SISSA

Scuola Internazionale Superiore di Studi Avanzati

Neuroscience Area – PhD course in
Functional and Structural Genomics

FUNCTIONAL CONSEQUENCES OF AGGREGATED ALPHA-SYNUCLEIN HIPPOCAMPAL ACCUMULATION IN RATS

Candidate:

Kasongo

Walu Emakana Danielle

Advisors:

Prof.Giuseppe Legname

Co-advisor:

Prof.Giampiero Leanza

Academic Year 2020-2021

LIST OF ABBREVIATIONS

PD	Parkinson’s disease
AD	Alzheimer’s disease
ALS	Amylotrophic lateral sclerosis
HD	Huntington's disease
FTD	Frontotemporal dementia
DLB	Dementia with Lewy bodies
NDs	neurodegenerative diseases
FTLD	frontotemporal lobar degeneration
PrP	Prion protein
PrP^{C}	Cellular prion protein
PrP^{Sc}	Misfolded, pathogenic form of PrP^{C}
PrnP	Prion gene
CJD	Creutzfeldt-Jakob disease
GSS	Gerstmann-Sträussler-Scheinker
FFI	Fatal familial insomnia
BSE	Bovine spongiform encephalopathy
PK	Proteinase K
Aβ	Amyloid β
CAA	cerebral amyloid angiopathy
PSP	progressive supranuclear palsy
CBD	corticobasal degeneration
NFT	Neurofibrillat tangles
α-syn	Alpha-synuclein
SOD1	Cu/Zn superoxide dismutase
TDP-43	TAR DNA-binding protein 43
PDD	PD with dementia
LBs	Lewy bodies
LNs	Lewy neurites
MSA	multiple system atrophy

APP	amyloid precursor protein gene
SNCA	alpha synuclein gene
APOE	apolipoprotein E
IDPs	intrinsically disordered proteins
IDRs	intrinsically disordered regions
PMCA	misfolding cyclic amplification
RT-QuIC	real-time quaking-induced conversion
SNpc	substantia nigra pars compacta
VTA	ventral tegmental area
MPTP	methyl-4phenyl-1, 2, 3, 6-tetrahydro-pyridine
TH	tyrosine hydroxylase
DA	dopamine
6-OHDA	6-hydroxydopamine
MWM	Morris water maze
RAWM	radial arm water maze
BH	Brain homogenates
Tg	Transgenic animals
EC	Entorhinal cortex
CTE	Chronic traumatic encephalopathy
TSEs	Transmissible spongiform encephalopathies
ThT	Thioflavin-T
APP	Aβ precursor protein
DMV	Dorsal motor nucleus of the vagus nerve
ENS	enteric nervous system
ThS	Thioflavin-S
WT	Wild type
AFM	Atomic force microscopy
EM	Electron microscopy
MCNSCs	Mouse cortical neuronal stem cells
PFFs	Preformed fibrils
p-Ser129	Phosphorylated Serine-129

CNS	central nervous system
BBB	blood-brain barrier
CWD	Chronic wasting disease

TABLE OF CONTENTS

ABSTRACT

Neurodegenerative diseases (NDs) include a broad range of age-related neuropathological conditions characterized by a slow but unstoppable highly selective degenerative process. It involves distinct subsets of neurons in specific anatomic systems leading to variable disease phenotypes such as cognitive impairment, movement disorders or a combination of both. However, the gradual accumulation of misfolded protein aggregates in well-ordered structures, habitually called amyloid represent a common feature of NDs and is thought to be at the root of these diseases. Some of these proteins are prion protein, beta amyloid, tau, TDP43 and alpha synuclein on which we focused our attention. Alpha-synuclein(α-syn) is a 140 amino acid protein widely expressed in the brain occurring as a soluble or membrane-associated protein at presynaptic nerve terminals. It is mainly involved in synaptic vesicle release and trafficking. In its membrane-bound protein form, α-syn has a predominantly α-helical structure which under certain conditions can alternatively fold into a β-sheet-rich structure that easily polymerizes into amyloid fibrils and aggregates. These aggregates acquire neurotoxicity affecting mitochondrial function, endoplasmic reticulum–Golgi trafficking, protein degradation and/or synaptic transmission, leading to neurodegeneration. Interestingly, aggregated forms of α-syn can recruit and seed the endogenous protein and initiate the spreading throughout cells, thus suggesting a prion-like mechanism. The occurrence of Lewy bodies/Lewy neurites containing misfolded fibrillar α-syn constitutes one of the pathological hallmarks of synucleinopathies such as Parkinson's disease, dementia with Lewy Bodies and multiple system atrophy, all linked to memory impairments. While it has been shown that brainstem Lewy bodies may contribute to motor symptoms, the anatomical and neuropathological substrates for cognitive symptoms are still elusive. Therefore, in this PhD thesis I sought to investigate the progressive pathologic alterations and spreading of synthetic α-syn fibrils bilaterally injected into the hippocampus of adult female Sprague-Dawley rats, up to the onset of memory impairments. Animals underwent behavioral testing for sensory-motor and spatial learning and memory abilities at different time-points post-injection. At no time-point was any sensory-motor deficits observed that could affect performance in the Morris Water Maze task, nor was any reference memory disturbances detected in any of the injected animals. By contrast, significant impairments in working memory performance became evident at 12 months post-injection. These deficits were associated to a time-dependent increase in the levels of phosphorylated α-syn at serine 129 and in the

stereologically-estimated numbers of proteinase K-resistant α-syn aggregates within the hippocampus. Interestingly, pathological α-syn aggregates were found in the entorhinal cortex and, by 12 months post-injection, also in the vertical limb of the diagonal band and the piriform cortices, all anatomically related to the injected sites. No pathological α-syn deposits were found within the Substantia Nigra, the Ventral Tegmental Area or the Striatum, nor was any obvious loss of dopaminergic, noradrenergic or cholinergic neurons detected in α-syn injected animals, compared to controls. This would suggest that the behavioral impairments seen in the α-syn injected animals might be determined by the long-term persisting α-syn neuropathology in the affected neurons rather than by neurodegeneration per se.

This study confirms and extends previous observations showing that hippocampal α-syn pathology contribute to specific memory impairment. In addition, the α-syn preformed fibrils infusion procedure in the rat may represent a feasible tool to model synucleinopathies with which to test possible therapeutic interventions.

CHAPTER I

INTRODUCTION

I Neurodegenerative diseases

Parkinson's disease (PD) together with Alzheimer's (AD), Amyotrophic Lateral Sclerosis (ALS), Huntington's disease (HD), Frontotemporal dementia (FTD), Dementia with Lewy bodies (DLB), belong to neurodegenerative diseases which enclose a broad range of age-related neuropathological conditions characterized by a slow but unstoppable highly selective degenerative process. It involves distinct subsets of neurons in specific anatomic systems leading to variable disease phenotypes such as cognitive impairment, movement disorders or a combination of both [1]. Another common feature of NDs is the accumulation in the human brain and peripheral organs of disease-specific proteins with altered physicochemical properties hence the name of conformational Diseases [2]. Comparatively, the disorders appear at the dawn of old age with a long clinical course followed by a complete disability which has a major negative impact at the professional, social and economic level on the lives of patients. Thus, NDs have become a tremendous burden for both families and society. They are almost 50 million affected worldwide and this number is expected to rise up substantially due to increasing life expectancy[3]. Despite the amount of work that has been carried out to develop disease-modifying treatments, none of them is able to stop the progression of the diseases, making NDs incurable until today.

1. Classification

The classification of NDs is based on the clinical presentation, anatomical regions and cell types affected, conformationally altered proteins involved in the pathogenetic process, and etiology if known (i.e., genetic variations or acquired pathways, for example, in prion diseases)[4]. Thus, the classification can be done following two different approaches subdivided in two groups:

The clinical classification

It is determined by the anatomical regions showing neuronal dysfunction or loss and allow focusing on early symptoms considering that in most NDs, there is an overlapping of clinical

symptoms, which occurs during the clinical course. Thus, involvement of the hippocampus, entorhinal cortex, limbic system, and neocortical areas can lead to clinical manifestations like cognitive decline, dementia and alterations in high-order brain functions. While, Movement disorders including hyperkinetic and hypokinetic disorders, are linked to the involvement of the basal ganglia, thalamus, brainstem nuclei, cerebellar cortex and nuclei, motor cortical areas, and lower motor neurons of the spinal cord[5][5]. In frontotemporal dementia, a subset of dementia, the neural degeneration mainly affects the frontal and temporal lobes (frontotemporal lobar degeneration, FTLD)[4].

The molecular pathological classification

The molecular pathological classification focuses on the distinction of synaptic, intracellular, extracellular protein accumulations and the subcellular location of the intracellular deposits (e.g., nuclear, cytoplasmic or cell process)[6]. With the development new antibodies, immunohistochemistry is mainly used for subtyping diseases, which describe novel immunostaining patterns whether biochemistry and genetic analysis are often required as a complementary examination to immunohistochemistry. However, there are some forms of NDs, like hereditary spastic paraplegia or some variants of spinocerebellar ataxia, where no specific protein inclusions are detected with currently available methods. According to the proteins associated with the majority of sporadic and genetic adult-onset NDs we can distinguish:

- **Prion diseases**

Prion diseases are a group of pathological conditions affecting both humans and animals and characterized by the aggregation within the brain of misfolded form of the cellular prion protein (PrP^{C}), called scrapie prion protein (PrP^{Sc}) or prion (PrP) [7, 8] which leads to brain damage. The classification of prion diseases is based firstly on the etiology as idiopathic/sporadic, acquired and genetic forms. Clinicopathological phenotypes include Creutzfeldt-Jakob disease (CJD: spongiform encephalopathy; sporadic, iatrogenic, variant or genetic), kuru, Gerstmann-Sträussler-Scheinker disease (PrP-amyloidosis), and familial or sporadic fatal insomnia (selective thalamic degeneration without prominent spongiform change) [9]. Secondly, it is based on immunostaining for disease-associated PrP, biochemical examination the size of the Proteinase K

(PK)-resistant core of PrP^{Sc} (i.e., type 1migrating at 21 kDa and type 2 at 19 kDa), and examination of the PrP gene (PRNP) (mutations and the genotype at the polymorphic codon 129; methionine, M, or valine, V) [9]. The combination of these molecular features distinguishes the bovine spongiform encephalopathy-related acquired form variant CJD, iatrogenic CJD, the recently described disorder termed variably protease-sensitive prionopathy (VPSPr), and certain genetic forms of disease. Morphologically, Major disease-associated PrP deposits comprise diffuse/synaptic, fine or coarse perineuronal immunopositivity, patchy/perivacuolar, plaque-like (lacking amyloid characteristics, thus called PrP plaques), and amyloid plaques. However, it is must be mentioned that florid plaque-like structures, which are amyloid plaques surrounded by a collar of vacuoles and additional PrP immunoreactivities such as multiple small cluster plaques, amorphous and star-like pericellular and perivascular PrP deposits [10] represent a characteristic sign of variant CJD, although already described in iatrogenic CJD [11].

- **Alzheimer disease**

The extracellular deposition of Amyloid β (Aβ) fibrils and the intraneuronal accumulation of abnormally phosphorylated tau protein represent the pathological hallmarks of AD. The accumulation of Aβ fibrils can occur in the parenchyma in the form of plaques and in the vessel walls as cerebral amyloid angiopathy (CAA). Parenchymal Aβ deposits display different morphologies, like stellate (probably related to astrocytes), diffuse deposits (further divided into fleecy, lake-like or subpial) or focal deposits (such as those with or without a dense core), and further rare morphologies like cotton-wool plaques [12]. Following the stereotypical pattern of protein pathology in AD, Braak and coworkers proposed either a staging scheme for neurofibrillary (tau) pathology or phases for Aβ deposition[13, 14]. Regarding tau pathology, strategic areas include the transentorhinal cortex (stage I), entorhinal cortex (stage II), inferior (stage III) and middle temporal gyri (stage IV), while for the end stages an examination of the occipital cortex is needed (peristriate for stage V and striate cortex for stage VI) [13]. Furthermore, it has been shown that subcortical nuclei also display early tau pathology and is indicated as early subcortical stages a, b, c [15], or as early pre-cortical evolutional phase [16]. Regarding Aβ deposition, five phases were proposed following the progressive involvement of isocortical areas (phase 1), hippocampus and entorhinal cortex (phase 2), basal ganglia and diencephalon (phase 3), brainstem (phase 4) and cerebellum (phase 5). Recently, the Braak

stages and Thal phases, together with the classical semiquantitative scoring of neuritic plaques [17], have been inserted in the NIA-AA neuropathological criteria for AD [18].

- Tauopathies

Tauopathies account for a heterogeneous group of disorders characterized by pathological intracellular deposits of the protein tau. Taupathies can be subdivided in two main groups: the primary tauopathies when tau pathology is the driving force in the pathogenesis or secondary tauopathies. when tau pathology is not the driving force. Primary tauopathies are grouped based on the ratio of 3 repeat (R)-tau and 4R-tau isoforms and two or three major bands (60, 64 and 68 kDa) in western blot of sarkosyl-insoluble fractions. Further classification is related to the distinct involvement of anatomical areas and cell types, and ultrastructural features of tau filaments [4]. The 3R tauopathy Pick's disease is characterized by neuronal spherical Pick bodies, ramified astrocytes and less frequently, small oligodendroglial globular inclusions[19]. 4R tauopathies comprise progressive supranuclear palsy (PSP), corticobasal degeneration (CBD), globular glial tauopathies (GGT) and argyrophilic grain disease (AGD). Comparably less neuronal inclusions comprising 4R immunoreactive spherical inclusions, globular Neurofibrillat tangles (NFT) NFT-like structures and diffuse cytoplasmic tau immunoreactivity are seen. The mixed 3R and 4R tauopathy affecting the medial temporal lobe, termed also as NFT-predominant dementia, represents the severe end of primary age-related tauopathy (PART) [20]. Secondary tauopathies include AD, in which deposit of Aβ plaques is associated with tau pathology and chronic traumatic encephalopathy (CTE), in which tau pathology is thought to be induced by repeated mild head injuries [21].

- **Alpha-synucleinopathies**

Alpha-synucleinopathies are a group of diseases characterized by the abnormal accumulation of aggregates of α-syn protein in neurons, nerve fibers or glial cells, α-synucleinopathies are subdivided in two main groups: the neuron and glia predominant α-synucleinopathies [6]. The neuron-predominant α-synucleinopathies display Lewy body (LB) pathology and are further classified according to the earliest nature of symptoms (movement disorder or cognitive decline)

including DLB, PD, and PD with dementia (PPD). We can have also incidental Lewy bodies' diseases where Lewy bodies are potentially detected despite the lack of clinical symptoms. One of the neuropathological approaches for Lewy body pathology classification concern the staging of α-syn pathology according to Braak and colleagues. This includes the sequential involvement of the medulla oblongata (stage 1), pons (2) mesencephalon (3; e.g., the substantia nigra), limbic areas (4) and neocortical areas (5 and 6), [22]. However, the existence of cases, which do not strictly follow these stages, outlined the presence of disease forms with Lewy bodies where α-synuclein pathology is generated 'spontaneously' in a specific region, [22]. Another approach proposed by Kosaka et al is applied in the diagnostic criteria for DLB (ie, brainstem, limbic and neocortical types)[23]. Further suggestions for classification have emerged due to the subsistence of disease forms where Lewy bodies are restricted to the amygdala, [24, 25] while the olfactory bulb is known to be the earliest affected. The unified staging system for Lewy body disorders classifies Lewy body disorders as olfactory bulb only, brainstem-predominant, limbic-predominant, brainstem and limbic and neocortical [26]. Regarding the glia predominant α-synucleinopathies, represented mainly by multiple system atrophy (MSA), the simple presence of oligodendroglial inclusions (Papp-Lantos bodies) is enough for the diagnosis [27]. Based on the distribution of glial inclusions which can follow a striatonigral or olivopontocerebellar predominance, clinical subtypes such as MSA-P (Parkinsonism dominant) and MSA-C (cerebellar symptom-predominant) are defined. Nevertheless, these cannot be clearly translated into biochemical or morphological differences [28]. Recently, a further type has been described with FTLD [29]. Furthermore, α-syn immunoreactive deposits can be observed in the ependyma, perivascular cells, cranial nerves, retina, gastrointestinal tract, peripheral organs and skin [30].

- **TDP-43 proteinopathies**

Inclusions of pathogenic deposits containing TAR DNA-binding protein 43 (TDP-43) are one of common pathological hallmarks of amyotrophic lateral sclerosis (ALS) and a common[31] form of FTLD. Markedly, up to 40% of cases are linked to multiple gene mutations including C9orf72 (most frequent), granulin (GRN), valosin-containing protein (VCP), TARDBP (the gene encoding TDP-43) etc. [32, 33]. TDP-43 immunoreactive deposits can be found in the cytoplasm, nucleus, and neurites of neurons. Furthermore, skein-like and spherical inclusions are

described in ALS[34]. According to a harmonized classification system we distinguish four subtypes (A–D), based on the predominance and layer, predominance of neuritic and neuronal cytoplasmic, or intranuclear inclusions. Interestingly, these patterns can also predict the genes involved in hereditary forms [35]. Finally, a further type (E) has been described in rapidly progressive forms (duration <3 years) [36]; this awaits further confirmation from larger cohorts. TDP-43 pathology frequently associates with other disorders like AD, DLB, hippocampal sclerosis and chronic traumatic encephalopathy. Some of these associations are related to genetic or other risk factors [37, 38]. The cellular distribution of TDP-43 pathology can be similar to the FTLD-TDP one, with only rare neuronal nuclear inclusions and variable presence of glial deposits. Recently an entity termed limbic-predominant age-related TDP-43 encephalopathy (LATE) has been defined. LATE allows the recognition of a stereotypical medial temporal lobe-predominant TDP-43 proteinopathy in older adults, with or without coexisting hippocampal sclerosis pathology that is associated with an amnestic dementia syndrome mimicking AD-type dementia. While LATE-NC described the neuropathological changes[39]

- FET/FUS proteinopathies

Conditions characterized by intra-nuclear and intra-cytoplasmatic deposition of RNA-binding proteins belonging to the FET (FUS/TLS, EWS or TAF15) family. Rare sporadic disorders associated with FTLD, such as basophilic inclusion body disease, atypical FTLD-U and neuronal intermediate filament inclusion disease, show neuronal (cytoplasmic/ nuclear) and glial cytoplasmic inclusions immunoreactive for FET proteins [40, 41]. The inclusion types and their regional distribution in FTLD distinguish these forms in most cases. In contrast, FUS gene mutation-related ALS cases are only immunoreactive for FUS and not for further FET proteins [40].

- Rare disease forms

They group different types of disorders of which some of the most relevant are represented by a group of diseases such as hereditary ataxia and Huntington's disease that are associated with the expansion of unstable trinucleotide repeats in some genes that lead to the aggregation of genic

products [42]. Another group of disorders are neuroserpinopathies that result from point mutations in the Neuroserpin gene, a member of the serpin family of serine protease inhibitors, promoting the formation of neuroserpin-compound inclusion bodies in the brain [43]. Ferritin-related NDs are characterized by a genetic defect in the ferritin light polypeptide gene that leads to the accumulation of ferritin deposits in the brain and peripheral organs [44]. Furthermore, there are hereditary brain amyloidosis, where deposited proteins include Aβ, transthyretin, gelsolin, cystatin, PrP and BRI2 proteins. Finally, there are diseases for which specific inclusions have not been described (eg, FTLD-ni; no inclusions) [45]. A summary of the most relevant neurodegenerative disease is shown in the Table below:

Disease group	Protein	Disease types	Form	Phenotype
Prion diseases	PrP	sCJD, VPSPr, sFI iCJD, vCJD, Kuru gCJD, GSS, FFI, PrP-CAA	SP ACQ GEN	DEM/MD DEM/MD DEM/MD
Alzheimer disease	Aβ, Tau	Alzheimer disease	SP/GEN	DEM
Taupathies FTLD-Tau	Tau	Pick disease, GGT CBD, PSP AGD, NFT-dementia/PART FTDP-17T	SP SP SP GEN	FTD MD/FTD DEM FTD/MD
αsynucleinopathies	α-synuclein	Parkinson disease Dementia with Lewy body multiple sytem atrophy	SP/GEN SP/DEM SP	MD DEM/MD MD
TDP-43 proteinopathies	TDP43	FTLD-TDP(Type A-D) MND-TDP FTDL-MND-TDP	SP/GEN SP/GEN SP/GEN	FTP MD FTD-MD
FUS/FET-proteinopathies	FUS/FET	aFTLD-U, NIFID, BIBD MND-FUS	SP GEN	FTD/MD MD
Trinucleotide repeat expansion disorders (TRD)	Huntington Ataxin1,2,37, CACNA1A,TBP FMRP ARP	Huntington disease Spinocerebellar ataxia (SCA) 1,2,3,6,7,17 FXTAS SBMA	GEN GEN GEN GEN	MD MD MD MD
Neuroserpinopathy	Neuroserpin	Neuroserpinopathy	GEN	DEM
Neuroferritinopathy	Ferritin	Hereditary ferritinopathy	GEN	DEM/MD
Hereditary amyloidosis	ABri, Adan, Gelsolin, Cystatin, Transthyretin, Aβ	Hereditary amyloidosis/CAA	GEN	DEM

Table 1. Summary of the most relevant neurodegenerative diseases classified according to their protein deposits. Abbreviations: ACQ: acquired; ARP: androgen receptor protein; AGD: Argyrophilic grain disease; BIBD: Basophilic inclusion body disease; CAA: sporadic cerebral amyloid angiopathy;CACNA1A:1A subunit of the P/Q-type voltage-gated calcium channel (SCA6; Cytoplasmic aggregates); CBD: Corticobasal degeneration; CJD: Creutzfeldt-Jakob disease (i: iatrogenic, s: sporadic, v: variant, g: genetic); DEM: dementia; sFI: sporadic fatal insomnia; FFI: fatal familial insomnia; FMRP: Fragile X mental retardation protein; FTD: frontotemporal dementia; FTLD:frontotemporal lobar degeneration; aFTLD-U: atypical FTLD with ubiquitinat: FTLD-ni: FTLD no inclusion specified; FTDP-17T: Frontotemporal dementia and parkinsonism linked to chromosome 17 caused by mutations in the MAPT (tau) gene; FXTAS: Fragile X associated tremor and ataxia syndrome (here also astroglial inclusions); GEN: genetic; GGT: globular glial tauopathy; GSS: Gerstmann-Sträussler-Scheinker disease; INIBD: intranuclear inclusion body diseases; MD: movement disorder; MND: Motor neuron disease; NIFID: Neurofilament intermediate filament inclusion disease; PrP: prion protein; PSP: Progressive supranuclear palsy; SCA: spinocerebellar ataxia; SBMA: spinal and bulbarmuscular atrophy; SP: sporadic; TBP: TATA-Box binding protein (SCA17); VPSPr: variably protease-sensitiveprionopathy. [6]

2. Etiology and pathogenesis

Aging, genetic, and environmental factors

Generally, neurodegenerative diseases are multifactorial in origin although aging and genetic factors remain greatest risk factors. Indeed, peculiar hallmarks of aging like genomic instability, telomere attrition, epigenetic alterations, and loss of proteostasis, mitochondrial dysfunction, cellular senescence, deregulated nutrient sensing, stem cell depletion and altered intercellular communication correspond with susceptibility to neurodegenerative disease [46]. Moreover, DNA damage, mitochondrial dysfunction, cellular senescence and inflammation, which are often thought to lead to neurodegeneration, show great interconnection with the others ageing-related hallmarks.

For instance, defects in DNA repair contribute to genomic instability, which increases with age [47]. It has been shown that the proteostasis decline, consequent to dysfunctions in proteasome or autophagy observed in AD and PD, is highly linked to inflammation [48]. There is also a correlation between metabolic dysfunction observed in neurodegeneration and alterations in NAD+ levels, mitochondrial dysfunction and oxidative stress [49]. Furthermore, the Loss of functional stem cells is linked to most of the ageing hallmarks, including DNA damage, epigenetic deregulation, mitochondrial dysfunction, telomerase inactivation and cell senescence [50].

Beside contributing to the aging process, genetic factors have a crucial role in the development of neurodegenerative diseases which majority are sporadic in occurrence with 5-10% familial. Familial forms of neurodegenerative diseases show a strong genetic component and the identification of mutations that cause disease in some genes such as amyloid precursor protein gene (APP) for AD, alpha synuclein gene (SNCA) in PD and tau in FTD have provided insights into their pathogenesis. Regarding sporadic forms, they are presumably owing to the involvement of different genes of susceptibility to multiple loci and interaction between them and / or environmental factors [51]. In fact, the ε4 allele of the apolipoprotein E (APOE) gene has been found to be a strong risk factor for AD [52, 53] as well as variants in genes like SNCA, MAPT and LRRK2 for Parkinson disease [54]. Furthermore, SNCA represent also an important risk locus for both multiple system atrophy and DLB [55, 56], as APOE for dementia with Lewy bodies [56] and MAPT for both CBD and PSP [57].

In the other hand, environmental factors including nutrients, pollutants, chemicals, metals, physical activity, and lifestyle, physical and mental stress can modulate epigenetic markers in developing organisms and adults. Thus, this may result in the alteration of gene expression through DNA methylation, histone modification, and non-coding RNA-associated gene silencing, increasing the susceptibility risk to neurodegenerative diseases [58]. Indeed, it has been demonstrated that Presenilin 1 PSEN1 expression can be modulated by modifying the methylation homeostasis, with consequent alteration of the amyloidogenic pathway, senile plaques burden and specific cognitive tasks in AD mice [59, 60]. Likewise, exposure to lead (Pb) could induce the

hypomethylation of CpG dinucleotide in the APP promoter leading to abnormal APP processing [61].

Meanwhile, both Huntington's disease, ALS patients, as well as their respective mouse models showed DNA histone hypoacetylation that can ultimately trigger cell apoptosis and lead to neuronal death [62]. Regarding PD, the SCNA is potentially regulated by DNA methylation. Hypomethylation of the SCNA intron1 negatively correlates with its expression and was reported in the substantia nigra of affected patients [63]. miR-7 and miR-153 which negatively regulate alpha synuclein expression levels were also found to be reduced in PD brain [64]. There is evidence that exposure of humans or mice to the environmental toxins like MPTP, paraquat, or rotenone hinder mitochondrial function, in particular the complex I, which results in an elevated free radical production and oxidative stress leading to acute and irreversible Parkinsonism [65]. Furthermore, the fact that a single heterozygous mutation in the recessive PINK1 and Parkin genes could lead to PD in some patients, suggested that these heterozygous mutations raise sensitivity to environmental toxins that conjointly are enough to cause PD [66]. A study done to known about the concordance rate in twins for dementia with Lewy bodies (DLB) revealed a neuropathological discrepancy in the type of dementia between monozygotic couples hinting at the importance of environmental or epigenetic factors in Lewy body pathology [67]. Therefore, overall these data highlighted the interplay between aging, genetic and environmental factors in the etiopathogenesis of neurodegenerative diseases.

According to increasing evidence and the molecular pathological classification of NDs, the gradual accumulation of misfolded protein aggregates in well-ordered structures, habitually called amyloid is thought to be at the root of these diseases [68]. This occurs within specific brain regions often showing significant neuroinflammation and increased oxidative stress with final degeneration of neural tissue [69]. Although there is, a clear difference between proteins aggregates implicated in distinct NDs, protein-misfolding procedure, its intermediates, final products, and principal characteristics are notably identical [68].

Protein misfolding and aggregation

Proteins are the operators of cellular functions and the correct folding of a protein into its native three-dimensional structure guarantees its biological functionality [70]. The sequence of amino acids as well as local low-energy chemical bonds between atoms in both the polypeptide backbone and the amino acid side chain determine the structure of a protein [71]. Indeed, following translation, each protein occurs as a specific sequence of covalently bonded amino acids, called polypeptide chain, which represent it primary structure. Then, depending on hydrogen bonds forming within the polypeptide chain, the latter can acquire an α-helix or β-sheet structure that constitute the secondary structure. α-helix is formed when polypeptide chains twist into a spiral, whereas in β-sheets polypeptide chains run alongside each other. Furthermore, the α-helices and ß-sheets can fold into a compact conformation stabilized by hydrogen bonds or ionic interactions referring to the three-dimensional tertiary structure of a protein. The quaternary structure designates the number and arrangement of multiple folded polypeptide chains known as subunits in a multi-subunit complex **Fig 1.1**.

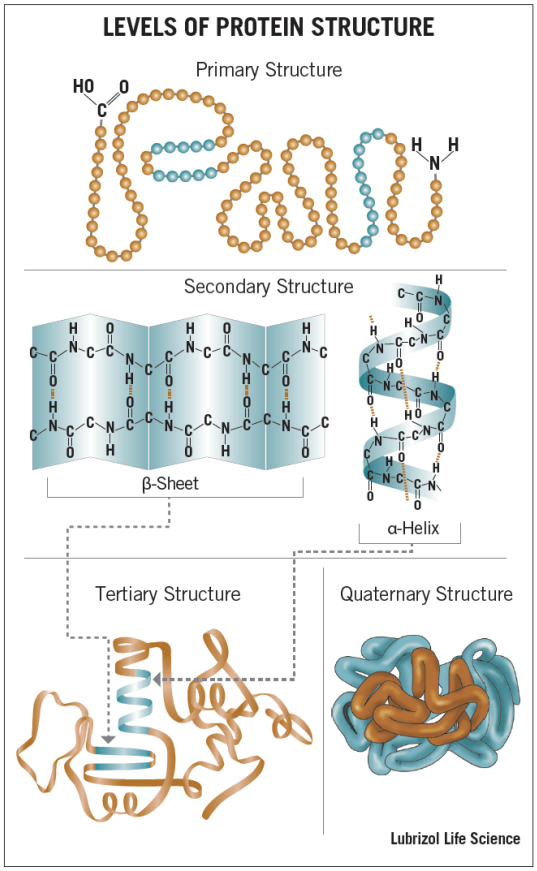

Figure 1.1 Level of Protein structure

Thermodynamically, the folding process is represented as an energy funnel where the unfolded state is associated with more chaos, higher entropy, and free energy, which leads the protein to curve and twine in order to reach a maximum stability or lowest energy state: the three-dimensional native conformation [72]. However, the principal driving force of the folding process is due to the tendency of hydrophobic amino acids to cluster together within the protein in view of lessening the amount of hydrophobic side chains exposed to water [73, 74]. Given the importance and complexity of the folding process, incipient proteins are assisted by chaperones. Moreover, chaperones monitor the quality of folded proteins by either reorienting non-native species to their native state or targeting them for degradation through the ubiquitin proteasome system or via the autophagy pathway or sequestration into cellular compartments [75].

However, some proteins are devoid of a stable tertiary and/or secondary structure under physiological conditions, existing as dynamic ensembles of interconverting structures

termed intrinsically disordered proteins (IDPs) or hybrid proteins due to the presence of both structured domains and biologically important intrinsically disordered regions (IDRs). It therefore results in a unique structural plasticity and a conformational adaptability allowing these proteins/regions, to interact with a broad range of unrelated partners, hence, serving as hubs in cellular protein-protein interaction network [76]. Consequently, IDPs/IDRs are involved in numerous biological processes and their disregulation and/or misfolding can lead to potentially fatal pathologies. Indeed, most proteins involved in some neurodegenerative diseases also known as proteins misfolding diseases like α-synuclein, Aβ, prion, tau and TDP43 have been shown to contain IDRs[76]. The suppleness of this structural form is essential for the conformational reordering, driving the formation of the core cross-beta structure of the amyloid fibril, which is a common characteristic of misfolded proteins [71]. However, both natively folded proteins and IDPs can undergo misfolding and aggregation under certain conditions. While ordered or folded proteins need to be first destabilized before going through fibrillation, natively unfolded proteins has to be partially folded [77]. Effectively, the consequential mainly unfolded conformation ensures distinct intermolecular interactions, including electrostatic attraction, hydrogen bonding and hydrophobic contacts, which are required for oligomerization and fibrillation [78]. Thus, environmental partially denaturing conditions such as low/high pH, high temperature, agitation, elevated glucose or oxidative agents and change in metal ions can trigger protein misfolding [79]. Furthermore, there could be several other causes of protein misfolding listed below [80]:

- somatic mutations in the gene sequence which induce the synthesis of a protein incapable to adopt the native folding underlying most of the inherited neurodegenerative disease.
- errors on the processes of transcription or translation leading to the production of modified proteins unable to properly fold.
- failure of the folding and chaperone machinery.
- Mistakes on the posttranslational modifications or trafficking of proteins.

Subsequently, misfolded proteins, in search of a lower energy levels and more stability, have a propensity to aggregate. Indeed, the misfolding process leads to the exposure of

hydrophobic fragments to the solvent while these fragments were ordinarily hidden inside the protein, resulting to a great rank of tackiness. Thus, the exposed hydrophobic fragments may interact with exposed hydrophobic patches of other proteins leading to the most favorable organization in the β-sheet structural motif of these protein aggregates [81, 82]. They can be classified in three categories ranging from small oligomers, intermediate protofibrils to large amyloid fibrils. Oligomers are soluble, low-molecular weight structures varying in size from dimers to decameters [83, 84] whose structural and biochemical characterization has been challenging due to their unstableness. However, evidence suggested that oligomers differ from primarily disordered [85] to structures similar to those of fibrils [86]. In particular, FTIR (Fourier-transform infrared spectroscopy) and NMR studies showed that oligomers are devoid of the parallel in-register β-sheet structure present in fibrillar form, but they have the β-loop-β secondary and tertiary folds as in fibrils [87]. Some oligomers share common immunological epitopes which are recognized by conformational antibodies, A11 (spherical) and αAPF (annular) [88], while fibrillary oligomers are recognized by conformational antibodies OC [89]. Protofibrils are short, flexible, rod-like structures consisting of unbranched polymers with 4-11 nm width and can reach a length of 100mm. They show a high β-sheet content and like the fibrils of which they are the direct precursors, they can bind the amyloid-specific dyes Congo red and thioflavin [90]. Amyloid fibrils are linear and unbranched structures of approximately 10 nm diameter and generally various micrometers in length. They show a classical "cross- β" X-ray diffraction paradigm consisting of two major reflections at 4.7 Å and 10 Å found on orthogonal axes [82].

The mechanism of protein misfolding and aggregation comply with the so-called "seeding-nucleation" model first proposed by Jarret and Lansbury [91] and subsequently modeled kinetically in detail [92]. Accordingly, the initial step of misfolding is thermodynamically unfavorable and progresses slowly, until the formation of a minimum stable oligomeric unit: the nucleus or seed, which then rapidly grows by incorporating monomeric proteins to form larger polymers, the protofibrils an then amyloid fibril. Therefore, kinetics of amyloid formation can be plotted by a sigmoidal curve with a lag phase followed by rapid growth phase which reach a plateau or saturation phase. The slope of the elongation curve reflects the speed of the fibril formation, which can be

increased by addition of preformed seeds that reduce the length of lag phase and accelerate the grow phase. Indeed, during the process, off-pathway oligomers can be formed which do not finish in fibrils while prefibrillar or on-pathway oligomers do so. Furthermore, the mature fibrils, probably helped in vivo by mammalian Hsp70–Hsp40–Hsp110 tri-chaperone system, macro-autophagy, and the proteasome system can shear or fragment to form fibrillar oligomers (originated from fibril) that can again aggregate [93]. It results in a secondary nucleation catalyzed by mature fibrils fragments that act as a template to form diffusible oligomers from monomers as illustrated in **Fig 1.2**.

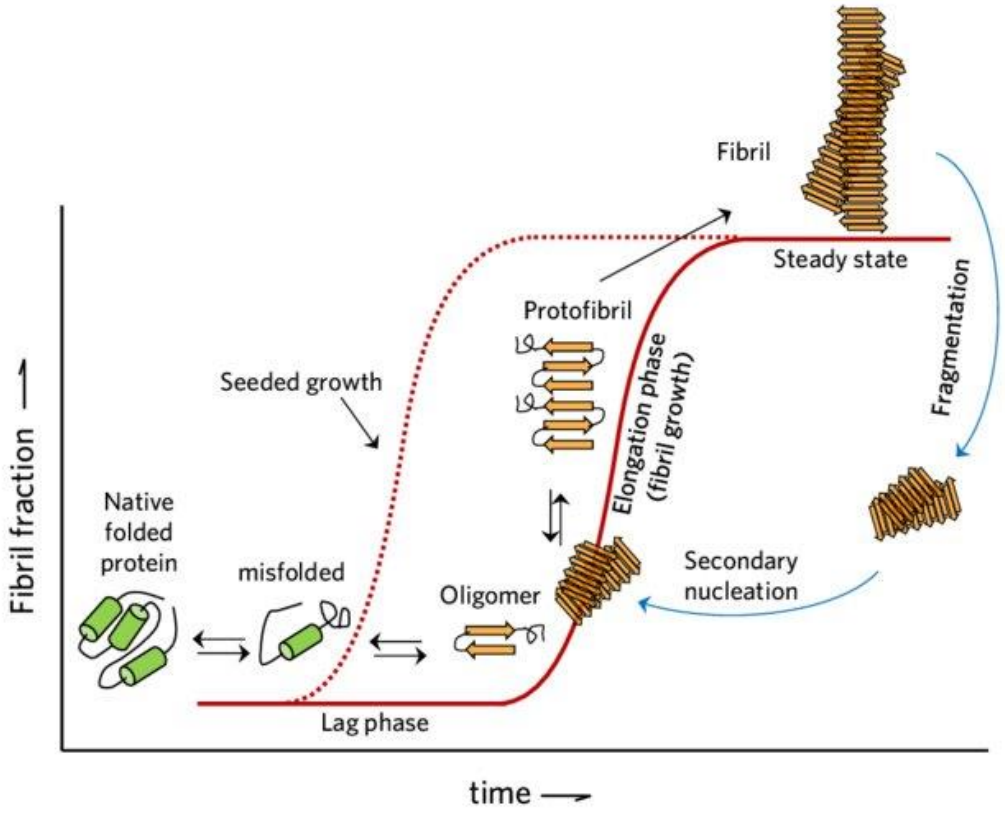

Figure 1.2 Illustration of amyloid protein fibrillation pathway. A nucleus is formed during the lag phase, and addition of monomer results in the formation of aggregates, which subsequently grow into mature fibrils. Preformed fibrils or fibril fragmentation may catalyze nucleation, and this is called secondary nucleation[94].

Thus, based on the seeding nucleation model several in vitro assays have been generated for the production of synthetic amyloid fibril as experimental model and are used as diagnostic tool for the detection of protein misfolding diseases. The most used techniques

are protein misfolding cyclic amplification (PMCA) and real-time quaking-induced conversion (RT-QuIC). The PMCA protocol was firstly developed by Soto's group for the detection of PrP^{Sc} from various biological samples like brain homogenates (BH), urine, blood, cerebrospinal fluid (CSF) and saliva [95]. The protocol implies a sonication and incubation phase that alternate several times. The sonication allows the proliferation of template units while the incubation phase promote the expansion of aggregates. Finally, PK digestion and western blot (WB) analysis are used for the characterization and recognition of pathological aggregates. However, the fact that PMCA must be carried out in several rounds, combined with the need for immunoblot make it time-consuming assay. Thus, Atarashi and colleagues elaborated the QuIC assay by modifying the protocol of PMCA [96]. In the QuIC assay, the PrP^{C} substrate originate from hamster's brain homogenate is switched by recombinant PrP^{C} and a strong intermittent shaking is used to promote seeded aggregation instead of sonication [97]. Of note, both assays necessitate the employment of discontinuous mechanical forces in order to mimic the fragmentation of newly formed fibrils, highlighting its importance since it produces thermodynamically unstable fibrils ends that act as seeds. In addition, as an alternative to WB analysis, the formation of β-sheeted aggregates is measured by Thioflavin T (ThT) fluorescence in real time as a read-out, hence the name RT-QuIC [96]. Furthermore, PMCA and especially RT-QuIC were found suitable for the detection and amplification of others misfolded protein aggregates like Aβ, α-syN, tau, and TDP43[98-101].

Toxicity of misfolded proteins

Once formed, misfolded protein aggregates can impair neuronal integrity leading finally to neurodegeneration. Their precise mechanisms of action are still unclear and seem to dissent depending on the protein species involved and whether the accumulation is intra or extracellular. Generally, misfolded proteins act by toxic gain-of function although loss-of-function effects are sometime observed. Extracellular aggregates like amyloid fibrils of Aβ and PrP might activate a signal transduction pathway that leads to apoptosis by interacting with specific cellular receptors as RAGE (receptor for advanced glycation end-products) [102]. Alternatively, their neurotoxic effects can be translated by

membrane disruption and depolarization mediated by ion-channel formation, ensuing the impairment of ion homeostasis and disfunction of cellular signal transduction, resulting in neuronal death. While intracellular aggregates might damage cells by recruiting factors that are essential for cell viability into the fibrillar aggregates [68]. Indeed, huntingtin and alpha synuclein aggregates usually contain components of the proteasome, chaperone proteins, cytoskeletal proteins, and transcription factors [103]. Beside of their proteotoxic effects, misfolded proteins may exert genotoxic effects by disturbing nuclear DNA replication and repair enzymes [104]. That leads to the impairment of the entire cellular interactome by jamming both the integrity of proteasome (proteostasis) and the genome [105]. Another consequence of misfolded protein aggregates is the generation of oxidative stress owing to the production of free radical species, which leads to protein and lipid oxidation, increasing of intracellular calcium and mitochondrial disfunction (Abramov et al 2020). Misfolded protein aggregates might trigger astrogliosis and microgliosis leading to neuroinflammation which is thought to be a double-edged sword since it can have both negative and positive effects simultaneously [106]. Furthermore, there is a co-interaction between protein misfolded aggregates and symptoms of cellular distress including calcium signaling abnormalities, mitochondrial dysfunction, oxidative stress, and neuroinflammation which in many cases worsen reciprocally. For instance, misfolded aggregates as amyloid-β, α-syn, tau and mHtt are known to induce oxidative stress in neuron and or astrocytes [107] while, conversely, oxidative stress triggers protein misfolding, aggregation and proteostatic collapse[108]. Thus, it results in a vicious cycle that inevitably leads to neuronal death. It was firstly thought that misfolded aggregates in the form of amyloid fibrils were the neurodegeneration cause. However, increasing evidence suggests that oligomers could be the most neurotoxic species and that amyloid-like fibrils formation might be a way to isolate and protect the cell against toxic misfolded intermediates [83, 109, 110]. Indeed, oligomers, due to their smaller size, thermodynamic instability and their structural arrangement in particular the abnormal exposition of hydrophobic groups on their surface and the more number of open active ends [110] can easily diffuse and interact improperly with many functional cellular components like membranes and organelles [111]. Alternatively, both soluble misfolded intermediates and amyloid-like fibril aggregates might exert their toxicity through

different mechanisms. While soluble oligomeric species might trigger apoptotic-signaling pathways, amyloid-like aggregates might take up tissue space, damage neuronal connections and recluse essential cellular factors. In addition, some neurons might show a specific vulnerability to apoptotic stimuli triggered by different misfolded proteins, resulting in distinct cellular damage, which translates to an ineffective elimination of protein aggregates from these cells [68]. For example, dopaminergic neurons in the substantia nigra pars compacta (SNpc) seem to be the population affected first in Parkinson's disease (Brichta et al 2014). However, even inside SNpc there is about 90% of dopaminergic neurons loss in the ventral tier compared to circa 25% dopaminergic neurons loss in the dorsal tier [112]. Conversely, dopaminergic neurons in the ventral tegmental area (VTA) degenerate in a lower amount [113]. Moreover, while cholinergic neurons in the basal forebrain and in the pedunculopontine nucleus are affected, GABAergic neurons in the same regions are not. Thus, GABAergic neurons indifferently of their location seems to resist to Lewy body pathology (Kingsbury et al 2010, Surmeier et al 2017). Another study using induced pluripotent stem cells (iPSCs) from patients harboring an APP mutation to quantify AD-relevant phenotypes, following directed differentiation to rostral fates of the brain and caudal fates showed that the rostral neurons are more vulnerable to the pathology compared to caudal neurons. Interestingly, authors found that both the generation of Aβ and the responsiveness of tau to Aβ were affected by neuronal cell type confirming the influence of cell-autonomous factors on selective neuronal/regional vulnerability [114]. Thus, the subsistence of diverse mechanisms of cellular toxicity may be related to the differences in the protein sequence, cellular emplacement and biophysical characteristics of the aggregates [109]. Finally, there is a dynamic equilibrium between misfolded intermediates, monomers and amyloid fibrils (Teplow 1998, Kim et al 2002), which accentuates the difficulty to distinguish the involvement of the different mechanisms into neurodegeneration.

Propagation and transmission of misfolded proteins

One of the common characteristics of neurodegenerative diseases rely on the highly predictable spatiotemporal patterns of the distribution of pathological proteins in the

brain of patients. For instance, in PD patients, alpha-synuclein pathology firstly appears in the olfactory bulb and the dorsal motor nucleus of the glossopharyngeal and vagal nerves. Then, the pathology propagates in a rostral direction from the brainstem to the midbrain and forebrain eventually reaching the cerebral cortex [22, 115]. In AD brains, pathological tau is primarily found in the locus coeruleus and transentorhinal cortex. Then it propagates to the entorhinal and hippocampal regions, followed by the basal temporal cortex and the insular cortex with an eventual reaching of the neocortex in the later stages of the disease [13, 116]. While Aβ pathology follows a different pattern of distribution, occurring first in the orbitofrontal neocortex and basal temporal cortex, and then spread throughout the neocortex with the ultimate attainment of the hippocampus, midbrain, brainstem and cerebellum [14, 116]. These patterns of distribution were historically attributed to vulnerability between brain regions [112] or the progressive spreading of pro- inflammatory cytokines [117]. However, several studies during the past decade have provided evidence for a "prion like" propagation of these pathogenic proteins that might be at the heart of the pathogenesis mechanisms of neurodegenerative diseases [118-122]. Indeed, the propagation rely on the intrinsic feature of these pathogenic proteins, to corrupt similarly the conformation of their physiological counterparts upon interaction with them. Such a phenomenon is peculiar to prion disease, which can be infectious, genetic, or idiopathic in origin [9]. The infectious agent represented by the misfolded prion protein (PrP^{Sc}), spreads the disease by acting as seeds to start up the misfolding and aggregation of the native, monomeric prion protein in the host [7]. Thus, the seeding nucleation mechanism combined with the resilience of aggregates to the cellular clearance machinery allow PrP^{Sc} to spread from cell to cell, throughout the central nervous system and sometimes even to the periphery. Generally, PrP^{Sc} propagation occur silently for a long period of time until achievement of toxicity limit required to spark cellular dysfunction, brain damage, and clinical disease [120]. Furthermore, PrP^{Sc} can be efficiently transmitted between hosts of the same species while the efficiency of the transmission is minimized between diverse species. This could be due to the discrepancies between amino-acid sequences of hosts and donors prevent PrP^{Sc} to trigger the conformational conversion of the native one leading to the so called "species barrier" [123, 124]. However, under certain conditions like a high sequence

homology, intrinsically unfolding and high flexibility of proteins the species barrier might be traversed [125]. A typical example of species barrier overcrossing refers to the BSE epidemic in Britain in the 1980s in cattle, which caused variant Creautzfeldt-Jakob disease (vCJD) in the humans due to natural transmission of prion diseases from livestock to humans after consumption of infected livestock [7, 126].

Similarly, protein misfolding-related neurodegenerative diseases behave almost like PrP^{Sc}. Of note, the concept of prion-like behavior of these proteins was and still under significant debate since they are not strictly speaking "infectious" under natural conditions [122, 127]. Indeed, this was supported by studies showing no infective transmission between humans of AD and PD occurred in cadaver-derived human growth hormone (HGH) recipients [128] or blood transfusion recipients [129] as it should have been the case in classical prion diseases like CJD. However, other studies reported a potential transmission of Aβ-pathology via pituitary-HGH and dura mater transplants in recipients' patients [130, 131]. Similarly, transmission of α- synuclein pathology was shown from the host to the graft in patients who have received transplants of human fetal brain-derived cells as a therapy for PD [132, 133]. Thus, further epidemiological and longitudinal studies will be of great help in clarifying the true infectious nature of protein misfolding related neurodegenerative diseases.

Nevertheless, as enounced above, various studies using cellular and animal models of diseases have demonstrated that several NDs can be experimentally transmitted through a prion-like spreading. In fact, inoculation of brain homogenates from patients affected by NDs or transgenic mouse models rich in protein aggregates like Aβ, tau α-syn, results in the induction of disease pathology in the recipient cellular or animal models [134-137]. Moreover, injection of synthetic aggregates in wild type animals was able to induce a de novo pathology like infectious prions [138-141]. Indeed, Pathological induction can be lessened by decreasing the inoculum of protein aggregates [142-144]. Thus, the induction rate might be directly proportional to the amount of seeds as shown by titration experiments in some cases [145]. Furthermore, ALS and FLTD-related proteins, including SOD1 and TDP-43, have been shown both in stem-cell culture and animal studies to follow self-perpetuating seeded aggregation, congruent with prion-like transmission [146, 147]. Similarly, drosophila models of HD have proven evidence of a

prion-like spreading of Huntindton aggregates [148], as confirmed by further cellular and in vivo studies [119, 149]. Interestingly, peripherally disease transmission was shown even when seeds were administered systemically. In particular, repeated injections of α-synuclein fibrils into the rodent tail vein and an intraperitoneal inoculation of tau extracts or amyloid beta seeds, triggers intracerebral aggregation of deposits and relevant pathology [150-154].

Overall, these data combined with the previously discussed adaptability of PMCA and RT-QuIC techniques to the proteins misfolding related neurodegenerative diseases demonstrate that the seeding nucleation mechanism underpin the propagation/transmission of misfolded proteins confirming thus the prion like hypothesis. However, diverse subcellular pathways and cellular connections may contribute to the spreading process, to favor interaction between misfolded aggregates and the native protein. Misfolded aggregates can be sequestered in aggresomes which are targeted to elimination by macroautophagy and degradation into lysosomes [155]. In pathological conditions, the autophagy–lysosome pathway is dysregulated or inhibited [156, 157] allowing both autophagosomal and lysosomal vesicles to propagate aggregates within the cell, constituting thus a reservoir of misfolded proteins [155]. Both retrograde and anterograde axonal transport may be also a way of propagation of misfolded aggregates along neuronal processes [158, 159]. Misfolded aggregates can be release in the extracellular space upon cellular death or trough exocytosis [160]. Furthermore, exosomes can serve as a vehicle for the release and delivery of misfolded aggregates between cells [161]. Indeed, plasma and other body fluid are enriched of exosomes which could contribute to systemic spread of proteins misfolding related neurodegenerative diseases [162]. Growing evidence suggest that tunneling nanotubes, which are membrane bridges between cells for intercellular long-distance communication, may participate to the spreading of misfolded aggregates [163-165]. Then misfolded aggregates can be taken up from the extracellular space via diffusion, endosomes, receptor-mediated transport, or fusion of the transporting vesicles with the plasma membrane allowing entrance in the recipient cells [166-169]. In order to interact with their physiological counterparts and begin templated amplification, pathological seeds need to exit the endosomal vesicle once internalized in the recipient cells. In fact, a- Synuclein, tau and

mutant Huntington fibrils were shown to induce vesicle rupture to access the cytosol [170, 171].

Intriguingly, pathological seeds composed by one misfolded protein were found to promote the polymerization and greatly accelerate the aggregation process of a different proteins [172]. This phenomenon acquaintes as cross-seeding or heterologous seeding and may explain the contemporaneous presence of different misfolded proteins aggregates, the occurrence of more than one PMD in the same individual (Fig 1.3). For instance, Aβ aggregates can seed the polymerization of prions and alpha-synuclein, which can lead to the increased polymerization rate of soluble Aβ [172]. Indeed, 50% of the AD patients display a-synuclein aggregates accompanied by more severe pathological symptoms [173]. Similarly, Aβ aggregates have been observed in typical prion plaques either in sporadic CJD or GSS syndrome cases [174, 175]. Moreover, Transgenic mice developing both Aβ, α-syn and tau deposits shown a strengthen cognitive decline which is thoroughly linked to the deposition of all three amyloidogenic proteins [176]. Therefore, cross-seeding phenomenon may be considered as modulator of transmission/spreading of misfolded proteins and might explain the fact that one Protein misfolding diseases (PMD) may be a risk factor for occurrence of a second PMD. Another important modulation factor of transmission/spreading pattern lies on the conformation of pathological seeds which will be discussed below.

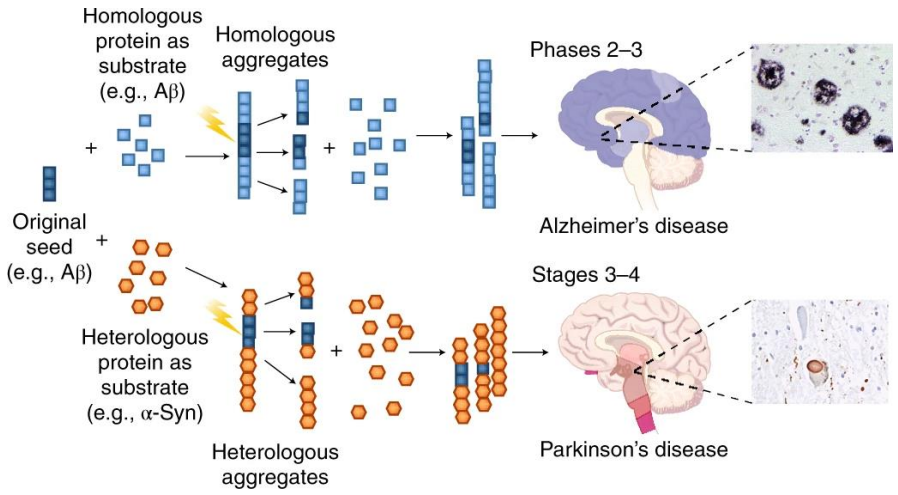

Figure 1.3 Illustration of cross-seeding between different proteins [109]

The structural polymorphism of misfolded proteins and the related strain concept

Initial results from X-ray analysis following investigations on the common cross-β structure of amyloid fibrils, shown a strict organization in which the β-strand direction is perpendicular to the fibril axis [177, 178]. However, recent progress in biophysical techniques led to the discovery that amyloid fibrils do not have a universal tertiary and quaternary structures [179], occurring either as parallel [180, 181] or antiparallel β-sheet conformation[182, 183] and other structural elements. Moreover, David Eisenberg and colleagues, in order to understand the precise composition of the β-cross structure, used X-ray microcrystallography to analyze small peptides that developed both microcrystals and fibrils. These fibrils were consisted of a pair of β-sheets where each β-sheet was formed by β-strands. One β-strand corresponds to a single peptide, and these β-strand peptides compose β-sheets with a close "dry" interface called a steric zipper. These steric zippers are repeated structures running up and down the fibril axis, excluding water from the interface between the β-sheets where the side chains of one β-strand are located between the side chains of another strand. Van der Waals interactions and hydrogen bonds between the side chains are the principal forces which lead to the formation of this interface [184]. Extending these observations to the structure of several amyloid proteins, Eisenberg and colleagues uncovered a difference between the basic organization of steric zippers in amyloid fibrils. Thus, they proposed eight possible structural classes of steric zipper (Fig. 1.4) based on three structural principles: first, whether their β-strands were antiparallel or parallel; second, whether the β-sheets were packed "face-to-face" or "face-to-back"; and third, whether the orientation of the β-sheets was "up-up" or "up-down" with respect to each other [185].

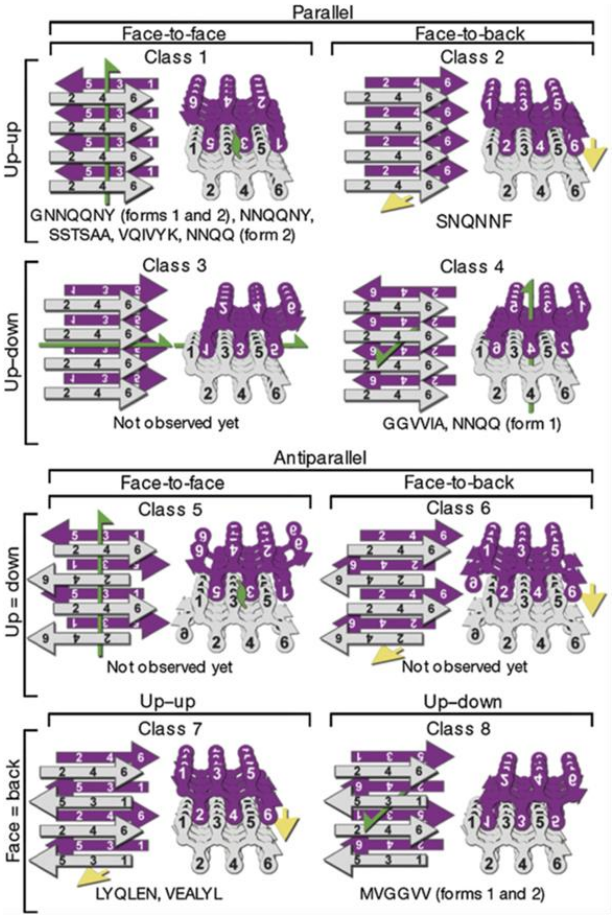

Figure 1.4 | The eight classes of steric zippers. Two identical sheets can be classified by: the orientation of their faces (either face-to-face or face-toback), the orientation of their strands (with both sheets having the same edge of the strand up, or one up and the other down), and whether the strands within the sheets are parallel or antiparallel. Both side views (left) and top views (right) show which of the six residues of the segment point into the zipper and which point outward. Green arrows show two-fold screw axes, and yellow arrows show translational symmetry. Below each class are listed protein segments that belong to that class [185].

Interestingly, the same polypeptide can display steric zippers of different structural classes based on the experimental conditions. Therefore, a major fount of amyloid fibrils polymorphism could be due to the diversity of steric zippers that amyloidogenic sequences are able to develop [186]. The majority of the eight possible structural classes of steric zipper proposed by Eisenberg and colleagues were shown in amyloid proteins like insulin, tau, amyloid-β and prion [185]. Indeed, in prion diseases (PrDs), the protein aggregates show a structural heterogeneity which is due to ability of PrP^{Sc} to self-propagate distinct 'conformational variant resulting in diseases with different

characteristics including incubation period, individual patterns of PrP^{Sc} distribution and spongiosis, and relative severity of the spongiform modifications within the CNS. These conformational variants are termed prion strains, analogously to strains of classical infectious agents[187-189]. Various prion strains can maintain permanently their properties to the detriment of the normal prion protein, and this process has been replicated in a cell-free system in vitro, suggesting that strain variation is dependent on PrP^{Sc} properties [190]. However, the local brain environment may interfere in the generation of protein strains. Different intracellular environments could affect both the initial protein misfolding process and the templated amplification process. This could lie on the affinity level between seeds and physiological monomer present in different intracellular environments as well as the strong assimilative capacity of the seed [191]. Interestingly, auxiliary substances present in the intracellular environments can both modify the intrinsic properties of the protein by forming or breaking covalent bonds such as PTMs and truncation and also influence the fibril assembly by noncovalent binding of extrinsic factors such as chemical metabolites, lipids, poly (ADP-ribose) (PAR) and metal ion [192-195]. Moreover, in pathological seeds composed of a mixture of different conformations or strains, there could be a selection and amplification of a specific conformation from the mixture, depending on the optimal adaptability to the host's biological environments [196] (Fig 1.5). This process may induce the disappearance of the old strain and the appearance of a new strain resulting thus in a phenomenon termed strain evolution [197, 198].

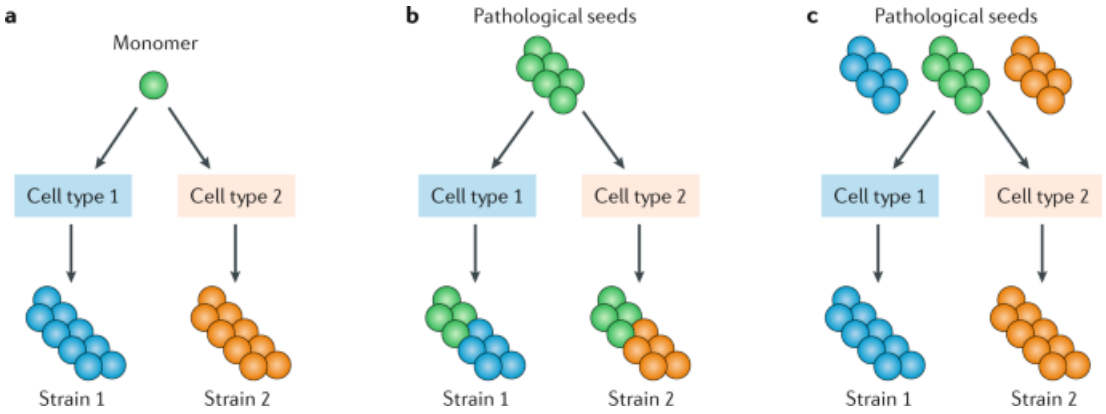

Figure 1.5 generation of different pathological protein strains. Different intracellular environments can result in different pathological protein strains and several potential mechanisms for this differentiation have been suggested. a | Different intracellular environments could affect the initial protein misfolding process. b | Different intracellular environments could affect the templated amplification process. c | If pathological seeds were a mixture of different conformations or strains, different intracellular environments could lead to the selection and amplification of a specific conformation from the mixture [196].

Similarly, to prion strains, strains like-behavior have been observed for several protein misfolding related neurodegenerative diseases. Indeed, initial in vitro generation of Aβ 40 fibrils that undergone agitation step or not resulted in different structures. Aβ 40 fibrils subject to agitation have a predominantly 'striated-ribbon' morphology, while fibrils grown without agitation have a predominantly 'twisted 'morphology. In addition, the two kinds of fibrils show different neurotoxicity in cell culture [199]. Subsequent fibrillation of Aβ using seed from two different AD patients exhibiting different neuropathology and clinical history, have led to the production of two structurally diverse Aβ forms, confirmed by Electron microscopy and solid-state NMR techniques[200]. Using strictly controlled in vitro fibrillation conditions it was possible to produce Aβ 40 and Aβ 42 providing further evidence of the existence of Aβ strains [201]. Thus, it has been proposed at least two distinct strains of Aβ in AD patient brains which are serially transmissible during serial passages in mice [202].

Furthermore, a comparative study of the topographical distribution of protein amyloid lesions showed differential clinical profiles of various disorders in tauopathies, synucleinopathies, and TDP-43 proteinopathies [203]. Indeed, at least seven different diseases have been associated with the accumulation of tau aggregates, including AD, frontotemporal dementia, progressive supranuclear palsy, corticobasal degeneration, argyrophilic grain disease, and chronic traumatic encephalopathy [204]. While PD, multiple system atrophy, and Lewy body dementia have been linked to the accumulation of alpha synuclein aggregates [205]. Analogously to prion strains causing diseases, tauopathies and synucleinopathies can be discriminated by the clinical symptoms, brain-region-specific pathology, and preference of the aggregates to accumulate in different cell types and/or by the distinct morphological and biophysical characteristics of the aggregates, their toxicity, and their seeding ability [204-206]. Kaufman, and colleagues

isolated and characterized 18 different tau strains in a cell culture model, each of which displayed different biochemical and biological properties[207]. After inoculation of transgenic mice with these strains, they found strain-specific intracellular tau aggregates in distinct cell types and brain regions, exhibiting different rates of propagation [207]. Thus, different tau species can self-propagate, resulting in distinct neuropathological presentations as found in human tauopathies and supported by another study where different tau strains were isolated from 29 patients affected by five distinct tauopathies [208]. Cryo-electron microscopy allowed the construction of atomic models of tau aggregates which are organized either as paired helical or straight filaments. Filaments are made of two identical protofilaments spanning residues 306–378 of tau, which adopt a combined cross-β –β -helix structure. Paired helical and straight filaments differ in their inter-protofilament packing, providing a model to explain how the same protein can adopt different conformational variants [206]. Indeed, Cryo-EM studies showed that at the atomic level, Tau fibrils isolated from the brains of patients afflicted by various tauopathies including AD, Pick's disease, CBD, and chronic traumatic encephalopathy (CTE) display distinct folds of Tau molecules and fibrillar assemblies [195])[206, 209-212] (Fig 1.6). Likewise, structural differences between α-syn fibrils purified from the brains of patients with MSA and DLB have been observed after cryo-EM analyses [213]. Interestingly, brain extracts from MSA patients but not from PD or DLB patients induced α-syn aggregation in mice expressing α-syn (A53T) mutation suggesting that MSA is caused by a strain of α-syn, which is different from those causing PD or DLB [214]. It has been found that Lewy bodies (LBs) in the substantia nigra showed biochemical differences from LBs in neocortical areas of patients afflicted by PD with dementia (PDD), which is a particular form of PD, [215]. Even within the same disorder of MSA, α-syn display distinct early foci of aggregation in different clinical cases of striatonigral degeneration and with olivopontocerebellar atrophy although converge with longer disease duration [216]. Thus, there could be a presence of different abnormal conformations within the same pathological condition. α-syn prominently accumulates into cytoplasmic inclusions in oligodendrocytes of the brain in MSA whereas it found majorly as neuronal inclusions in PD and DLB [27]. It has been demonstrated that α-syn in glial cytoplasmic inclusions is more potent than that in Lewy bodies in terms of

neuropathology and seeded propagation [217]. Again, this study highlighted the influence of different cellular environments on the generation and effect of α -syn strains. Analogously, inducing α -syn aggregation in vitro in the presence of distinct concentrations of salts results in either cylindrical fibrils or flat, twisted ribbons [218]. Detailed characterization of these alternative structures has made it possible to observe a big difference in terms of proteolytic resistance, secondary structure, X-ray fiber-diffraction patterns, distribution of secondary structure elements determined by solid-state NMR, cellular toxicity, in vitro seeding, and propagation in mammalian cells [218]. Further evidence indicates the existence of multiple different conformations for others misfolding protein-related neurodegenerative disorders, including SOD1[219] and Mutant HTT [220]. Overall, these data show that Different conformations of the same pathological protein can display dramatically different seeding capacities and spreading patterns, leading to the pathological and clinical diversity of neurodegenerative disease.

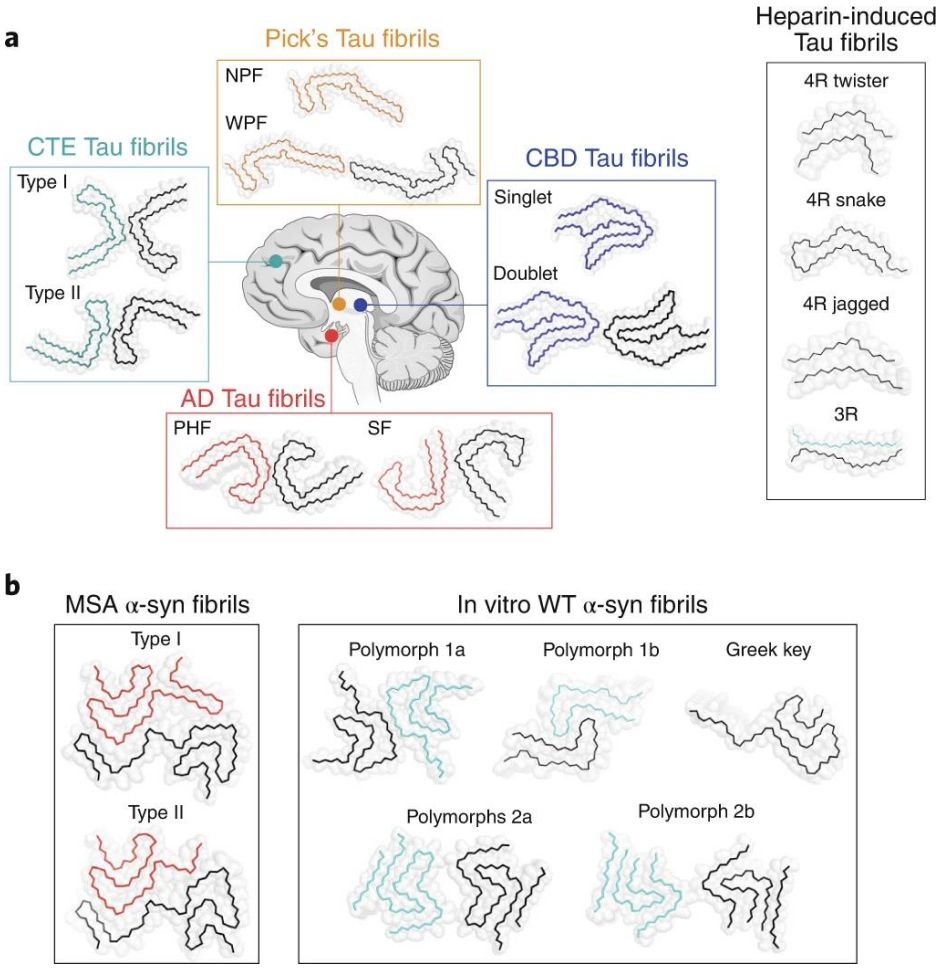

Figure 1.6 Environment-sensitive amyloid fibril formation of Tau (a) and α-syn Proteins(b)[195].

II- ALPHA-SYNUCLEINOPATHIES

The abnormal accumulation of alpha synuclein protein in distinct cellular populations of the brain is a common pathological feature of synucleinopathies. However, the variety of cell and brain structures involved as well as different clinical manifestations observed in affected patients even though with some overlapping symptoms, constitute the basis for differential diagnosis and categorization.

1.Parkinson disease

PD is the most widespread form of α-synucleinopathies with an overall prevalence of 0,3%, 1.0% in people over 60 years old and 3.0% in people over 80 years old [221]. Men are more affected than women, with a ratio of 1.5 to 1.0 respectively [222]. The rates of incidence of PD are estimated among 8 and 18 per 100 000 persons/year [222]. Thus, by the year 2030, there will be 8–9 million subjects in the world suffering from this disease [223]. As the majority of NDs, it is prevalently a sporadic disease, however with 10-15% of familial forms. The genes responsible of familial form are known as "PARK" with different number following the order of identification. Up to know, 23 PARK genes have been linked to PD with mutations showing either autosomal dominant (e.g., *SCNA*, LRRK2, and VPS32) or autosomal recessive inheritance (e.g., PRKN, PINK1, and DJ-1) [224]. In addition, exposure to some environmental toxin like 1-methyl-4phenyl-1, 2, 3, 6-tetrahydro-pyridine (MPTP), the herbicide paraquat and the pesticide rotenone have been linked to the development of PD [225, 226]. The diagnosis of PD is based on clinical manifestations including cardinal motor symptoms, like bradykinesia, rigidity, rest tremor, postural and gait impairments [227]. According to the features of motor symptoms, PD can be distinguished in the tremor-dominant PD, which is relatively absent of other motor symptoms, and the non-tremor-dominant (akinetic/rigid) PD, including phenotypes as akinetic-rigid syndrome and postural instability gait disorder. Moreover, some PD patients show a mixed or an indeterminate phenotype having several motor symptoms of comparable severity [228, 229].The tremor-dominant PD patients

often exhibit a slower rate of progression and less functional disability than the non-tremor-dominant PD [230]. Besides motor symptoms, various non-motor symptoms have been observed in PD patients. These include olfactory dysfunction, cognitive impairment, psychiatric symptoms (depression, visual hallucinations, and anxiety), insomnia, rapid eye movement (REM) sleep disorder (RBD) [231], autonomic dysfunction (constipation, orthostatic hypotension, and urinary incontinence), pain, and fatigue. Cognitive impairment includes specific cognitive domains such as visuospatial or executive. Symptoms, like impaired olfaction, constipation, depression, excessive daytime sleepiness, and RBD, appear well before the onset of the motor symptoms [232]. The non-tremor-dominant PD patients exhibit autonomic deficits early [233, 234]. The loss of pigmented dopaminergic neurons in the SNpc and the formation of a-syn-containing intraneuronal inclusions represent the main pathological hallmarks of PD. SNPc dopaminergic neuron death induces the disruption of the nigrostriatal pathway with a reduction of dopamine levels in the striatum, resulting in the occurrence of the cardinal motor symptoms of PD. However, neuronal loss has been also observed in various other brain areas such as the locus coeruleus, the nucleus basalis of Meynert, the dorsal motor nucleus of the vagus nerve, the pedunculopontine nucleus, the VTA, the raphe nuclei, and also the hypothalamus and the olfactory bulb [235]. Other neurotransmitter systems including the cholinergic, adenosinergic, glutamatergic, GABAergic, noradrenergic, serotonergic, and histaminergic also undergone degeneration [236]. This is thought responsible of some of the non-motor symptoms of PD that do not respond well to dopamine replacement therapies [237], even though the precise pathological mechanisms underlying the non-motor symptoms in PD are still relatively unclear.

α-syn-containing intraneuronal inclusions can occur either in the in neuronal somata and neurites and are named respectively LBs and LNs, or collectively known as Lewy related α-syn pathologies (LRP) [238, 239]. LB are round, eosinophilic inclusions consisting of a granular and fibrillar hyaline core with a surrounding halo (Fig 1.7). They size can range from 5 to 30 μm in diameter, and numerous LB can be found inside a single neuron [240]. According to literature, LB are subdivided in 2 types: classical brainstem and cortical LBs which are devoid of the halo, have less distinct outlines, and have usually small size. In SN, structures like cortical LBs are sometimes called “pale bodies” and are

considered LB precursors [241]. Filamentous a-synuclein is the main components of LB followed by, several proteinsn including ubiquitin, tau, parkin, heat shock proteins (HSPs), oxidized/nitrated proteins, cytoskeletal proteins (such as neurofilaments, MAPs, and tubulin), proteasomal and lysosomal elements, and others [242].

In 2003, Braak and colleagues proposed a staging scheme of PD based on the topographical location of LRP as previously described (see classification of NDs) A further revision of Braak hypothesis proposes that LRP may in fact be initiated in nasal and intestinal mucosal sites, specifically in the olfactory bulb and the enteric cell plexuses ("dual-hit hypothesis") [243].

2. Dementia with Lewy Body

DLB is the second major synucleinopathy, and the most frequent cause of degenerative dementia after Alzheimer's disease [244]. It accounts for about 5% of all dementia cases in older populations [245] with a mean age of appearance of 75 years, ranging from 50 to 80 years. there is a small male predominance and a mean disease duration of 9 years, ranging from 1 to 20 years [246]. Approximatively, 70% of cases are sporadic while 30%are familial [247] with the convincing involvement of gene like APOE, GBA and *SNCA* [248]. Of note, DLB belongs to Lewy bodies disorders which are dementia syndromes associated with Lewy bodies and are subdivided into DLB, AD, PD, and PDD, usually used to define the cognitive impairment occurring in people diagnosed with Parkinson's disease [249]. The timing of dementia relative to parkinsonism allow the clinical distinction between PDD and DLB. indeed, DLB is diagnosed when cognitive impairment precedes parkinsonism or begins within a year of parkinsonism while PDD is diagnosed when parkinsonism precedes cognitive impairment by more than 1 year [250]. The main clinical features of DLB are fluctuating cognition (periods of inattention interspersed with periods of lucidity, with deficits involving the naming of objects, verbal fluency, visuospatial abilities, and executive functions), complex visual hallucinations, parkinsonian motor features and REM sleep behavior disorder (failure to enter paralysis during REM sleep and subsequent physical acting of dreams) [251]. Additional features, such as severe autonomic dysfunction, hallucinations outside of the visual modality and

depression may also appear. The occurrence of widespread limbic and cortical Lewy bodies and Lewy neurites composed of aggregates of α-syn, as well as the loss of midbrain dopamine cells and loss of cholinergic neurons in ventral forebrain nuclei are shared neuropathological feature of DLB and PDD [252]. However, some differences have been observed. Indeed, most of DLB cases display an advanced Braak stage, with cortical involvement [26]. In contrast to PD, in DLB patients the degeneration of dopaminergic neurons in the substantia is less pronounced with a relative lack of D2 receptor upregulation in the striatum [253]. Moreover, there is a significant amyloid deposition in the striatum, hippocampus and cortex [238, 254] of several patients with co-occurrence of Aß and tau pathology at postmortem observations in some patients [255, 256].

3. Multiple system atrophy

MSA is a neurodegenerative disease that encompasses disorders such as olivopontocerebellar atrophy, Shy–Dragers syndrome, and striatonigral degeneration. The mean onset age varies from 40–60 years old with male predominance [257]. It has been estimated that there is about 3–4 cases per 100,000 person in the age group 50–99 years per year [258] with an average survival time of 6–10 years after onset [257]. MSA is essentially a sporadic disease with genes like MSA – *SNCA*, COQ2, MAPT, GBA1, LRRK2 and C9orf72 which have been identified as susceptibility genes [259]. MSA is characterized by parkinsonism, cerebellar ataxia, autonomic failure, motor weakness, and cognitive decline [260]. Additional symptoms may include autonomic failure and parkinsonism or cerebellar syndrome [261]. Based on the motor phenotypes it possible to distinguish parkinsonian (MSA-P) and cerebellar (MSA-C) forms. MSA-P seems to predominate in Europe (58%), with respect to MSA-C that dominates in Asia (84%) [262, 263]. MSA-P patients exhibit a hypokinetic-rigid parkinsonian syndrome, which tends to be more symmetrical and less responsive to Levodopa than in PD, with an irregular, higher-frequency postural tremor. In MSA-C, the most common symptom is gait ataxia with wide-based movements. Furthermore, ataxia of the limbs, cerebellar oculomotor impairments, scanning dysarthria, and intention tremor are common in MSA-

C [264]. As in PD and DLB, MSA is pathologically characterized by the presence of alpha synuclein inclusions throughout the brain. However, in MSA α-synuclein filaments accumulate prevalently in the cytoplasm and nuclei of glial cells. We distinguish glial cytoplasmic inclusions (GCIs) in oligodentroglia which is the most diffuse, nuclear inclusions (GNIs), neuronal cytoplasmic inclusions (NCIs), neuronal nuclear inclusions (NNIs) [265].

Given the unwavering presence of abnormal aggregates of alpha synuclein in LRP and GCIs **(Fig 1.7)**, the main pathological hallmarks of the above described synucleinopathies, it is well accepted that alpha synuclein may play key role in their pathogenesis even though its physiological function is not yet well defined.

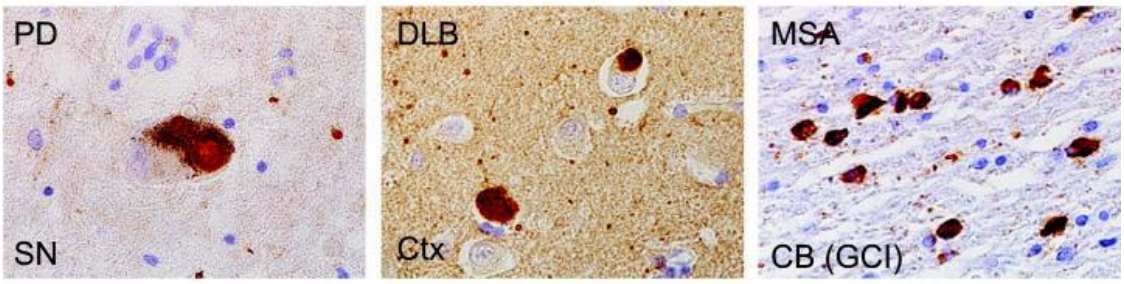

Figure 1.7 Neuropathology of α-synuclein deposits in different synucleinopathies.

α-synuclein aggregates stained by anti-α-synuclein antibody showing different aggregates morphologies and distinct affected areas in PD (SN: substantia nigra), DLB (Ctx: cortex) and MSA (CB: cerebellum; GCI: glial cytoplasmic inclusion

4. Alpha-synuclein protein: structure localization and physiological functions

α-syn, together with beta-synuclein, and gamma-synuclein belong to the evolutionary conserved synuclein family that share a highly conserved alpha-helical lipid-binding motif with other protein like apolipoproteins, 14-3-3 chaperones and several small heat-shock-proteins [266]. In humans, SNCA is localized on chromosome 4, position 4q22.1 where it is organized into 10 exons, with a size vary from 42 to 110 base pairs and length of about 117 kb. α-syn protein exist at least in 4 different alternative splicing variants for functional polypeptide synthesis [267]. The prevalent variant is a 14kda polypeptide

made of 140 amino acid residues 20 whose primary structure is characterized by three different regions **(Fig 1.8)**:

- The amino-terminal sequence going from residue 1 to 60 that contains the hexamer conserved repeats consisting of 11 residues with the consensus sequence KTKEGV which refers to highly conserved alpha-helical lipid-binding motif. It is also in this portion of the protein that were found the A30P, A53T, and E46K mutation sites related to familial PD cases.
- A central hydrophobic region of residues 61to 95, known as NAC (non-amyloid-β component) since it was firstly purified from Alzheimer's disease senile plaques of patients [268]. This domain contains two additional KTKEGV motifs and is specific to the alpha synuclein among the synuclein family [269]. The NAC domain was found to promote alpha-synuclein fibrilization, suggesting its importance for the protein aggregation [270]. Indeed, mutation of only one single amino acid within NAC can alter the aggregation properties of the protein [271].
- The carboxy-terminal sequence, from residue 96 to 140, is highly negatively charged, enriched in proline residues, and is used for interaction with metals, small molecules, proteins, and other α-syn domains [272]. In fact, the ability to interact with the NAC domain gives it a regulatory role in the aggregation and fibril formation of the protein. Moreover, it is responsible for the intrinsically disordered nature of α-syn since it lacks rigid well-defined structure [273]. Importantly, the phosphorylation site at Ser129 is localize in the C terminal region and this major post-translational modification is a main pathological hallmark in synucleinopathies [274].

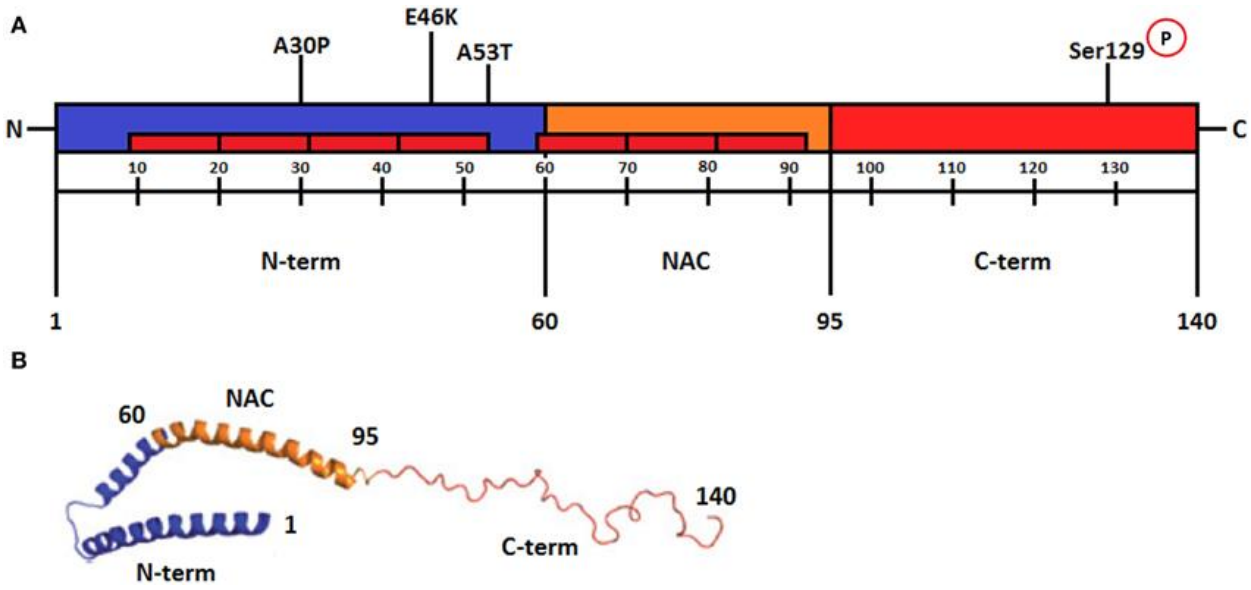

Figure 1.8 Schematic representation of α-syn regions. The amino-terminal from amino acids 1–60 is an amphipathic region responsible for α-syn-membrane interactions. It contains the hexamer conserved repeats represented by the red rectangles, and the A30P, E46K, and A53T PD linked mutations. The central region from amino acids 61-95, termed NAC (non-β amyloid component), is the most hydrophobic portion of the protein and is required for the aggregation process. The C-terminal from amino acids 96–140 is characterized by the presence of acidic residues and several negative charges. The residue serine 129 in this region is phosphorylated in Lewy bodies. (B) Schematic representation of micelle-bound α-synuclein. The N-terminal region with antiparallel α-helices is shown in blue, the NAC region is also an α-helix and is shown in orange, and the unstructured C-terminal part is shown in red. Numbers refer to amino acid residues. Modified from [275].

Numerous studies using different biochemical and biophysical methods demonstrated that α-syn purified from bacteria, red blood cells, mammalian cell lines, human and rodent brain exists predominantly in a partially unfolded monomeric state, hence it belonging to the IDP family [276, 277]. However, it has also been reported that in physiological conditions when α-syn binds to lipid vesicles or membranes, it can adopt an helically folded tetramer form of 58 kda which is resistant to aggregation [278]. In particular, the N-terminal portion of the protein acquires the α-helical conformation, extending it in helix or antiparallel helices connected by a short linker, depending on the membrane properties, while the C-terminal portion remains unstructured, as illustrated in

Fig 1.8 B [279, 280]. Moreover, Wang and colleagues have shown that recombinant α-syn, produced in bacteria and purified under nondenaturing conditions, forms stable tetramers in vitro in the absence of lipid bilayers or micelles. These oligomeric forms of a-syn are resistant to fibrillation, do not readily form pores in membranes, and are not toxic to cells [281]. Together these data suggest that that native α-syn exists in equilibrium between different conformational and/or oligomeric states and this equilibrium can be influenced in vivo by several factors that were shown to modulate α-syn structure and oligomerization in vitro such as post-translational modifications, oxidative stress, proteolysis, concentration of lipids and metal ions [282]. Thus, α-syn occurs prevalently as a partially unstructured monomer which can possibly forms a stable multimer and/or adopt different structures under specific stress-induced conditions or upon interaction with other proteins, specific ligands, lipids and/or biological membranes, probably required for it physiological functions.

α-syn owes its name to Maroteaux and colleagues who first identified it in synapses and the nucleus in the torpedo ray [283]. It is highly expressed in the nervous system including neocortex, hippocampus, substantia nigra, thalamus, and cerebellum, but it is also present in erythrocytes, platelets, and as well as in other tissues [284]. α-syn is prevalently a neuronal protein but can also be found in the neuroglial cells and represents about 1% of cytosolic protein in the brain [285]. As an IDP, alpha synuclein may serve as a hub in protein interaction networks, being central to the normal function and stability of the network. Indeed at least 69 proteins have been found as alpha synuclein interactors [286], and this makes coherent its diverse subcellular localization even though its physiological function in each subcellular compartment is not well understood. For example, in the nucleus it may interact with histones and affect histone acetylation, thereby modulating gene expression [287, 288]. Moreover, α-syn can bind DNA, induce DNA fragmentation, and modulate repair processes [289, 290]. α-syn has been found in the mitochondria where it acts in part like a physiological regulator of mitochondrial fusion. α-syn binds to curved membrane sites on the outer mitochondrial membrane (OMM), blocking the fusion stalk buildup, a necessary structure for mitochondrial fusion, thus favoring mitochondrial fission [286]. α-syn is also associated with endoplasmic reticulum (ER) and Golgi membranes [291] where it is involved in the regulation of

endoplasmic reticulum and Golgi vesicle trafficking. It was recently demonstrated that a fraction of α-syn is localized in mitochondria-associated membranes, a region mainly composed of intracellular lipid rafts, which interconnects the ER with mitochondria [292]. It is also present in the endolysosomal system [293].

Results from numerous interaction studies led to the involvement of α-syn in regulating synaptic neurotransmission, function, and plasticity [282, 285, 294, 295]. At the presynaptic terminal, asyn associates with synaptic vesicles [285], binds membranes [296] and induces membrane curvature [297]. α-syn regulates soluble NSF attachment protein receptor (SNARE) complex assembly [298] by binding the SNARE protein synaptobrevin-2/vesicle-associated membrane protein 2 (VAMP2) to promote synaptic-vesicle fusion [299]. Furthermore, α-syn was shown to help stabilize vesicles by protecting them from premature fusion with target membranes as a result of curvature stress [300]. α-syn can also modulate the late steps of exocytosis. In fact, this was confirmed by a study showing a rescue of the assembly and function of exocytic SNAREs after transgenic expression of α-syn in mice lacking cysteine string protein alpha (CSPα)[298]. Since CSPα is a presynaptic chaperone, these findings suggested that α-syn can act as a chaperone as well. Indeed, α-syn has the ability to inhibit thermally induced protein precipitation [301] and as described above share structural motif with and binds to 14-3-3 proteins, a family of molecular chaperones [302]. In addition of showing decreased levels of the SNARE protein SNAP-25 and impaired SNARE complex assembly, mice lacking CSPα display a strong neurodegeneration, suggesting a link between these events [298].

Several studies also reported an involvement of α-syn in dopamine (DA) biosynthesis and release. Indeed, in the presynaptic terminals of neurons α-syn was shown to interact physically with tyrosine hydroxylase (TH), the rate-limiting enzyme in DA synthesis, leading to the inhibition of the TH activity [303]. α-syn can increases the ratio of the less active, non-phosphorylated form of TH to the more active phosphorylated form through the activation of protein phosphatase 2A (PP2A)[304]. In addition, it has been found that α-syn can physically interact with human dopamine transporter hDAT and modulate dopamine reuptake [305, 306]. Other physiological functions have also been ascribed like an anti-apoptotic function against several insults, including oxidative stress and serum

deprivation [307-309] and involvement in cellular differentiation via ERK/MAPK pathways [310].

5. alpha synuclein: role in pathology

As reported above, α-syn is thought to play a key role in the pathogenesis of synucleinopathies where it adopts an amyloid like structure and aggregates in the patients' brains. As for the others misfolding proteins related neurodegenerative diseases the aggregation process follows the seeding nucleation model previously described. It has been found that α-syn filaments within pathological inclusions display a core which extends over about 70 amino acids, including the repeat region of a-synuclein (residues 30–110)[271, 311]. High resolution structure obtained by solid-state nuclear magnetic resonance, scanning transmission electron microscopy and X-ray diffraction, revealed that the core residues of the a-synuclein fibril were organized in parallel, in register ß-sheets with the topology of a Greek key common to amyloid structures [312].

The exact cause of α-syn aggregation is still unknow but various factors were shown to influence such process. Given the implication of SNCA mutations as cause of familial forms of PD, it has been suggested that these mutations can have an impact on the protein structure increasing the α-syn propensity to aggregation. Indeed, Ala53Thr, Ala30Pro, and Glu46Lys which are three PD-related point mutations have been shown to accelerate a-syn aggregation [313, 314], probably through changes in net charge, hydrophobicity and secondary structure propensity, leading to the destabilization of the long-range interactions in the α-syn monomer [315]. NMR spectroscopy allows to discover that the Ala30P substitution strongly attenuates the helical propensity in the N-terminal region, possibly resulting in a decreased interaction between α-syn and lipid membranes [316]. In addition, β-strand formation does not necessarily require the involvement of proline, thus the introduction of a proline residue in the N terminus, slows the incorporation of the N terminus in the fibrils resulting in an increased oligomer formation [273]. The Ala53Thr mutation was suggested to expend the region of β-sheet structure in the NAC domain leading to increased intermolecular contacts that induces an elevate tendency to form oligomers. Moreover, this mutation also stabilizes the β-sheet structure in the mature

fibril, explaining the faster rate of formation [273]. However, The Glu46Lys mutation does not disrupt long-range interactions even though a-SYN with this mutation has an increased fibrillization rate [317]. It was suggested that this increased fibrillization rate may be due the overall change in net charge [318]. Moreover, glutamate residues in the Lys-Thr-Lys-Glu-Gly-Val (KTKEGV)-type repeats (such as Glu46) may be greatly involved in the regulation of α-syn fibrillization [313]. Increased level of α-syn concentration because of triplication or duplication of SNCA increase the probability of oligomer and fibril formation[273].

Post-translational modifications like phosphorylation (Ser87, Tyr125, and Ser129), ubiquitination, oxidative modifications, have been suggested to have an effect on aggregation. Among them the most recurrent is the phosphorylation at residue Ser129 whom site is positioned within the C-terminal region of α-syn and G-protein-coupled receptor kinase, casein kinases 1 and 2 were suggested as the responsible kinases [319] . Only 4% of native α-syn is phosphorylated under physiological conditions, while in LRP this percentage increases to approximately 90%, highlighting its importance as pathogenic event [320, 321]. Subsequent studies confirmed the promotor effect of the phosphorylation at residue Ser129 in α-syn aggregation [322, 323]. Nevertheless, the phosphorylation of the Ser87 induces an expansion of α-syn structure, increasing its conformational flexibility, and blocking its aggregation in vitro. Similarly, the phosphorylation at Thr125 attenuates the conversion of α-syn to toxic oligomers [324]. Therefore, based on the sites involved, phosphorylation may increase or decrease the fibrilization potential of α-syn.

Accordingly, the ubiquitination process, in particular the position of the modified residues was also suggested to influence α-syn aggregation. Ubiquitin is a small protein that can be linked to lysine (Lys) residues of target proteins that must be proteolytically degraded by proteasome complex. There are 15 lysine residues in α-syn structure and only Lys6, Lys10, and Lys12 were shown to be involved in vivo [325]. It has been found that the modification of Lys6 induced a slower aggregation respect to the un-ubiquitinated protein [326], while the multiple lysine modification induced the formation of an aggregated toxic form [325].

In COS-7 cells, an unidentified Lys residue located at the N-terminal part of α-syn protein was shown to be modified by SUMO1 which is a small ubiquitin-like modifier promoting α-syn aggregation [327].

Oxidative modifications including tyrosine (Tyr) and methionine (Met) oxidation can influence α-syn aggregation. Indeed, tyrosine cross-linking following exposure to oxidative agents promotes the α-syn oligomerization and inhibits its transition to fibrils[328]. The methionine-oxidized protein has been shown disrupts "end-to-end association" of α-syn necessary for fibril growth and thus guides its aggregation toward less structured, non-toxic oligomers [329].

Also, nitration is thought to influence α-syn aggregation. Beside the fact that nitrated α-syn was found in LBs [330], nitrated α-syn was found to accelerate fibril formation of unmodified α-syn [331].

In addition, environmental factors like metal ions, pesticides were shown to accelerate the fibrillation rate of α-syn [332].

6. Mechanisms of a-synuclein neurotoxicity

Even though some issues remain to be clarified regarding to the precise mechanisms through which α-syn aggregation induce neurodegeneration, various toxic mechanisms have been linked to the α-syn aggregation process, oligomeric and fibrillar products.

Given the principal localization and function of α-syn at the synapse, the aggregation process might lead to a loss of function resulting in synapse dysfunction. Indeed, it has been found that α-syn large oligomers bind to synaptobrevin-2 and disrupt SNARE complex formation by obstruction of vesicle docking [333]. In addition, the binding of α-syn aggregates with vesicles induces clusters formation that constrains physiological vesicles trafficking [334]. The formation of pores on the vesicles surface may be another consequence of the interaction between oligomeric α-syn and vesicle which leads to neurotransmitter leakage [335, 336]. Overexpression of α-syn in nigral dopamine neurons resulted in reduction of dopamine reuptake and defective DAT function, thus a disruption of dopamine turnover [337].

Mitochondria has been also suggested to be a cellular target for α-sync neurotoxicity. Indeed, overexpression of both α-syn A53T or WT induced an increased release of cytochrome c from the mitochondria and its accumulation in the cytosol was also associated with increased caspase-3 and-9 activities over time [338] which could further lead to apoptosis. In addition, increased level of α-syn has been linked with higher concentrations of mitochondrial Ca^{2+}, that triggers apoptotic pathways [339]. Similarly, soluble, prefibrillar α-syn oligomers, were shown to decrease the retention time of exogenously added $Ca^{2+,}$ promoted Ca^{2+}-induced mitochondrial swelling and depolarization, and accelerated cytochrome c release. Interestingly, these mitotoxic effects of α-syn were mitochondrial complex I dependent [340]. Indeed, it has been found that α-syn oligomers can also inhibit the import of proteins, including some subunits of complex I, into the mitochondria by binding to the translocase of the outer membrane (TOM20) and inhibiting its interaction with the co-receptor TOM22 [341]. Cells overexpressing α-syn, shown a high level of mitochondrial ROS that could impair mitochondria functions by decreasing the mitochondrial membrane potential [342]. Intriguingly, the impaired mitochondria ROS production can induce α-syn expression, oligomerization, and aggregation via oxidative damage [330, 343]. ROS produced during mitochondrial dysfunction, such as in complex I inhibition may increases the vulnerability of mutations in mitochondria DNA (mtDNA) given the proximity between the mitochondrial electron transport chain (ETC) and mtDNA [344] and especially considering mtDNA is not protected by histone proteins as seen in nuclear DNA [345]. Coherently, α-syn overexpression was linked to mtDNA damage [346] and mitophagy [347]. Alternatively, α-syn toxicity may indirectly induces mitochondrial dysfunction decreasing levels of the mitochondrial biogenesis factor PGC-1α as shown in cell models that express oligomeric α-synuclein, mice that express A30P α-synuclein [348] and the brains of patients with PD [349].

Considering the important role of the ER in protein folding, trafficking to the Golgi, calcium buffering, overexpression, or accumulation of mutant α-syn within the ER, may interfere with protein folding and induces ER stress, which may contribute to neurodegeneration via activation of cell death cascade [291]. In fact, elevated ROS levels owing to ER stress and mitochondrial dysfunction contribute to A53T α-syn-induced cell

death [338]. Toxic α-syn oligomers were found within the ER/microsome compartment, after examination of postmortem tissues of human PD patients and mouse cases of α-synucleinopathy, supporting a direct pathological link between α-syn oligomers and ER stress in vivo [291]. Moreover, accumulation of α-syn in the ER induces calcium leakage into the cytosol which in turn promote further α-syn aggregation [350, 351]. Aggregated forms of α-syn induce the impairment of the ubiquitin-proteasome system which leads to ER stress and triggers the unfolded protein response [352, 353].

α-syn accumulation can induce defects in ER-Golgi trafficking, by both sequestering Rab1, a central regulator of membrane trafficking and activating transcription factor 6 (ATF6) which prevents the vesicular transport to the Golgi [354]. Recently it has been found that α-syn can directly affect the Golgi apparatus, by inducing it fragmentation, as part of apoptotic cascade [355].

Autophagy is a cellular process which allows the degradation of damaged organelles, invading microorganisms, and aggregated proteins [356]. Overexpression of α-syn in SKNSH cells was shown to disturb autophagy by reducing autophagosome synthesis trough sequestration of Rab1 [357]. Moreover, A53T and A30P α-syn have a stronger binding affinity for the lysosomal receptor LAMP2A respect to WT α-syn, suggesting a defections degradation of mutant forms of α-syn by protein clearance mechanisms, which results in increased α-syn burden of chaperone-mediated autophagy (CMA) and inhibits the loading and clearance of other cargo [358]. CMA can be also blocked by dopamine-modified α-synuclein, which might contribute to selective dopaminergic vulnerability in PD [359]. α-syn preformed fibrils (PFFs), were shown to induce defective lysosomal fusion and autophagic cargo accumulation [360], when incubated with neurons even though autophagosomes formed normally. It has been suggested that these defects might be due to an impaired autophagosome axonal transport [361]. Indeed, α-syn may partially disrupt axonal transport by interacting with tau protein that stabilizes and promotes microtubule assembly [362] or disrupts actin turnover and actin waves along axons, owing to cofilin inactivation [363]. Given the link between efficient autophagic degradation and lysosomal enzymatic activity, α-syn accumulation may potentially affect the correct lysosomal activity. In fact, in iPSCs from PD, it has been found that overexpression of α-syn reduced the enzymatic activity of multiple lysosomal

enzymes, like GCase, which is fundamental for the correct functioning of the auto-phagolysosom [364, 365].

Importantly, the presence of α-syn in MAMs [292], structures that mediate several key processes such as Ca^{2+} signaling, mitochondrial and ER stress, macroautophagy, and lipid synthesis may explain how α-syn accumulation may lead to cellular pathologies [366].

Of note, the diversity of pathway that are involved in α-syn neurotoxicity may be explained by the fact that distinct pathways might be affected in different synucleinopathies at different time points of disease progression. In addition, these differences might be intensified by differences in α-syn strain characteristics, specific cell types affected and diverse protein interactions accordingly to it prion-like behavior.

7. Prion-like spreading of α-syn: insight from cells and animal models of synucleinopathies.

Based on the hypothesis that α-syn has a key role in the pathogenesis of the synucleinopathies, a number of paradigms have been generated over the last two decades entailing different methodologies, such as duplication, triplication or genetic mutations in the α-syn gene (A53T, A30P, E46K, G51D, etc.), all linked to autosomal dominant PD, leading to the development of multiple transgenic PD models [367-370]. These models have the advantages to express α-syn at moderate, near-physiological or supra-physiological levels for long periods as it occurs in the disease, allowing the study of disease-relevant pathways and the assessment of therapeutic interventions for familial forms of PD [371, 372]. However, transgenic PD models do not appear to recapitulate other pathological hallmarks of the disease, including the robust nigrostriatal degeneration and the consistent motor deficits [373, 374]. For some decades, neurotoxic models have been used, based on the intracerebral injection of the hydroxylated dopamine analogue 6-hydroxydopamine (6-OHDA) in rodents [375] or MPTP in non-human primates [376], both leading to a rapid nigrostriatal degeneration associated to robust, well characterized motor deficits [377]. However, none of these models appears to display α-syn and LBs/LNs pathology [371, 378]. Therefore, toxin models are preferred for the assessment of symptomatic therapies or the study of sporadic forms of

PD. In order to model both hallmarks, i.e., the nigrostriatal degeneration, α-syn and LBs/LNs pathology, viral vector-based models of PD have also been generated [379]. When viral vector-mediated overexpression of WT or mutant human α-syn is targeted to the nigrostriatal system of naïve mice or rats, this induces a robust degeneration of nigrostriatal system with aggregation of the pathological α-syn forms [380, 381]. However, in these models the time course of the pathology is often relatively short (1-2 months) and the α-syn aggregation is limited to nigrostriatal circuits while in PD subjects, the α-syn pathology seems to be time-dependent and widespread through the brain [22]. Moreover, the viral vector-based models of PD require a supra-physiological level of α-syn overexpression to produce a robust PD phenotype, which is in contrast with the findings in the human condition [382]. A recent model was generated based on the prion-like spreading of α-syn. Indeed, the Braak staging of α-syn pathology progression first suggested a prion like spreading between neurons, but molecular evidence was only provided by the discovery of α-syn pathology in grafted neurons in PD patients. The similarity in spreading with prion diseases was confirmed by the observation that α-syn inclusions in these neurons were positively stained for thioflavin-S, ubiquitin and were proteinase k resistant [383, 384] being also phosphorylated at serine129 [274] Moreover, the affected transplants showed reduced levels of dopamine transporter and tyrosine hydroxylase suggesting a spreading of PD pathology from host to graft neurons.

It has been also found that MSA or PD patient-derived brain homogenates could induce pathological α-syn deposition when injected in recipient cells, or in the brain of mice and monkeys [214, 385] confirming the prion like mechanism. Accordingly, the α-syn pre-formed fibrils (α-syn PFFs) were developed through the conversion of recombinant monomeric α-syn protein to a pathologic fibrillar form. Several studies shown that under certain conditions like incubation at 37°C, buffer, pH, and shaking conditions, the monomeric α-syn converts into β-sheet rich fibrils similar to those found in synucleinopathies [386, 387]. The resulting assemblies can either be added to the culture media or microinjected into the brain [388-391]. Indeed, in previous studies α-syn PFFs have been observed to become detergent-insoluble, able to trigger p-Ser129 α-syn pathology, synaptic dysfunction, perturbations in cell excitability, and induce cell death in both cell lines overexpressing α-syn as well as primary neuronal cultures from WT

mice [392, 393]. Interestingly it has been proven that α-syn PFFs were not able to trigger LB like aggregates and related cellular pathological events in neurons non expressing the α-syn protein endogenously [393]. Moreover, Sacino and colleagues after performing mixed neuronal-glial cultures from P0 C3HBL/6 mice showed that WT and mutant recombinant α-syn fibrils were able to recruit endogenous α-syn into morphologically distinct inclusions in neurons, providing a further proof of the prion-like self-templating mechanism of α-syn pathology [394]. The same authors also provide evidence that α-syn inclusion pathology can be passaged in primary astrocyte cultures. Similarly, to other reported studies, the aggregates formed were partially ubiquitinated, phosphorylated (p-Ser129) and stained by ThS dye. This study also pointed out the existence of α-syn strains, that replicated in morphologically distinct inclusions. Furthers studies generated α-syn PFFs strains. In fact, using different salts concentrations Bousset and coworkers developed two strains exhibiting different structures, levels of toxicity, in vitro and in vivo seeding and propagation properties [218]. Other strains were generated in the presence or absence of lipopolysaccharide (LPS). These strains showed distinct molecular features and degradation/internalization kinetics by neurons and microglia [395], thus pointing out the involvement of environmental factors in the generations of α-syn aggregates. Moreover, they confirmed previous suggestions according to which different cell types in the brain, such as oligodendrocytes, astrocytes, and microglia, can uptake α-syn assemblies [396, 397]. Therefore, the spreading of α-syn aggregates can occur not only between neurons, through several mechanisms. Indeed, as previously described above, α-syn aggregates shared several mechanisms of transfer between cells with others misfolded proteins. An alternative pathway is the misfolding-associated protein secretion pathway (MAPS), that involves the recruitment of α-syn to the ER-associated deubiquitylase USP19, which is later encapsulated into late endosomes and secreted to the extracellular space[398]. It has been also found that the uptake of pathological forms of α-syn can be mediated by receptors, such as lymphocyte activation gene 3 (LAG3) [399], or heparan sulfate proteoglycans [400]. In addition, membrane proteins like the α3 subunit of the Na+/K+-ATPase (Shrivastava et al., 2015), the Fc gamma receptor IIb [401], or neurexin 1α [399, 402] are known to interact with different

of α-syn species at the cell surface. Interestingly recent studies discovered the cellular prion protein as potential sensor of α-syn aggregates [403, 404].

When switching to the in vivo model, α-syn PPFs showed a better representation of synucleinopathies respect to the previous models. Indeed, injections of α-syn pre-formed fibrils into the rodent Striatum, Somatosensory Cortex, EC, Olfactory Bulb, SNpc, or muscle have been shown to produce inclusions that closely resemble those found in PD and DLB, not only in the proximity of the injected sites but also in distally located, and anatomically related, brain areas, suggesting a widespread propagation of α-syn pathology [388, 405]. Intramuscular injection induced spinal motor neuron degeneration and the loss of neuromuscular junctions [406], suggesting that α-syn PFFs can act also through retrograde transport from the injection site [407]. Intravenous injection in non-Tg rats revealed the α-syn deposits in the CNS after 4 months (in cortical neurons, spinal cord), indicating that the peripheral injection leads to the crossing of the blood-brain barrier (BBB)[154]. Interestingly, accordingly to the gut-brain hypothesis of α-syn propagation Kim and colleagues showed that gut injection of α-syn PPFs converts endogenous α-syn to a pathologic species that spread to the brain resulting in features of Parkinson's disease. However, vagotomy and α-syn deficiency prevent the neuropathology and neurobehavioral deficits induced by transmitted pathological α-synuclein [408]. This study provides further proof of the prion like gut-brain spreading of α-syn pathology, validating the α-syn PPFs model.

In addition, α-syn PPFs model exhibited altered behavior along with neuropathological changes. Indeed, injections into the rodent Striatum or Olfactory Bulb have been shown to induce a progressive loss of dopaminergic neurons in the SN with a further appearance of motor and/or olfactory impairments akin those seen in the human condition [388, 405, 409-413].

By contrast, it seems like deficits and abnormalities in learning and memory behavior are spared in the α-syn PFF models up to 6 months after injection. This could be due to the injection site (such as the striatum, olfactory bulb, and peritoneum) and/or the duration of pathological spreading [414]. Therefore, further investigations are required.

8. Hippocampal α-syn pathology

The hippocampus is a part of brain belonging to the limbic system and encompasses several structures, including the dentate gyrus, the CA1-CA3 layers, and the subiculum. The entorhinal cortex (EC), located in the parahippocampal gyrus, is considered as part to of the hippocampal region because it serves as the main ‘‘interface’’ between the hippocampus and other parts of the brain [254]. The hippocampus is known to play important roles in the consolidation of new memory, emotional responses, navigation, and spatial orientation which are frequently impaired in synucleinopathies [254]. Indeed, PD is clinically characterized not only by motor deficits but also by cognitive disturbances affecting both executive functions and memory [415] that may lead to overt dementia in 30 to 40% of the patients as the disease progresses [13, 416]. In addition, memory impairment is often a prominent hallmark of DLB which shares numerous features with AD and PDD [417-419]. While brainstem LBs are thought to contribute to motor symptoms, the neural substrate for cognitive symptoms in synucleinopathies remains a matter of debate. Cykowski and colleagues shown that the occurrence of globular NCIs in the neocortex was associated with cognitive impairment [420]. In contrast, other authors found that 33 out of 102 (i.e., about 33%) autopsy-proven MSA patients developed some degree of cognitive impairment and had a greater burden of NCIs in the dentate gyrus rather than the neocortex, compared to those without cognitive impairment[421].

Consistent with Braak hypothesis which suggests a caudal to rostral spread of LB/LN pathology from the brainstem to cerebral cortex [22], several studies have reported that cortical or limbic LBs/LNs are the best correlate of dementia in PD [422-426]. However, other studies pointed out no correlations between cognitive dysfunction and the distribution of LBs in the brain [427-429]. In a previous study, the deficits in reference memory observed following neurotoxic ablation of dopaminergic neurons in the Ventral Tegmental Area (VTA) were seen to affect also working memory when cholinergic neurons in the Medial Septum/vertical limb of the Diagonal Band of Broca (MS/vDBB) were targeted as well, suggesting that both neuron systems might be critical for the regulation of specific aspects of memory function [430]. Moreover, it has been

demonstrated that similar behavioral deficits could be obtained independently of dopaminergic and cholinergic cell loss following targeted overexpression of human WT α-syn in these regions in rats using recombinant adeno-associated viral vector, suggesting that a severe α-syn pathology in target regions such as the hippocampus may induce substantial effect on behavior [431]. Indeed, like in DLB patients, some genetic mouse models overexpressing α-syn display predominant cortical and hippocampal pathology with associated deficits in hippocampal function as impairment of contextual fear memory and long-term spatial memory in the Morris water maze, as well as deficit in amygdala functions like cued fear memory, at middle or old age (8-9 months at the earliest) [432-434]. Interestingly, the notion of a possible involvement of hippocampal LB pathology in cognitive impairments is further supported by a recent study in patients with autopsy confirmed DLB where the degree of post-mortem Lewy pathology in hippocampal CA1 and EC was seen to correlate with their impaired cognitive performance while alive [435]. Similarly, Miki and coworkers found that neuronal cytoplasmic inclusion burden in the hippocampus and parahippocampus was linked to the occurrence of memory impairment in multiple system atrophy [436]. Surprisingly, however, no study to date has addressed the anatomical, molecular and functional effects of α-syn PFFs following injection in the hippocampus, a region known to be crucial for learning and memory.

CHAPTER II

AIM OF THE STUDY

Cognitive deficits represent common significant non-motor manifestations of synucleinopathies including Parkinson's disease, dementia with Lewy body and multiple system atrophy. Besides being social and economic burden for community, such deficits are firstly known to deteriorate daily living activities leading to reduced independence, quality of life, and survival of affected patients. The anatomical and neuronal substrates underlying cognitive impairment are still poorly understood despite the multitude of studies already carried out. Considering the previously described results and limitations, the present study sought to investigate the progressive pathologic alterations and spreading of synthetic a-syn fibrils bilaterally injected into the hippocampus of adult rats, up to the onset of memory impairments.

CHAPTER III

MATERIALS AND METHODS

1.Expression and purification of recombinant mouse α-syn

α-syn was prepared as described previously [437]. Briefly, recombinant α-syn protein was purified from Escherichia coli BL21 (DE3) cells expressing mouse α-syn construct from the pET11a expression vector. E. coli cells were grown in minimal medium at 37°C in the presence of ampicillin (100 g/ml) until OD600 of ≈0.6, followed by induction with 0.6 mM IPTG for 5 h. The protein was extracted from periplasm by osmotic shock, followed by boiling for 20 min and ammonium sulfate precipitation. The protein was next purified by anion exchange chromatography (HiTrap Q FF column, GE Healthcare), and fractions were analyzed by SDS-PAGE. Finally, the protein was dialyzed against water, lyophilized, and stored at -80°C.

2. Fibrillation of mouse α-syn

Prior to fibrillation, the protein was filtered (0.22 µm syringe filter) and the concentration was determined by absorbance measured at 280 nm then the fibrillation was performed as described previously [403]. Briefly, purified mouse α-syn (1.5 mg/ml) was incubated in the presence of 100 mM NaCl, 20 mM Tris-HCl pH 7.4. Reactions were performed in a black 96-well plate with a clear bottom (Perkin Elmer), in the presence of one 3-mm glass bead (Sigma) in a final reaction volume of 200 µl. Plates were sealed and incubated in BMG FLUOstar Omega plate reader at 37°C with cycles of 50 s of shaking (400 rpm, double-orbital) and 10 s of rest. After fibrillation, the reaction mixtures were ultracentrifuged for 1h at 100 000g (Optima Max-XP, Beckman), sonicated for 5 min (Branson 2510) and resuspended in sterile phosphate-buffered saline (PBS), aliquoted and stored at -80 °C until use. The resulting α-syn fibril assemblies were then structurally characterized by atomic force microscopy (AFM) as previously described [403].

3. Animals and experimental groups

Thirty-six young adult female Sprague-Dawley rats (provided by the animal facility at the University of Trieste) weighing 220-250 g at the time of surgery were housed in high efficiency, particulate air-filtered, double-decker cage units (Tecniplast, Italy), and maintained under standard conditions of temperature, light and humidity, with ad libitum access to food and water. The animals were randomly assigned to groups receiving bilateral intrahippocampal injections of recombinant mouse α-syn PFFs (n=18) or phosphate-buffered saline (PBS) alone (sham-injected, n = 10) whereas the remaining animals (intact, n = 8) were not injected and served as unoperated controls. Subgroups of randomly selected animals (5 α-syn-treated, 3 sham-injected and 2 intact rats) were formed to be sacrificed at about 7- and 9-months post-surgery, whereas the remaining subjects (8 α-syn-treated, 4 sham-injected and 4 intact rats) were allowed to survive up to 12 months post-injection. Behavioral analyses were begun at about 3 months post-injection and consisted in the sequential administration of tests specifically designed to evaluate sensory-motor, as well as spatial reference and working memory abilities. Upon completion of the last testing session, at each of the predetermined time-points, the animals were sacrificed, and the brains processed for quantitative immunohistochemistry or western blot analyses **(Fig 3.1).** All the experimental procedures were carried out following the Italian Guidelines for Animal Care (D.L. 116/92 and 26/2014) which are in compliance with the European Communities Council Directives (2010/63/EU) and were approved by the Ethical Committee at the University of Trieste.

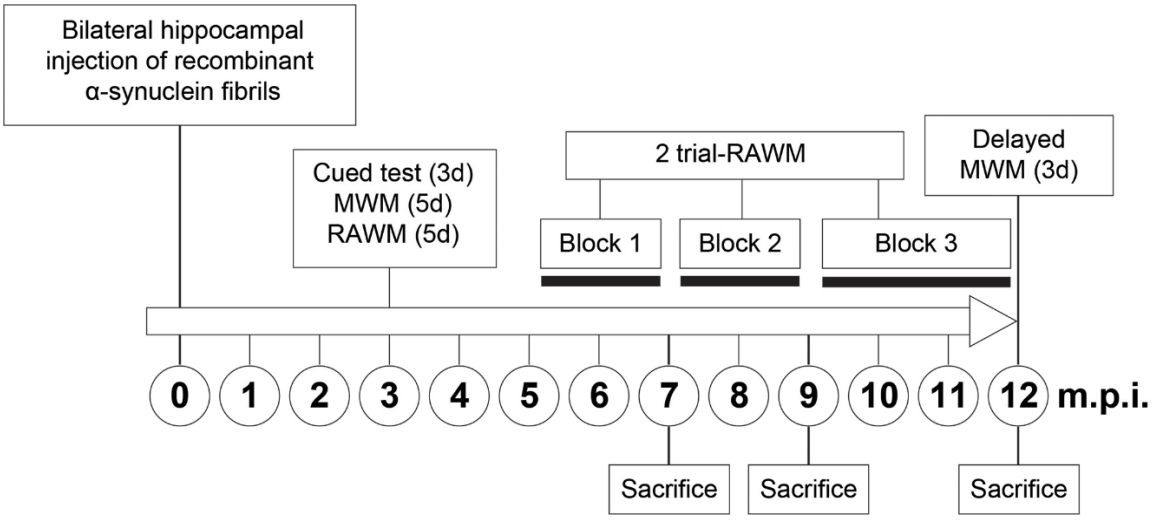

Figure 3.1 Experimental time-line diagram illustrating the temporal sequence of surgery, behavioral tests, killings, and the intervals between them.

4. Surgical procedures

Stereotaxic injections of recombinant, freshly sonicated mouse α-syn PFFs bilaterally into the hippocampus were performed on rats under deep anesthesia (sodium pentobarbital, 40 mg/kg, i.p.). Briefly, 7.5 µg of the protein was injected using a 10 µl Hamilton microsyringe (Hamilton, Bonaduz, Switzerland), in a volume of 5 µL sterile PBS per side at the following stereotaxic coordinates according to Paxinos and Watson [438] : AP = - 3.6; ML = ± 1.8; DV = - 3.6 (in mm, relative to bregma and outer skull surface). The dose and volume were chosen based on the results of pilot experiments. Each infusion was carried out over 5 min, waiting for additional 2 min before withdrawal, in order to prevent backflow and reduce tissue damage. For sham treatment, sterile PBS was injected using the same coordinates, volume and speed.

5. Behavioral tests

Starting from about 3 months post-injection, the animals underwent a battery of behavioral tests (normally administered between 9.00 am and 3.00 pm) conducted at different time-points, in order to evaluate possible effects of the treatments upon sensory-

motor and cognitive functions and their time course (Fig 3.1). All the behavioral paradigms were based on modified versions of the water maze task originally developed by Morris [439] for the assessment of spatial learning and memory in rodents. The test apparatus consisted of a circular pool, 140 cm in diameter and 50 cm deep, filled with room temperature water to a depth of 35 cm and located in a room with several external cues that could be used for orientation. Four equally spaced points (conventionally indicated as North, South, East, and West) served as start locations, also dividing the tank into four quadrants. A circular platform (10 cm in diameter) was fixed to the bottom of the pool with it top 2 cm below (and thus invisible from) the water surface. In the middle of each quadrant, a circular area of about 20 cm in diameter (termed annulus) indicated the site where the escape platform could have been, if placed in that quadrant. For each animal, the latency to find the hidden platform, the distance swum, and the swim speed were recorded by a computer-based video tracking system.

Three different paradigms, designed to evaluate the sensory motor, as well as reference and working memory abilities [440, 441], were implemented.

6. Cued test

All animals first received a free 60-second swim to become familiar with the swimming pool, followed by a 3-day cued learning session to exclude the occurrence of noncognitive (e.g. visual) deficits, induced by the treatment, that may interfere with the correct execution of the test. During the cued task, the position of the escape platform was made visible by a 10x15 cm striped flag and randomly changed on each of 4 daily trials.

7. Morris water maze test

Three days after conclusion of the cued test, the animals were subjected to the Morris water maze test for the assessment of reference memory. The animals were given four trials per day over five consecutive days with a 30 s intertrial time. On each trial, the animal was released into the pool from one of the starting points and then given 60

seconds to locate the platform (constantly kept in the North-East, NE, quadrant) and climb onto it. If the submerged platform was not found, the rat was gently guided by the experimenter and left on it for about 30 s, prior to be placed in the next predetermined starting point, whose sequence was defined randomly, and it was changed every day. On the fifth day of testing, after the fourth trial, the platform was removed and a spatial probe trial commenced, during which the animals were allowed to swim freely for 60 s. In this test, generally used to evaluate the efficiency of the previous learning, the distance swum as well as the collisions with the annuli in each of the four quadrants, were recorded. In order to check for possible delayed long-term effects of the α-syn treatment upon reference memory, a separate 3-days Morris water maze test, with a spatial probe trial, was administered to the animals just before sacrifice, at about 12 months post-injection.

8. Radial Arm Water Maze Test

Spatial working memory was tested using a radial arm water maze (RAWM) apparatus consisting in 6 swim alleys (50 cm length x 20 cm wide, numbered 1 to 6) radiating out of an open central area in the same pool. The submerged escape platform was placed at the end of an arm (referred to as the goal arm) and its position was changed every day over five consecutive days. In each of the 5 daily trials, the animals were released from a different starting position and given up to 60 secs to locate the hidden platform with a 30 s intertrial time. Entering an incorrect arm (i.e. an arm that did not contain the platform or an already visited arm) was counted as an entry error. For each trial, the latency to find the platform and the number of arm selection errors prior to locating the goal arm were recorded. The task design entails that the animals locate the platform by chance on the first trial each day (and thus no group difference is expected), whereas in the second and subsequent trials the acquired information on the novel platform location for that day would determine substantial improvements in performance. Therefore, differences in latency or error scores between trials 1 and 2 across days, both in absolute terms and as percentage of trial 1 (savings) provided measures of working memory performance.

9. Two-trial radial arm water maze test

In the original 5-trials-a-day paradigm, the RAWM testing is conducted over 5 consecutive days, allowing animals to get used to the task contingencies and to exclude all the unspecific factors that may affect performance. In this case, the RAWM standard paradigm was modified by cutting the general duration of the test from 5 to 2 days, as the animals were already well habituated to the environment and have learned the rules of the task. In addition, the number of trials administered every day was reduced from 5 to 2 as it was noticed previously that the main improvement in the RAWM performance mainly occurs between the first and second trial. Thus, from 5 months post-injection and onwards, two 2-trial RAWM tests were administered over two consecutive days each week, organized as two adjacent blocks of 6 weekly sessions each. Starting from approximately the 9th month post injection, the animals received the same two 2-trial RAWM testing sessions, but every second week, until significant group differences in the savings for both latency and errors were detected over three consecutive testing sessions. Subsequently, the delayed 3-days Morris water maze test was administered, as mentioned above (see also **Fig3.1**).

10- Postmortem procedures

Upon conclusion of behavioral tests, at about 7- and 9-months post-injection, the animals under terminal anesthesia (chloral hydrate 350 mg/kg i.p.) were perfused through the ascending aorta with room temperature saline, followed by ice-cold phosphate-buffered 4% paraformaldehyde (pH 7.4). The brains were rapidly removed, kept in the same fixative for 2 hours and then transferred in a phosphate-buffered 20% sucrose solution at 4°C until they had sunk. Coronal sections at 40 µm thickness were cut using a freezing microtome (Leitz Welzlar) from the prefrontal cortex level through the basal forebrain to the level of the caudal hippocampus and collected into 6 series. The sections were then stored at –20 °C in a phosphate-buffered antifreeze solution containing 30% glycerol and 30% ethylene glycol, pending immunohistochemical analysis.

Animals allowed to survive up to 12 months post-injection, under terminal anaesthesia as above, were perfused through the ascending aorta with room temperature saline. After rapid removal, and using a counterbalanced left–right dissection schedule, the whole hippocampus, the prefrontal, fronto-parietal and entorhinal cortices from one hemisphere were dissected free onto a chilled glass plate, immediately frozen in crushed dry ice and kept at –80 °C for Western blot assay (see below). The remaining portions of the brain, which comprised the cortical and hippocampal regions from the opposite hemisphere, both striata and the entire basal forebrain were fixed by 24 h immersion in ice-cold phosphate-buffered 4% paraformaldehyde (pH 7.4), soaked in phosphate-buffered 20% sucrose and then cut as above.

11. Immunohistochemistry

For the detection of PK resistant α-syn aggregates, one series of free-floating coronal sections were first quenched in 3% H2O2 and 10% methanol for 10 minutes to eliminate endogenous peroxidase activity, and then treated 30 min with 5μg/ml of PK. After blocking unspecific binding sites with 5% normal goat serum (NGS, Immunological Sciences), and 0.3% Triton X-100 in phosphate-buffered saline (KPBS, pH 7.4) for 2 h, the sections were incubated overnight with a rabbit anti-α-syn primary antibody (C20-R, Santa Cruz, 1:500), 2% NGS and 0.3% Triton X-100 in KPBS. Subsequently the sections were incubated with a biotinylated secondary antibody (goat anti-rabbit 1:300, Vector), 2% NGS and 0.3% Triton X-100 in KPBS for 1 hour. After this step, the sections were incubated with avidin biotin peroxidase complex (Vectastain ABC alite kit, Vector) for one hour and then reacted with 0,025% diaminobenzidine and 0.01% H2O2 in KPBS for 3-5 minutes. The sections were mounted on gelatin-coated slides, dehydrated through steps in ascending alcohol concentrations, clarified in xylene and coverslipped for subsequent microscopical analyses. In order to ensure consistency during morphometric analyses (see below), tissue processing and staining were carried out under identical conditions, using all relevant sections at a time. Control tissue specimens, not exposed to the primary antibody, were also used to check for nonspecific labelling. All steps were performed at room temperature.

For double immunofluorescence, free-floating sections were incubated overnight at room temperature with a rabbit anti-phospho-α-syn (Ser129) (D1R1R) primary antibody (Cell Signaling, 1:1000) and a monoclonal mouse anti-GFAP antibody (SIGMA, 1:400). The sections were then incubated with an Alexa 488-conjugated goat anti-rabbit secondary antibody (Life Technologies, 1:200) and then with an Alexa 594-conjugated goat anti-mouse (Life Technologies, 1:200) for 2 hours in the dark. The 4′,6-diamidino-2-phenylindole (DAPI, Sigma 1:200) compound was used for nuclear staining. Slides were coverslipped with Fluoromount™ Aqueous Mounting Medium (Sigma) and images were acquired using a Leica confocal microscope (Leica TCS SP2, Wetzlar, Germany).

12. Western blotting

The cortices and the hippocampi dissected for the measurement of non-phosphorylated, Ser129-phosphorylated α-syn and PrP^c expression levels, were homogenized using a manual dounce homogenizer in a RIPA (radioimmunoprecipitation assay) buffer containing 150 mM NaCl, 0.1% Triton X-100, 0.5% sodium deoxycholate, 0.1% SDS (sodium dodecyl sulphate), 50 mM Tris-HCl (pH 8.0), 1× phosSTOP (Roche Diagnostic) and 1× protease inhibitor cocktail (Roche Diagnostic). The homogenates were centrifuged at 10000 rpm for 10 min at 4 °C and the supernatants collected and stored in aliquots at -80 °C until use. Total protein content of brain homogenates was measured using bicinchoninic acid protein (BCA) quantification kit (Pierce) and 25 μg/ml of brain homogenates were resuspended in Laemmli loading buffer, boiled for 5 min at 100 °C for denaturation. Subsequently the samples were loaded onto the Mini-PROTEAN® TGX™ Precast Gels (Biorad), transferred to PVDF membranes (Immobilon-P, Millipore) and incubated for 30 min with 4% PFA in PBS to better detect endogenous Ser129-phosphoryated α-syn [442]. By contrast, no PFA treatment was employed for the detection of non-phosphorylated α-syn and PrPc. After incubation, the membrane was washed in TBS-T (0.1% Tween 20 in TBS) for 10 min, treated with 5% non-fat milk or BSA (w/v, in PBS) blocking solution for 1 h at room temperature in agitation and then incubated overnight at 4 °C with the following primary antibodies: rabbit polyclonal anti-phospho S129 α-syn (Abcam, ab59264 1:1000); rabbit polyclonal anti-α-syn (C-20-R,

Santa Cruz, 1:1000); mouse monoclonal anti PrPc (clone P, kindly provided by Prof. S. Prusiner, San Francisco 1:1000) and a mouse monoclonal anti β-actin (1:50000, A3854 Sigma-Aldrich), all diluted in blocking solution.

Membranes were washed with TBST and incubated in horseradish–peroxidase (HRP)-conjugated goat anti-rabbit (DAKO, 1:1000) or goat anti-mouse (DAKO 1:1000) secondary Ab for 1 h. The membranes were washed in TBST, and proteins were visualized following the manufacturer's instructions using Amersham ECL Western Blotting Detection Reagent (GE Healthcare) with UVITEC Cambridge. Quantitative densitometry analysis of proteins was performed using UVBand software (UVITEC Cambridge).

13. Stereology

All analyses were carried out on coded slides by investigators blinded to the groups' identity. The occurrence of PK-resistant α-syn immunoreactive deposits, as either LB-like inclusions (defined as dense, darkly stained intraneuronal cores) or LN-like inclusions (defined as dense, darkly stained neurites) in the hippocampal formation, was quantified using an unbiased stereological estimation method based on the optical fractionator principle [443]. α-syn immunoreactive neurons and processes were counted bilaterally in the CA1 subfield of the hippocampus and in the dentate gyrus (i.e. the areas in close proximity to the injection site), using about 10 sections per rat located between 2.1 and 4.5 mm caudal to bregma. The same analyses were also carried out to quantitatively estimate the presence of α-syn immunoreactive deposits in projection areas outside the injection site, namely the EC. The sampling system consisted of an Olympus BH2 microscope (fitted with an X-Y motorized stage and a microcator to measure distances in the Z-axis) interfaced with a color video camera (Sony) and a personal computer. The CAST GRID® software (Olympus Denmark A/S, Albertslund, Denmark) was used to delineate the hippocampus area at 4x magnification, as well as to generate unbiased counting frames which were moved randomly and systematically until the entire delineated area was sampled. Using a 100x oil objective, unambiguously positive aggregates were identified and counted. For each animal, estimates of the total numbers

of neuronal and neuritic aggregates in the hippocampus and EC were obtained according to the optical fractionator formula and then plotted as mean ± SEM for each time-point analyzed. Accuracy of the stereological procedure was evaluated following [444], and values < 0.1 were considered acceptable.

14. RNA extraction and Real Time-quantitative PCR (RT-qPCR) analysis

Total RNA was isolated from about 300 mg of prefrontal cortex from frozen postmortem rat brain tissue. RNA processing and qPCR experiment were the same as reported previously [445] and the primers sequences were as follows: For *Actb* Forward CTGTGTGGATTGGTGGCTCT reverse CAGCTCAGTAACAGTCCGCC; for *SNCA* Forward TGTCAAGAAGGACCAGATGGG reverse TAGTCTTGGTAGCCTTCCTCT and for *Prnp* forward CGGTACCAGTCCGGTTTAGG reverse GCTTTTTGCAGAGGCCAACA. Differential gene expression of SNCA and *PrnP* was normalized to *Actb* expression. The relative expression ratio was calculated using the ΔΔCT method[446].

15. Statistical analysis

Data fulfilled the criteria for normal distribution and were therefore analyzed using parametric tests for all statistical comparisons. Group differences in behavioral performance as well as in the numbers of immunostained profiles or α-syn expression levels were evaluated by either repeated or one-way analysis of variance (ANOVA), as appropriate, followed by Fisher's Protected Least Significant Difference (PLSD) post-hoc test. All data are presented as mean ± SEM, and differences were considered significant at $p < 0.05$.

CHAPTER IV

RESULTS

1. Behavioral analyses

All animals, regardless of their treatment, increased in body weight and exhibited fairly normal sensory-motor functioning when evaluated in the three-day cued test at 3 months post-injection (Fig. 4.1). In fact, the groups improved their performance over time (repeated measures ANOVA, effect of day on latency, $F_{2,66} = 51.79$; on distance, $F_{2,66} = 42.44$; both $p < 0.001$) and did not differ from each other (main group effect on latency $F_{2,33} = 0.11$; on distance $F_{2.33} = 0.13$; group x day on latency $F_{4,66} = 0.23$; on distance $F_{4,66} = 0.23$; all n.s.). Moreover, swim speed, monitored as a measure of motor ability throughout the execution of the various tasks, averaged 0.2-0.3 m/sec and did not differ between groups at any time-point, indicating that the treatments did not produce any sensory or motor impairments that would affect navigation search in the pool. As revealed by statistics, rats with sham injections did not differ from the intact animals on any of the behavioral or morphological parameters analyzed. These animals were therefore combined into a single Control group (n = 18) for all illustrations.

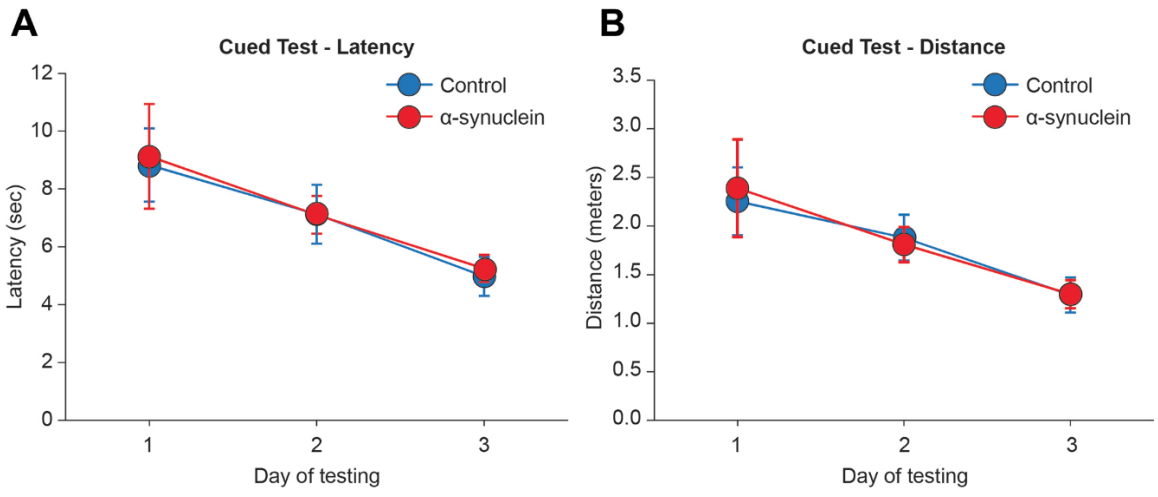

Figure 4.1 Groups performance during the cued version of the Morris water maze test at 3 months post injection. In this task, the visually cued escape platform was moved to a different quadrant on each of the four daily trials, and average escape latencies (A) and swim distances (B) were recorded. Each point represents the mean value ±SEM for the block of four trials administered each day, over the three training days.

2. Morris water maze test

Mean latencies and swim distances required to find the hidden platform in the reference memory version of the Morris water maze task administered at 3 months post-injection, are shown in Fig. 4.2 A, B. All animals rapidly learned to locate the platform and improved significantly over the five testing days (repeated measures ANOVA, effect of day on latency, $F_{4,132} = 43.93$; on distance, $F_{4,132} = 40.58$; both $p < 0.001$), reaching an asymptotic performance already on day three. The animals appeared to learn the tasks at similar rates, and no significant differences were observed between the groups (main group effect on latency $F_{2,33} = 0.47$; on distance $F_{2.33} = 0.60$; group per day on latency, $F_{8,132} = 0.16$; on distance $F_{8,132} = 0.18$; all n.s.). During the spatial probe trial, on the last day of testing, when the platform was removed for a 60 s free swim **(Fig. 4.2 C-E),** all animals swam primarily in the training (NE) quadrant, where the platform was originally located (repeated measures ANOVA, effect of quadrant on swim distance, $F_{3,99} = 36.73$; on annulus crossings, $F_{3,99} = 74.06$, both $p < 0.001$), with equal efficiency (main group effect on distance $F_{2,33} = 0.67$; on annulus crossings, $F_{2,33} = 1.87$; group per quadrant interaction for distance, $F_{6,99} = 1.35$; for annulus crossings $F_{6,99} = 1.39$, all n.s.). In addition, no group difference was observed in the total number of collisions with the annuli or swim speed (one-way ANOVA, main group effect, respectively, $F_{2.33} = 1.87$ and $F_{2,33} = 0.01$; both n.s.), indicating an equally active and spatially focused search behavior in all animals.

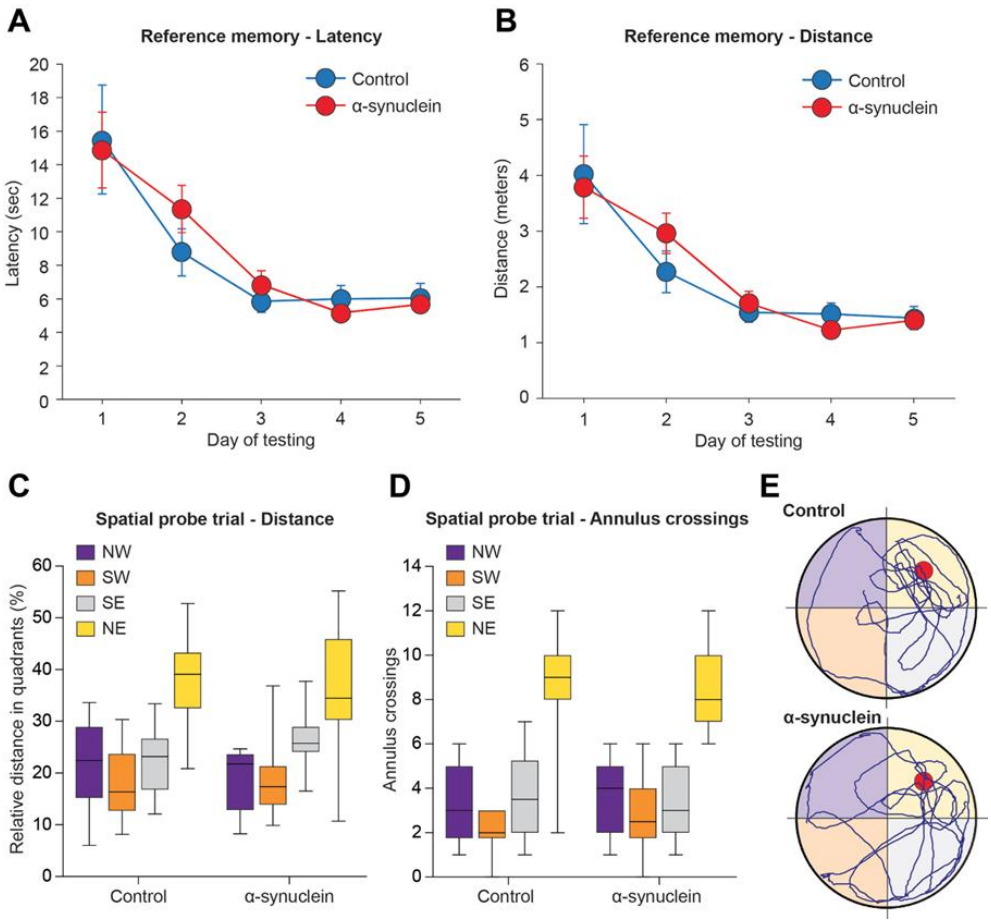

Figure 4.2 Performance during the Water maze reference memory test at 3 months post injection. Average latency (A) and swim distance (B) required to locate the submerged platform during the acquisition phase of the spatial navigation task. Each sample point represents the mean value ±SEM for the block of four trials on each of the five consecutive days of testing. Lower diagrams illustrate the mean relative distance swum (C) and the average number of annulus crossings (D) in each quadrant during the spatial probe trial, once the escape platform was removed from the NE (training) quadrant. In E, the actual swim paths taken by representative animals from the different groups are shown. All groups exhibited an equally efficient performance, indicating that the α-syn injection had no effects on this task. NE, North-East; NW, North-West; SE, South-East; SW, South-West

At about 12 months post-surgery, upon conclusion of the last 2-trial RAWM session (see below), the animals were tested again in the Morris water maze task in order to evaluate possible delayed effects of the injected α-syn PFFs, as a result of their progressive spreading. Only the data referring to the spatial probe trial will be reported here **(Fig. 4.3 A-C)**. Consistent with the observations at the 3 months' time-point, the α-syn treatment

produced no long-term impairments in reference memory abilities. In fact, all tested animals exhibited an equally efficient and focused search behavior in the spatial probe trial (repeated measures ANOVA effect of quadrant on swim distance, $F_{3.39} = 9.31$; on annulus crossings $F_{3.39} = 19.49$; both $p < 0.001$), with no obvious group differences (main group effect on distance, $F_{2,13} = 1.29$; on annulus crossings, $F_{2,13} = 2.00$; group x quadrant interaction for distance, $F_{6,39} = 1.25$; for annulus crossings $F_{6,39} = 1.76$, all n.s.). This applied also to the total number of crossings or swim speed.

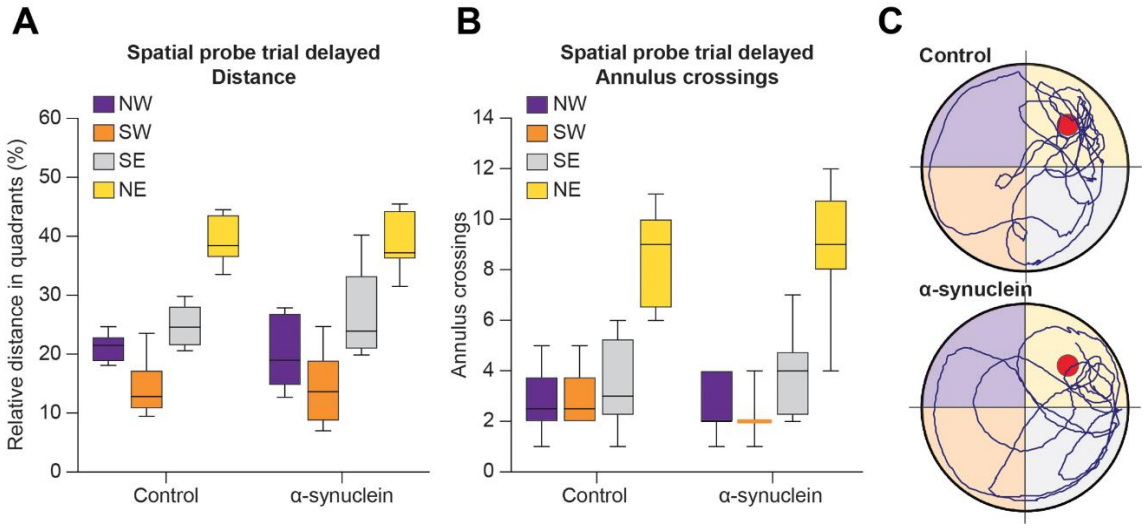

Figure 4.3 Performance during the spatial probe trial of the separate 3-d Morris water maze test administered just before killing, at 12 months post injection. The mean relative distance swum (A), the average number of annulus crossings (B), and the actual swim paths taken by representative animals from the different groups (C) are illustrated. Consistent with the observations at the 3 months' time point, no long-term impairments in reference memory abilities were produced by the α-syn treatment.

3. Radial arm water maze test

Group performances in the RAWM task, when first administered at 3 months post-injection, are shown in **Fig. 4.4 A-E**. In this design, the platform position was moved to a new arm daily, thus the animals had to re-learn its position within the five trials of each testing day by developing a new search strategy. As expected, all animals required a longer latency and made a higher number of arm selection errors (i.e., entering an arm not

containing the platform or an arm which had already been visited) during the first trial of each day, but they improved over the five trials (repeated measures ANOVA, effect of trial on latency, $F_{4,132} = 57.76$; on errors, $F_{4,132} = 45.69$; both $p < 0.001$). At the 3 months' time-point, the ability to progressively reduce the latency and errors required to locate the hidden platform was similar for all animals, and no group difference was detected (main group effect on latency, $F_{2,33} = 0.19$; on errors $F_{2,33} = 0.45$; group per trial interaction on latency $F_{8,132} = 0.67$; on errors, $F_{8,132} = 0.55$; all n.s.). Inspection of latency and errors savings, calculated as percentage improvement between trials 1 and 2, confirmed a ~ 40-48% reduction of latency and entry errors, with no obvious group difference (one-way ANOVA with Fisher's PLSD post-hoc test, all n.s.). The swim paths obtained on the fifth day of training from representative animals are shown in **Fig. 4.4 E.**

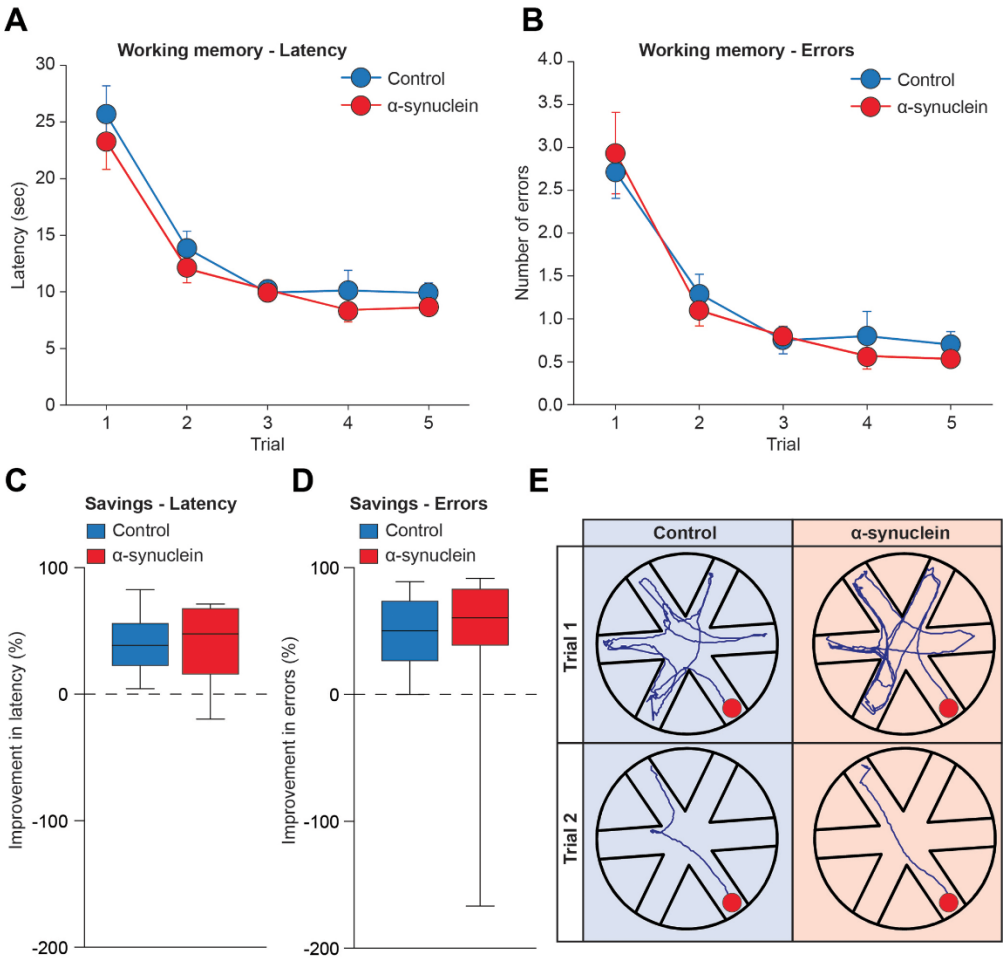

Figure 4.4. Working memory performance in the RAWM task, at 3 months post injection, illustrating latency (A) and number of entry errors (B) required by the animals to find the hidden platform. Each sample point represents the mean latency and errors ±SEM recorded during each 60-s trial over five consecutive testing days. In the lower diagrams, performances are plotted as percent savings between trials 1 and 2 for latency (C) and errors (D). In E, the actual swim paths taken by representative animals from the different groups are illustrated. All groups exhibited an equally efficient performance, indicating no clear-cut effects of α-syn on working memory at this time point.

4. Two-trials radial arm water maze test

Starting from 5 months and up to about 12 months post-injection, the animals were tested using a modified version of the RAWM task, with two daily trials administered over two consecutive days. The testing was then organized, with intervening sacrifices of randomly selected subjects from the various groups at different time-points post-injection, so as to have three main blocks of six sessions administered weekly or every two weeks, as outlined above. By such design, latency and error savings, calculated as percentage improvement from trial 1 to 2, provided a measure of working memory performance and its possible changes over time **(Fig. 4.5 A-C**). During the first two blocks (weekly sessions 1-6 and 7-12 starting at 5 and 7 months post-injection, respectively) animals in the groups were equally efficient in reducing both escape latency and number of errors across trials, and no significant group difference was detected (one-way ANOVA, all $p > 0.05$, n.s.). By contrast, in the third block of sessions (administered every two weeks starting from the 9th month post-injection), α-syn-treated animals were seen to progressively worsen their performance. In fact, the calculated percent improvements in both latency and errors appeared significantly lower than those exhibited by the Sham-injected and Intact groups already on session 15 (one-way ANOVA, $p < 0.01$ or $p < 0.05$ for both measures), and remained unmodified up to session 18, when the training criterion (i.e. significant group differences in at least three consecutive sessions) was considered fulfilled and the 2-trial RAWM testing was interrupted (actual swim paths from representative animals are illustrated in **Fig. 4.5 C**).

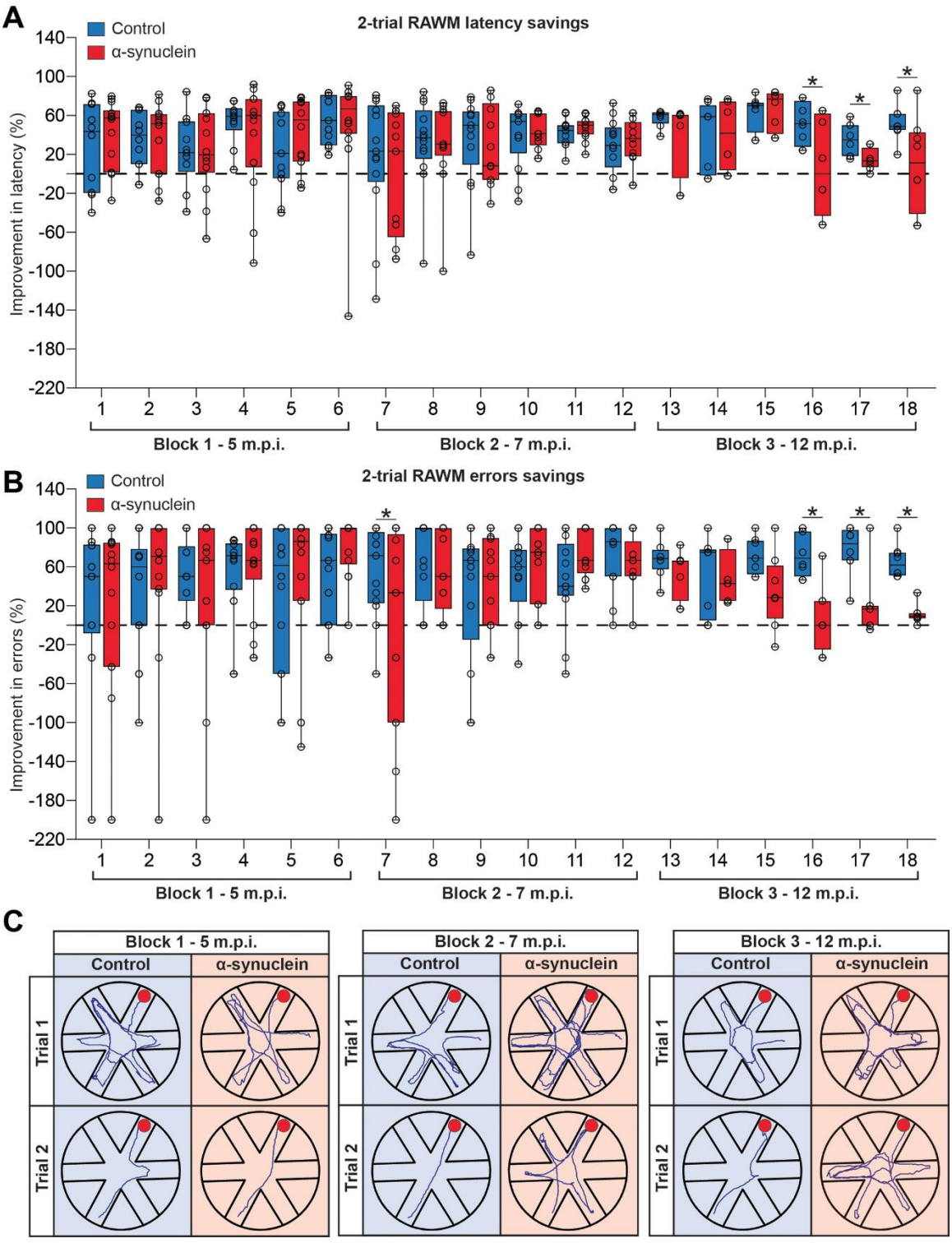

Figure 4.5 Working memory performance during the two trials RAWM, from 5 to 12 months post injection. Data represent the percentage rate of improvement between the first and the second trial (savings) in latency (A) and errors (B). All groups exhibited an equally efficient working memory during

the first two blocks of weekly sessions, administered at 5 and 7 months post injection, respectively; however, α-syn-treated animals progressively worsened their performance and appeared significantly impaired during the third block of sessions, administered every two weeks. In C, the actual swim paths taken by representative animals from the different groups in the various blocks are illustrated. Asterisks indicate significant difference from control at $p<0.01$.

5. Morphological analyses

Consistent with previous observations [403], sonication of α-syn fibrils resulted in the formation of relatively small and homogeneous fibrillary assemblies, as revealed by AFM (**Fig. 4.6).** By contrast, no such pattern was exhibited by the non-preaggregated protein (not shown).

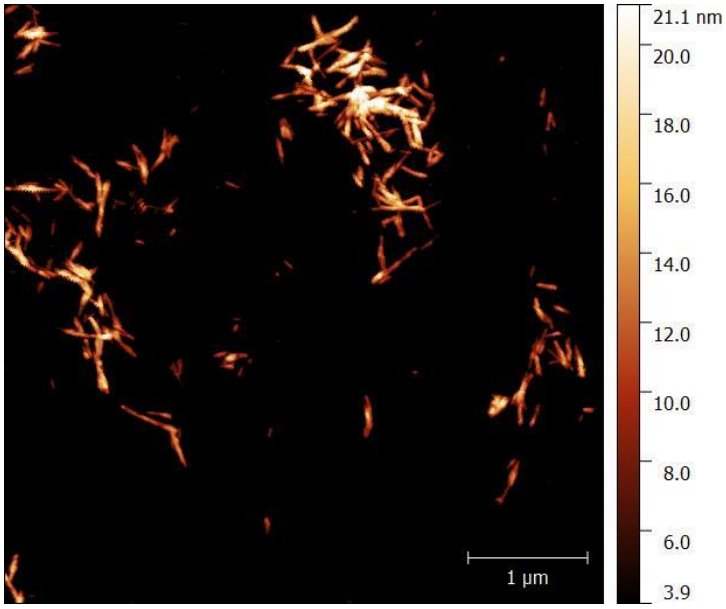

Figure 4.6 Atomic force microscopy image of sonicated of α-syn fibrils. Image was acquired with tapping mode in air, at room temperature working in dynamic mode by the use of a commercially available microscope (Solver Pro AFM from NT-MDT – NT-MDT Co. – Moscow – Russia) endowed with a closed-loop scanner[403].

The bilateral injection of synthetic mouse α-syn fibrils into the hippocampus resulted in the occurrence and progressive accumulation of α-syn-immunoreactive aggregates in

various hippocampal subfields (e.g. Dentate Gyrus, DG, Fig. 4.7A-F and Cornu Ammonis, CA1, Fig. 4.7G-L') whereas no such α-syn aggregates were found in the brain of sham-injected or intact animals (compare e.g. with corresponding regions in Control animals, **Fig. 4.7A–F'**). In general, the strong PK-resistant α-syn immunoreactivity occurred as both LB-like and LN-like deposits (**Fig. 4.7M-N**) and was detected not only in the proximity of the injection site but also in distinct anatomically related regions, with a morphology and distribution pattern that varied in a time-dependent fashion. Thus, as estimated by stereology, relatively few α-syn-immunoreactive LB-like inclusions were found in the hippocampal CA1 and dentate gyrus subfields at about 7 months post-injection, their numbers showing a significant 2.2- and 5.8-fold increase at 9 and 12 months, respectively (one-way ANOVA with Fisher's PLSD post-hoc test, $P < 0.05$; **Fig. 4.7O**). Conversely, the number of LN-like deposits in the same regions was slightly higher at 7 months post-injection and exhibited a non-significant reduction at 9 and 12 months (Fig. **4.7P**).

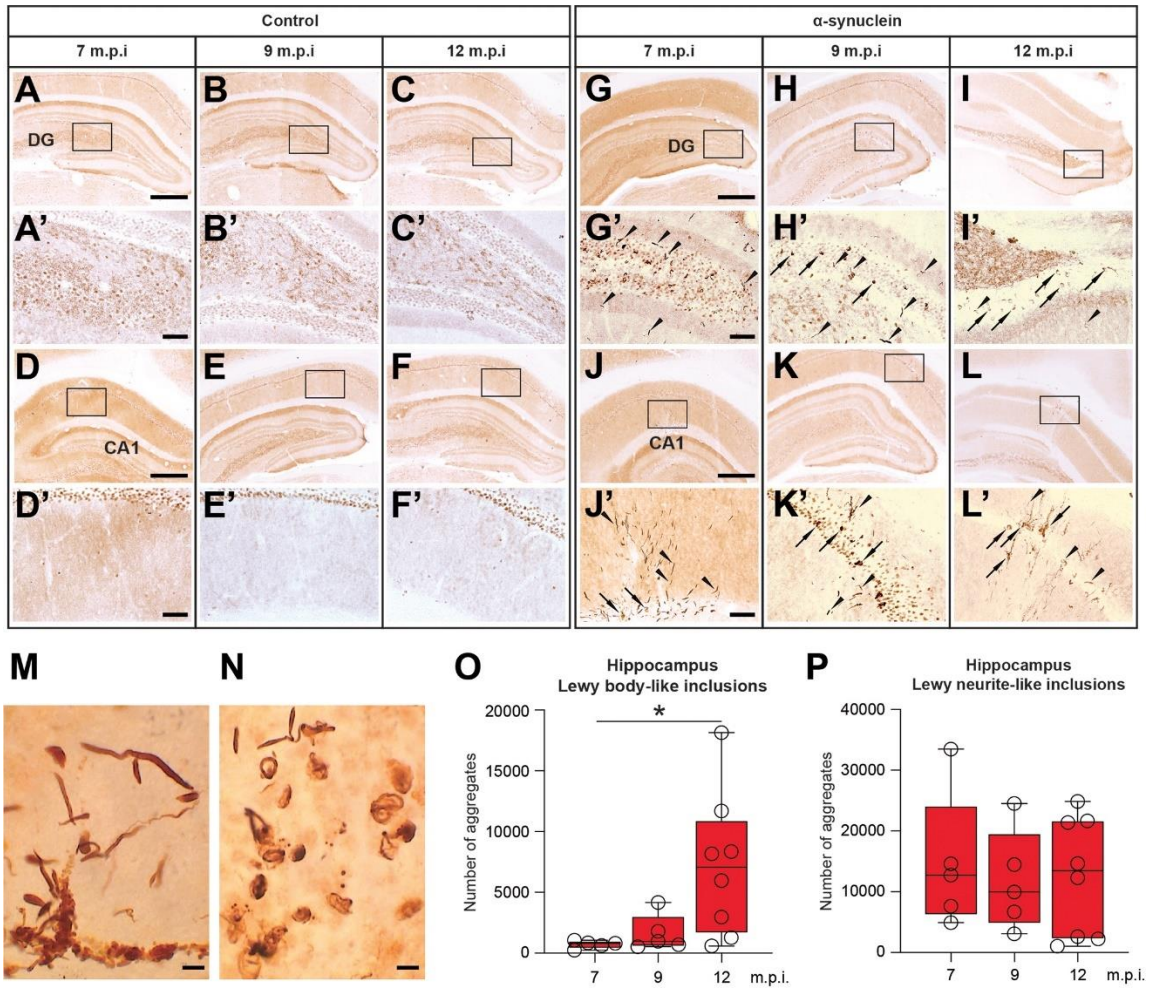

Figure 4.7. Representative micrographs illustrating, on the coronal plane, the negligible expression of PK-resistant a-syn immunoreactivity at 7, 9 and 12-months post-injection in the hippocampal DG (A–C, insets shown in A'–C') and in the CA1 region (D–F, insets shown in D'–F') of control rats. Progressive aggregation of a-syn after injection of recombinant mouse a-syn fibrils into the hippocampus. Compared with control, a strong PK-resistant a-syn immunoreactivity was found at seven, nine-, and 12-months post-injection in the DG (G–I, insets shown in G'–I') and in the CA1 region (J–L, insets shown in J'–L') of injected rats. PK-resistant a-syn aggregates occurred as darkly stained LB-like (arrows) and LN-like deposits (arrowheads) and are shown at higher magnification in M, N. Box-whiskers plots illustrate the stereologically estimated numbers at different time points 6 min to max value of LB-like (O) and LN-like (P) inclusions in the hippocampus of rats injected with the a-syn fibrils. Scale bars: 500 µm (in A, D, G, J for A–C, D–F, G–I, J–L), 100 µm (in A', D', G', J' for A'–C', D'–F', G'–I', J'–L'), and 5 µm (M, N). Asterisk in O indicates significant time dependent changes at $p<0.05$.

LB-like and LN-like inclusions in the EC were virtually undetectable or very sparse at 7 months post-injection but they became clearly visible already at 9 months (**Fig. 4.8A-F'**; compare with corresponding regions in Control animals, **Fig. 4.8A–C'**), and their numbers increased significantly over time (one-way ANOVA with Fisher's PLSD post-hoc test, both $p < 0.05$; **Fig. 4.8G-H).**

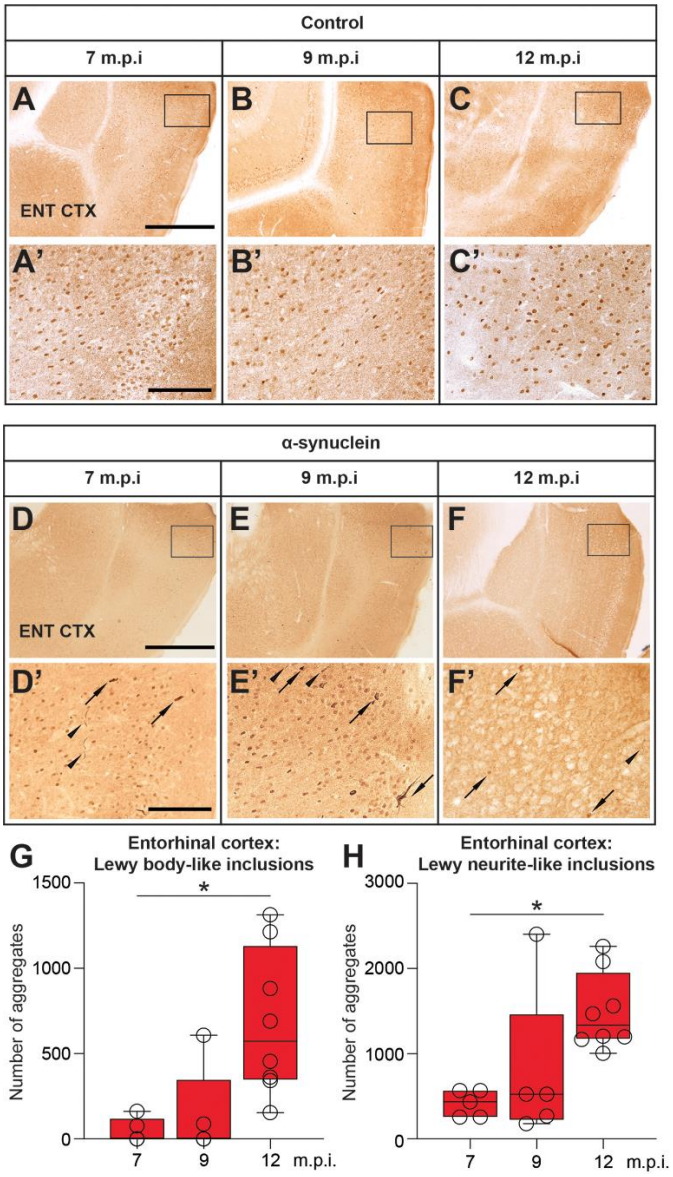

Figure 4.8. Representative micrographs illustrating, on the coronal plane, the negligible expression of PK-resistant a-syn immunoreactivity at 7, 9, and 12 months post injection in the entorhinal cortex (A–C, insets shown in A'–C') of control rats. Progressive a-syn aggregation after injection of

recombinant mouse a-syn fibrils into the hippocampus. A strong PK-resistant a-syn immunoreactivity occurring as both LB-like (arrows) and LN-like (arrowheads) deposits was also found at 7, 9, and 12 months post injection in the entorhinal cortex (D–F, insets shown in D'–F') of injected rats. Box-whiskers plots illustrate the stereologically estimated numbers at different time points 6 min to max value of LB-like (G) and LN-like (H) inclusions in the entorhinal cortex of the injected rats. Scale bar: 500 μm (in A, D for A–C, D–F) and 100 μm (in A', D' for A'–C', D'–F'). Asterisks in G, H indicate significant time-dependent changes at $p<0.05$.

By contrast, only at 12 months were α-syn immunoreactive LB-like and LN-like inclusions found in other projection areas, such as the vertical limb of the diagonal band, and the anterior and posterior piriform cortices, being barely detectable at earlier time-points (**Fig. 4. 9A-F'** compare with corresponding regions in Control animals **Fig. 4.9A–C'**).

In either form, occurrence of α-syn immunoreactivity in the hippocampus or entorhinal cortex did not appear to result in disrupted morphology or architecture of local neuronal populations (**Fig. 4.9 G–L**)

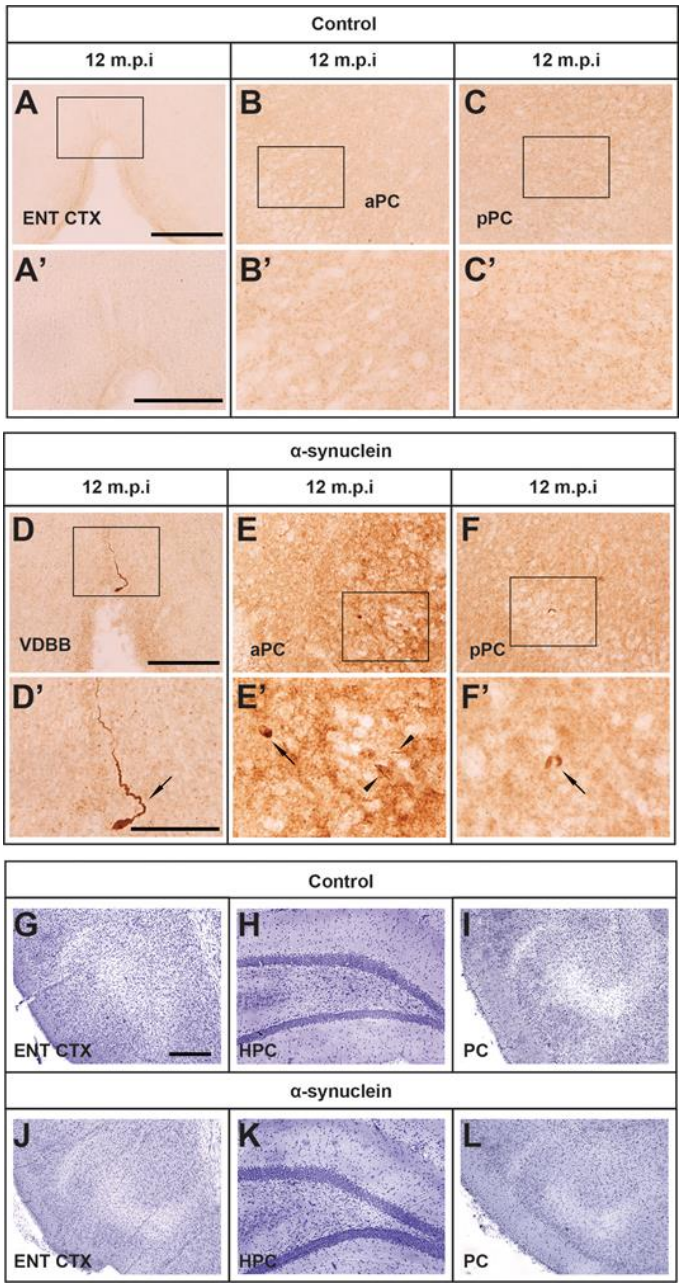

Figure 4.9. Representative micrographs illustrating, on the coronal plane, the negligible expression of PK-resistant α-syn immunoreactivity at 12 months post injection in the vertical limb of the DBB (vDBB; A, inset shown in A'), and the anterior and posterior piriform cortices (aPC and pPC; B, C, respectively, insets shown in B', C'). Spreading of a-syn aggregates. A strong PK-resistant α-syn immunoreactivity was also found at 12 months postinjection in the vDBB (D, inset shown in D', arrow) and the anterior and posterior piriform cortices (aPC and pPC, E, F, insets shown in E', F'; arrows and arrowheads indicate LB-like and LN-like inclusions, respectively). Scale bar: 100 µm (in A, D, for A–C, D–F) and 50 µm (D for D–F). Cresyl violet staining of the entorhinal cortex (ENT CTX), hippocampus

(HPC), and piriform cortex (PC) of control (G, H, I, respectively) and α-syn-injected animals (J, K, L, respectively). Scale bar: 100 μm (in G for G–L).

Moreover, separate morphometric analyses, carried out to assess the possible toxic effects of α-syn overexpression, revealed that at no time-point post-injection was any obvious loss of dopaminergic, cholinergic or noradrenergic neurons detected in the Substantia Nigra (SN), the Ventral Tegmental Area (VTA), Medial Septum/Diagonal Band of Broca (MS/DBB) or Locus Coeruleus (LC), respectively. Thus, occurrence and distribution of tyrosine hydroxylase (TH)-, choline acetyltransferase (ChAT)- or dopamine-beta-hydroxylase (DBH)-immunoreactive neurons did not differ between α-syn-injected and control animals in any of the analysed regions (data not shown)

Consistent with the above observations of a time-dependent increase of PK-resistant α-syn aggregates within the hippocampus, immunofluorescence confirmed the progressive, increase of Ser129-phosphorylated α-syn in the hippocampus of injected rats (**Fig. 4.10A-C)**, whereas no such immunoreactivity was detected in controls (not shown). Subsequent analyses of fluorescence intensity and localization profile in Ser129-phosphorylated a-syn P-α-syn-GFAP double immunostained specimens at 7, 9 and 12 months post-injection revealed virtually no co-localization of these markers. In fact, close inspection of the expression profile plots of P-α-syn and GFAP immunoreactivities showed very poor or no juxtaposition between the respective peaks, thus ruling out a glial occurrence of Ser129-phosphorylated α-syn as a result of intracerebral α-syn fibril treatment at any time-point post-injection (**Fig. 4.10A'-C' and A"-C").**

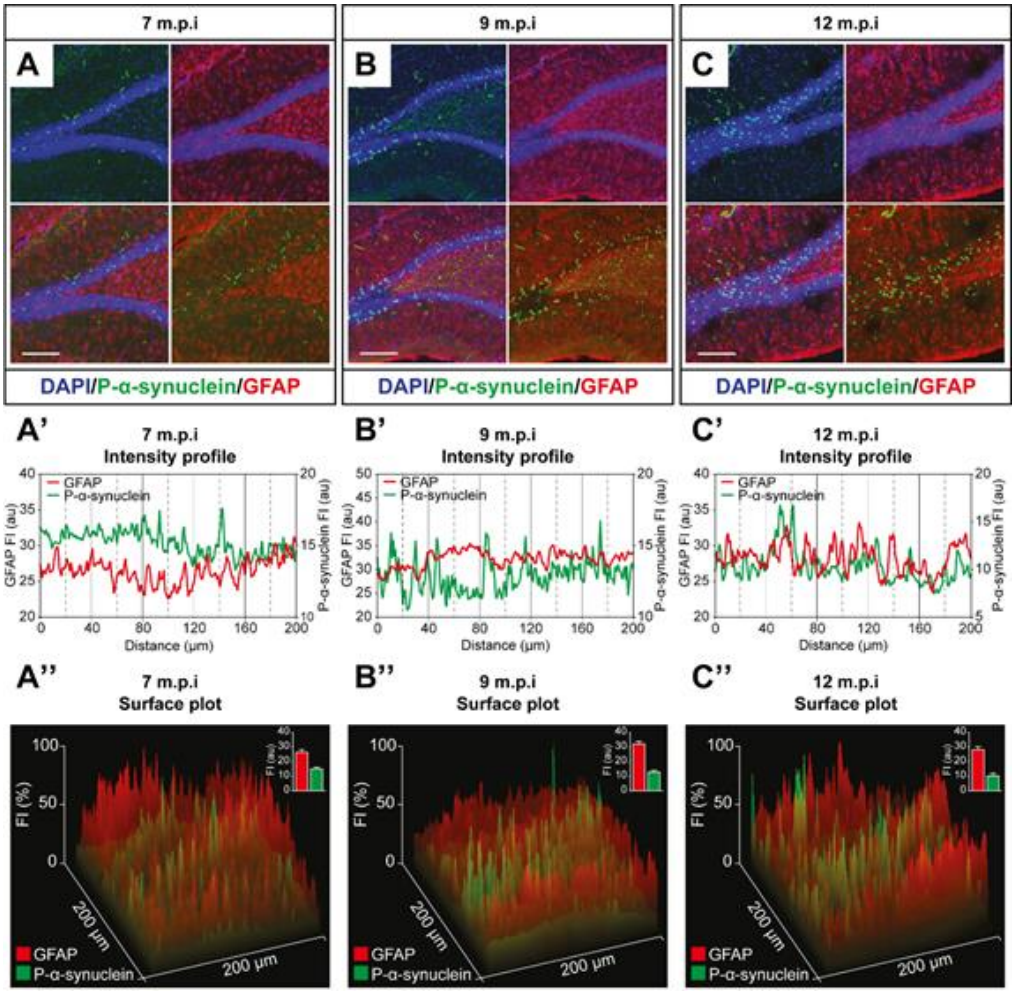

Figure 4.10. Confocal microscopy images illustrating the progressive increase of hippocampal Ser129-phosphorylated α-syn (A–C) and the lack of co-localization with GFAP at seven, nine, and 12 months after the injection of recombinant mouse α-syn fibrils into the hippocampus. In the lower diagrams, analysis of fluorescence intensity (A'–C') and surface plot profiles (A"–C") of confocal images in A–C indicate very poor or no glial occurrence of the Ser129-phosphorylated a-syn. Scale bars: 50 μm (A–C). Long-term effects of α-syn fibril injection

6. Western blot analyses

At 12 months post injection, Western blot analyses were carried out on tissue homogenates from the hippocampus and the prefrontal and frontoparietal cortices of control and α-syn-injected rats. Due to technical reasons (accidental loss of the homogenate samples), western blot analyses on the EC could not be carried out and will

not be reported here. The analyses were designed to obtain estimates of the relative levels of non-phosphorylated and Ser129-phosphorylated α-syn. The procedure (as described above) enabled the detection of a ~15 kDa band, that represents the non-phosphorylated α-syn [274], a ~80 kDa which correspond to Ser129-phosphorylated α-syn (**Fig. 4.11 A-C**) and a ~35 kDa for PrP^c (**Fig. 4.11D-F**). Densitometric analysis of the bands after normalization against β-actin revealed a significant 50% increase of the Ser129-phosphorylated α-syn level only in the hippocampus of α-syn treated rats compared to controls ($p < 0.01$; **Fig.4.11A'**). By contrast, no group differences in Ser129-phosphorylated α-syn expression were detected in prefrontal and frontoparietal cortices (**Fig.4.11B'-C'**), nor did the α-syn treatment affect the expression of non-phosphorylated α-syn in any of the analyzed regions. Likewise, the expression levels of PrP^c in these regions was similar in the two groups (**Fig. 4.11D'-F'**).

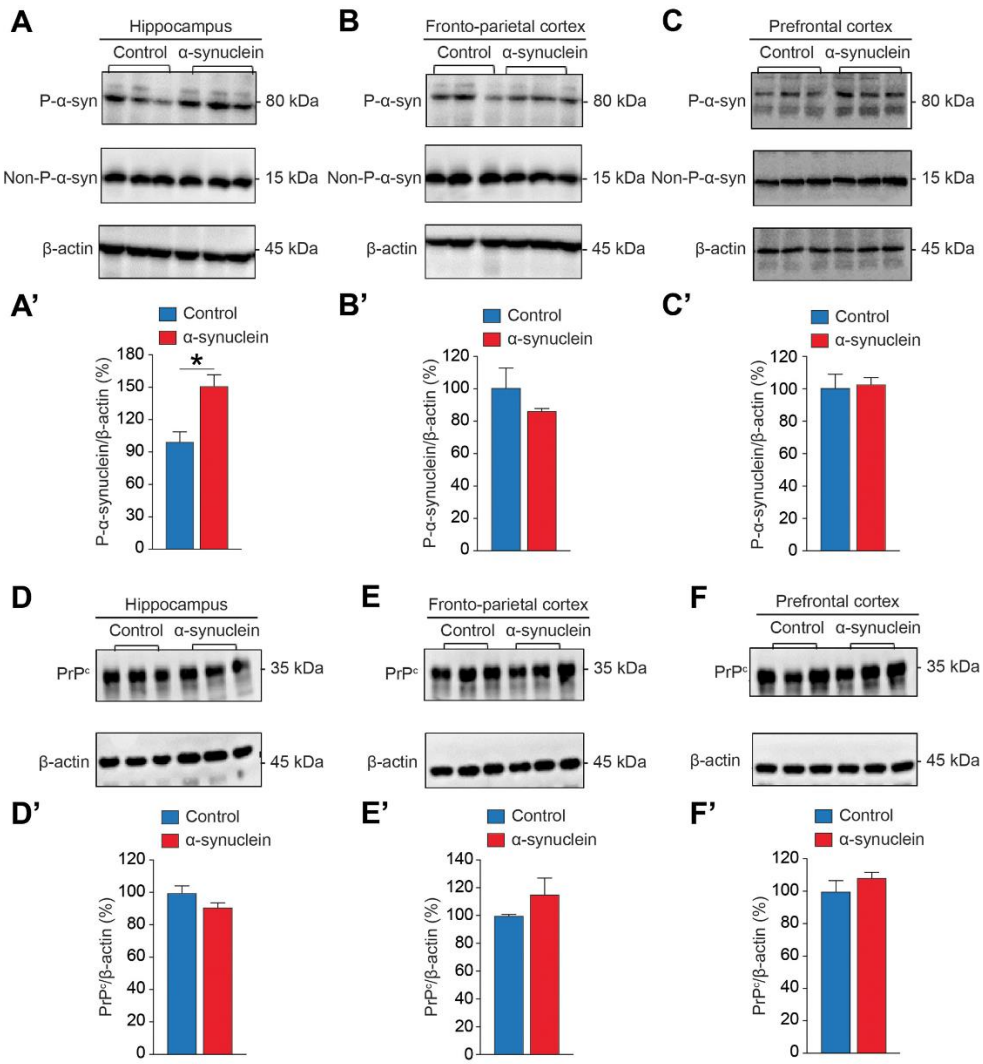

Figure 4.11. Long-term effects of intrahippocampal a-syn fibril injection on regional tissue levels of Ser129-phosphorylated a-syn (Pa-syn), non-phosphorylated a-syn (non-P-a-syn), and PrP^c. Representative Western blotting bands and densitometric analyses illustrate the expression levels of the various proteins in the hippocampus (A, A', D, D'), fronto-parietal cortex (B, B', E, E'), and prefrontal cortex (C, C', F, F') of rats injected with a-syn fibrils and controls at 12 months post injection. The values are shown as a percentage of P-a-syn, non-P-a-syn forms, or PrPc relative to b -actin, this latter being the loading control. Data are represented as mean ± SEM. Asterisk in A' indicates significant difference from control at $p<0.05$.

7. RT-qPCR analysis

To evaluate the differential gene expression of *SCNA* and *PrnP*, RT-qPCR analysis was performed on tissue homogenates from prefrontal cortex of control and α-syn-injected rats at 12 months post injection. There was no significantly increased expression level of *SCNA* mRNA and *PrnP* mRNA in α-syn injected rats compared to control (**Fig. 4.12).**

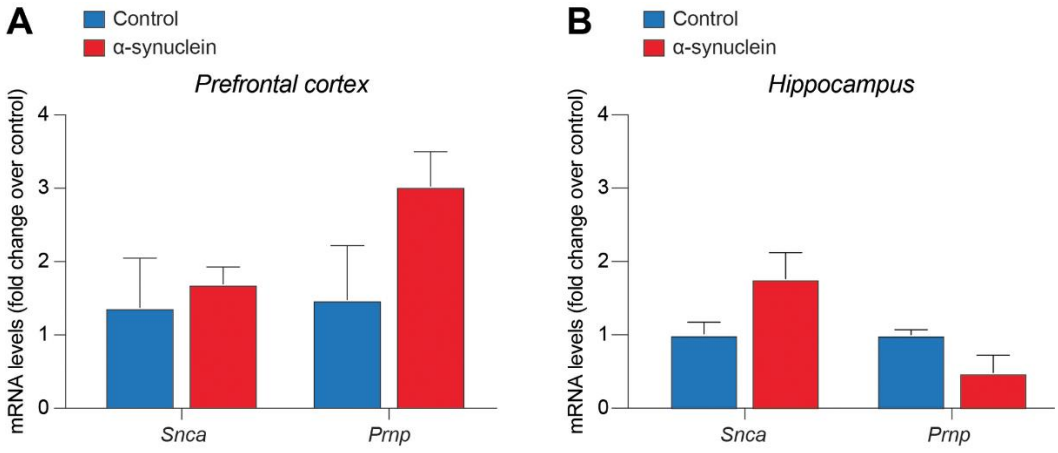

Figure 4.12 Quantification of the mRNA expression levels of *SNCA* and *PrnP* in prefrontal cortex (A) and in the hippocampus (B) of rats injected with a-syn fibrils and controls at 12 months postinjection. Data are represented as mean fold change over control ±SEM.

CHAPTERV

DISCUSSION AND CONCLUSION

The aim of this study was to evaluate the anatomical, neurochemical, molecular and behavioral effects of recombinant mouse α-syn PFFs following intrahippocampal injection in the adult rat. The injections resulted in the time-dependent occurrence of PK-resistant α-syn aggregates within the hippocampus suggesting that neurons in this region may be particularly susceptible to transmitted α-syn pathology. Moreover, in keeping with previous findings following intrastriatal/intracortical administration in mice [389] the present data lend support to the notion that pathological α-syn can spread over considerable distances to several central regions, which is also consistent with the prion like hypothesis. In fact, PK-resistant α-syn aggregates were also found in anatomically related areas, such as the EC, the vDBB and the piriform cortices, which, interestingly, was associated to the onset of specific deficits in spatial working memory, i.e. the kind of memory function that is commonly impaired in PD patients [447].

Thus, at 7 months post injection, α-syn immunoreactivity in the hippocampus was mainly associated to neuritic processes and relatively few intracellular inclusions were detected. This observation is consistent with previously suggested explanation according to which the onset of α-syn accumulation in axons may be due to the physiological high-level content of endogenous α-syn within the presynaptic terminals [283, 448]. In addition, the pathological staging of PD confirmed that Lewy neurite formation precedes Lewy body formation[22]. In the hippocampus, the numbers of Lewy-like neuritic inclusions did not vary significantly over time, whereas in the EC the estimated numbers of α-syn immunoreactive neurites were seen to increase between 7 and 9 months but remained virtually unchanged thereafter. In both regions, the immunoreactive material appeared to progressively invade somata and already at 9 months, the number of neuronal profiles with dense perinuclear LB-like inclusions was seen significantly increased. Interestingly, inclusions of α-syn immunoreactive material in both the hippocampus and EC exhibited the most dramatic increases (by about 6- and 10-fold, respectively) at 12 months post-injection. The time-course and dynamics of intracellular α-syn occurrence, with more

dramatic increases detected between 9- and 12-months post-injection, i.e. concurrently to the onset of cognitive impairments, points to a precise time window, relatively long after its injection into the brain parenchyma, when α-syn is capable to massively accumulate inside neurons and efficiently interfere with their functioning. The present findings appear consistent with previous observations of remarkably slow progression of α-syn pathology in PD patients [449, 450], thus confirming the feasibility of the α-syn PFF infusion paradigm as a tool for modelling aspects of cognitive loss in PD. In fact, a significant trend towards a worsened performance in the RAWM task was seen from 9 months post injection, to become dramatically evident at 12 months. Interestingly, at no time point post-injection was any motor disturbance detected in the injected animals, nor was α-syn found within regions rich in dopamine neurons and fibers, such as the SN, the VTA or the Striatum. In addition, no obvious loss in dopaminergic, noradrenergic or cholinergic immunoreactivity was detected in α-syn-injected animals compared to controls, thus the behavioural impairments seen in the α-syn injected animals appear to be determined by the long-term persisting α-syn neuropathology in the affected neurons rather than by neurodegeneration, which is consistent with the observations by Hall and colleagues [431]. These observations are also in keeping with the findings of a recent in vitro study [451] showing that treatment of excitatory hippocampal neurons with α-syn fibrils after 7 days induced neuronal dysfunctions before the occurrence of neuronal death when α-syn inclusions primarily localize to axons. Indeed, Froula and colleagues found that exposure of neurons to α-syn fibrils caused a Paradoxically, reduced postsynaptic spine density which was accompanied by increased frequency of miniature excitatory postsynaptic currents (EPSCs) and presynaptic docked vesicles, suggesting enhanced presynaptic function. In addition, neurons exposed to α-syn fibrils, showed reduced frequency and amplitudes of spontaneous Ca2+ transients confirming the detrimental effect of α-syn fibrils on synaptic activity as previously described in others studies[452, 453]. However, Action-potential dependent activity was unchanged, suggesting compensatory mechanisms responding to synaptic defects at the level of synapse. In fact, Froula and colleagues suggested that the transformation of normal α-syn into pathologic aggregates at the presynaptic terminal increased presynaptic activity with a reduction of dendritic spines which can be considered as a homeostatic response to the increase

presynaptic activity, thus causing no changes in spontaneous synaptic events. Furthermore, Wu and coworkers after using a whole cell patch clamp technique to investigate synaptic activity modulation after exposure to α-syn FFs at the single-cell level reported decreased synaptic activity within 10 min following the direct administration of PFFs to the neuron before neuronal death occurrence at 7 days post administration[452]. All together these data, in accordance with ours, suggested that neuronal α-syn pathology could induced negative changes in synaptic function which could lead to cognitive impairment before the occurrence of neuronal death. Moreover, the compensatory mechanisms (found by Froula and colleagues) responding to synaptic defects induced by α-syn fibrils could explain the long-time window before the onset of memory impairments observed in the present study.

Considering the occurrence of α-syn immunoreactivity in the EC and, at 12 months post-injection, in the vDBB and the piriform cortices, i.e. all regions involved in memory functions and the time-course and regional pattern of α-syn accumulation, the present data therefore suggest that hippocampal Lewy pathology must spread beyond its initial site, towards cognitively-relevant areas, to induce measurable memory dysfunctions. This is consistent with the model proposed by Adamowicz et al. [435] according to which learning, and memory impairment become apparent once Lewy pathology concurrently affects CA1 and EC.

The mechanism underlying the hippocampal Lewy pathology induced memory impairment needs to be further elucidated. However, it has been reported that deficits in learning and memory observed in α-syn transgenic mice are accompanied by alterations in post-synaptic densities [454] or reduction in presynaptic vesicle-associated proteins such as synaptophysin [433], suggesting that the toxicity of α-syn may be mediated by disturbances in synaptic transmission and plasticity [455, 456]. α-syn FFs have been also shown to hampers synapse formation, disrupt spine dynamics and morphology, all events known to be involved in learning and memory. In particular, the reduced spine density induced by α-synuclein pathology may be a pathophysiological phenotype contributing to dementia [457, 458]. Indeed, it has been demonstrated that increasing in spine density of CA1, CA3 and dentate gyrus neurons of the rat hippocampus is positively proportional to RAWM performance (thus reduced working memory errors and latency) in trained

rats[459]. Thus, α-syn PFFs induced disruption of spine dynamics and morphology may underly the working memory impairment observed in α-syn PFFs injected rats in this study. However, further analyses assessing spine dynamics and morphology in relevant areas and at different time points after α-syn PFFs injection are needed.

In a recent investigation, Aulić and coworkers([403] found that the PrP^c binds α-syn amyloids to get access into the cell and accumulate into cytoplasm, thereby facilitating the cell-to-cell spreading of the pathology. Likewise, it has been reported that α-syn oligomeric species interact with PrP^c through mGluR5, activating SFK kinases and, subsequently, NMDAR2B to induce neuronal dysfunction and cognitive deficits in Thy1-α-syn mice and also that the toxic effects induced by α-syn oligomers may be prevented using antibody-mediated inactivation of PrP^c [404]. Taken together these studies have identified previously unknown components of the signaling cascade triggered by α-syn, therefore suggesting that PrP^c signaling might be involved in the pathogenesis of synucleinopathies and may be used as a potential therapeutic target to prevent or slow down the progression of synucleinopathies. Surprisingly, in the present study, the immunoprecipitation approach provided no evidence of any complexes formed in the hippocampus between PrP^c (data not shown) with either non-phosphorylated or phosphorylated α-syn at 12 months post-injection. Considering that the α-syn-PrP^c interactions reported by both Aulic et al. (2017) and Ferreira et al. (2018) are detected in 5–8-month-old animals, it is possible to assume the existence of specific stages during which the interaction of these proteins may actually take place, leading to a massive α-syn spreading, to become less pronounced at later time-points, once the spreading is well ongoing. This may be of potential interest, as it may highlight a valuable window of therapeutic opportunity, whose full understanding, again, requires further investigation.

PrP^c level in the hippocampus, prefrontal and fronto-parietal cortices of α-syn-injected rats was similar to controls at 12 months post-injection, as well as PrP^c mRNA and α-syn mRNA levels in the prefrontal cortex which is consistent with previous observations [403]. This appear to confirm that the level of PrP^c and α-syn transcripts were not altered after fibrils injection and that the observed increase of pathological α-syn is likely to occur at protein accordingly to the already described prion like hypothesis.

Increased level of phosphorylated α-syn at serine 129 represents one of the hallmarks of PD. In fact, approximately 90% of α-syn deposited in LBs is phosphorylated at serine 129 (Ser129) while only 4% or less of the total α-syn is phosphorylated at this residue in brains from individuals without PD [274, 460]. Nevertheless, the significance of phosphorylation in the biology and pathophysiology of the protein is still controversial and both in vitro and in vivo studies, examining phosphorylation of α-syn at different sites, have reported conflicting results, showing either promotion [323], inhibition [461] or no effect [462] on inclusion formation. However, to assess the role, if any, of the phosphorylation of α-syn fibrils in the seeding and pathological accumulation of α-syn, Karampetsou and colleagues found that phosphorylated α-syn -PFFs are more efficiently uptaken by neurons after injection in wild type mice, leading to increased seeding and accumulation of the endogenous α-syn. This suggests that phosphorylation adds "aggregation" capacity to the α-syn assemblies and as such may regulate the onset of neuronal dysfunction[322]. Similarly, we found after injection of non-phosphorylated recombinant mouse α-syn fibrils in rats, a time–dependent increase of Ser-129 phosphorylated α-syn into the hippocampus with the overt manifestation of cognitive deficits. Our data, therefore, not only provide a further proof of the importance of phosphorylation in the pathogenesis of disease but also allow the validation of our experimental model.

In the present study we used the α-syn PFFs as a model to examine the long-term behavioral effects induced by misfolded α-syn within the hippocampus. However, we did not address the eventual neuroinflammation that could result from α-syn PFFs injection. Previous studies using α-syn PFFs revealed an increased microglial activation followed by the release of proinflammatory mediators which may be the cause rather than the consequence of neurodegeneration[414]. Indeed, intranigral injection of α-syn PFFs in rats induced the major histocompatibility complex (MHC) II response 24 hours post injection, which persisted over time, and was accompanied by CD163-positive cells, revealing the infiltration of scavenger macrophages from the periphery. Interestingly, SN was invaded by a high number of of CD45High/Cb11b macrophages and CD4+ T cells at 2 months post injection even though no changes in the number of microglia were evident suggesting changes in microglial activation instead of an increase in proliferation.

Furthermore, the lack of apparent nigrostriatal degeneration led to the suggestion according to which, the cause of degeneration may be due to the recruitment of peripheral immune cells expressing proinflammatory phenotypes triggered by MHC II activation[463]. Similar results were found in another study after intrastriatal injection of α-syn PFFs in rats suggesting that the activation of inflammatory components, like MHC II, represent a primary defense mechanism upon the presence of inclusions in hope of aggregate burden reduction[464]. Indeed, Olanow and colleagues showed that microglial inflammatory responses precede the propagation of Lewy body pathology in human fetal tissues grafted into patient brains, which indicates that in humans, immune responses are early events rather than late events in association with aggregate propagation[465]. However, these early immune responses might contribute to neuronal vulnerability and lead to degeneration[464]. Thus, in light of the previous studies, the apparent lack of neurodegeneration observed 12 months after α-syn PFFs injection in the present study may indicate a lack of neuroinflammation which however requires further investigation given the fact that differences in the inflammatory profile were shown to depend on the site of injection, type of seed, and time point of pathology assessment[322, 412, 463, 466].

In conclusion, our study shows that bilateral injection of recombinant mouse α-syn PFFs into the hippocampus of rat was sufficient to trigger α-syn pathology within the hippocampus and spread it in EC, vDBB and piriform cortex leading to working memory impairment. Although the mechanism behind α-syn-mediated working memory impairment has to be further elucidated, the present study provides an additional proof that α-syn may be one the main neuronal substrates for cognitive impairment in synucleinopathies.

REFERENCES

1. Ahmed, R.M., et al., *Neuronal network disintegration: common pathways linking neurodegenerative diseases.* J Neurol Neurosurg Psychiatry, 2016. **87**(11): p. 1234-1241.
2. Carrell, R.W. and D.A. Lomas, *Conformational disease.* Lancet, 1997. **350**(9071): p. 134-8.
3. Misiak, B., et al., *European studies on the prevalence of dementia in the elderly: time for a step towards a methodological consensus.* Int J Geriatr Psychiatry, 2013. **28**(12): p. 1211-21.
4. Kovacs, G.G., *Concepts and classification of neurodegenerative diseases.* Handb Clin Neurol, 2017. **145**: p. 301-307.
5. *<Current-Concepts-Of-Neurodegenerative-Diseases.pdf>.*
6. Kovacs, G.G., *Molecular Pathological Classification of Neurodegenerative Diseases: Turning towards Precision Medicine.* Int J Mol Sci, 2016. **17**(2).
7. Prusiner, S.B., *Novel proteinaceous infectious particles cause scrapie.* Science, 1982. **216**(4542): p. 136-44.
8. Bolton, D.C., M.P. McKinley, and S.B. Prusiner, *Identification of a protein that purifies with the scrapie prion.* Science, 1982. **218**(4579): p. 1309-11.
9. Quadrio, I., A. Perret-Liaudet, and G.G. Kovacs, *Molecular diagnosis of human prion disease.* Expert Opin Med Diagn, 2011. **5**(4): p. 291-306.
10. Peden, A.H. and J.W. Ironside, *Review: pathology of variant Creutzfeldt-Jakob disease.* Folia Neuropathol, 2004. **42 Suppl A**: p. 85-91.
11. Kretzschmar, H.A., et al., *Latrogenic Creutzfeldt-Jakob disease with florid plaques.* Brain Pathol, 2003. **13**(3): p. 245-9.
12. Duyckaerts, C., B. Delatour, and M.C. Potier, *Classification and basic pathology of Alzheimer disease.* Acta Neuropathol, 2009. **118**(1): p. 5-36.
13. Braak, H., et al., *Staging of Alzheimer disease-associated neurofibrillary pathology using paraffin sections and immunocytochemistry.* Acta Neuropathol, 2006. **112**(4): p. 389-404.
14. Thal, D.R., et al., *Phases of A beta-deposition in the human brain and its relevance for the development of AD.* Neurology, 2002. **58**(12): p. 1791-800.
15. Braak, H. and K. Del Tredici, *The preclinical phase of the pathological process underlying sporadic Alzheimer's disease.* Brain, 2015. **138**(Pt 10): p. 2814-33.
16. Stratmann, K., et al., *Precortical Phase of Alzheimer's Disease (AD)-Related Tau Cytoskeletal Pathology.* Brain Pathol, 2016. **26**(3): p. 371-86.
17. Mirra, S.S., et al., *The Consortium to Establish a Registry for Alzheimer's Disease (CERAD). Part II. Standardization of the neuropathologic assessment of Alzheimer's disease.* Neurology, 1991. **41**(4): p. 479-86.
18. Montine, T.J., et al., *National Institute on Aging-Alzheimer's Association guidelines for the neuropathologic assessment of Alzheimer's disease: a practical approach.* Acta Neuropathol, 2012. **123**(1): p. 1-11.
19. Kovacs, G.G., et al., *Neuropathology of the hippocampus in FTLD-Tau with Pick bodies: a study of the BrainNet Europe Consortium.* Neuropathol Appl Neurobiol, 2013. **39**(2): p. 166-78.
20. Crary, J.F., et al., *Primary age-related tauopathy (PART): a common pathology associated with human aging.* Acta Neuropathol, 2014. **128**(6): p. 755-66.
21. McKee, A.C., et al., *The spectrum of disease in chronic traumatic encephalopathy.* Brain, 2013. **136**(Pt 1): p. 43-64.
22. Braak, H., et al., *Staging of brain pathology related to sporadic Parkinson's disease.* Neurobiol Aging, 2003. **24**(2): p. 197-211.
23. Kosaka, K., K. Tsuchiya, and M. Yoshimura, *Lewy body disease with and without dementia: a clinicopathological study of 35 cases.* Clin Neuropathol, 1988. **7**(6): p. 299-305.

24. Popescu, A., et al., *Lewy bodies in the amygdala: increase of alpha-synuclein aggregates in neurodegenerative diseases with tau-based inclusions.* Arch Neurol, 2004. **61**(12): p. 1915-9.
25. Uchikado, H., et al., *Alzheimer disease with amygdala Lewy bodies: a distinct form of alpha-synucleinopathy.* J Neuropathol Exp Neurol, 2006. **65**(7): p. 685-97.
26. Beach, T.G., et al., *Unified staging system for Lewy body disorders: correlation with nigrostriatal degeneration, cognitive impairment and motor dysfunction.* Acta Neuropathol, 2009. **117**(6): p. 613-34.
27. Trojanowski, J.Q. and T. Revesz, *Proposed neuropathological criteria for the post mortem diagnosis of multiple system atrophy.* Neuropathol Appl Neurobiol, 2007. **33**(6): p. 615-20.
28. Jellinger, K.A., *Neuropathology of multiple system atrophy: new thoughts about pathogenesis.* Mov Disord, 2014. **29**(14): p. 1720-41.
29. Rohan, Z., et al., *Screening for α-synuclein immunoreactive neuronal inclusions in the hippocampus allows identification of atypical MSA (FTLD-synuclein).* Acta Neuropathol, 2015. **130**(2): p. 299-301.
30. Gelpi, E., et al., *Multiple organ involvement by alpha-synuclein pathology in Lewy body disorders.* Mov Disord, 2014. **29**(8): p. 1010-8.
31. Grad, L.I., et al., *Clinical Spectrum of Amyotrophic Lateral Sclerosis (ALS).* Cold Spring Harb Perspect Med, 2017. **7**(8).
32. Benussi, A., A. Padovani, and B. Borroni, *Phenotypic Heterogeneity of Monogenic Frontotemporal Dementia.* Front Aging Neurosci, 2015. **7**: p. 171.
33. Kovacs, G.G., et al., *Clinicopathological description of two cases with SQSTM1 gene mutation associated with frontotemporal dementia.* Neuropathology, 2016. **36**(1): p. 27-38.
34. Braak, H., et al., *Amyotrophic lateral sclerosis: dash-like accumulation of phosphorylated TDP-43 in somatodendritic and axonal compartments of somatomotor neurons of the lower brainstem and spinal cord.* Acta Neuropathol, 2010. **120**(1): p. 67-74.
35. Mackenzie, I.R., et al., *A harmonized classification system for FTLD-TDP pathology.* Acta Neuropathol, 2011. **122**(1): p. 111-3.
36. Lee, E.B., et al., *Expansion of the classification of FTLD-TDP: distinct pathology associated with rapidly progressive frontotemporal degeneration.* Acta Neuropathol, 2017. **134**(1): p. 65-78.
37. Nelson, P.T., et al., *Hippocampal sclerosis in advanced age: clinical and pathological features.* Brain, 2011. **134**(Pt 5): p. 1506-18.
38. McKee, A.C., et al., *The neuropathology of chronic traumatic encephalopathy.* Brain Pathol, 2015. **25**(3): p. 350-64.
39. Nelson, P.T., et al., *Limbic-predominant age-related TDP-43 encephalopathy (LATE): consensus working group report.* Brain, 2019. **142**(6): p. 1503-1527.
40. Neumann, M., et al., *A new subtype of frontotemporal lobar degeneration with FUS pathology.* Brain, 2009. **132**(Pt 11): p. 2922-31.
41. Munoz, D.G., et al., *FUS pathology in basophilic inclusion body disease.* Acta Neuropathol, 2009. **118**(5): p. 617-27.
42. Devys, D., et al., *Pathological mechanisms in polyglutamine expansion diseases.* Adv Exp Med Biol, 2001. **487**: p. 199-210.
43. Yazaki, M., et al., *Biochemical characterization of a neuroserpin variant associated with hereditary dementia.* Am J Pathol, 2001. **158**(1): p. 227-33.
44. Vidal, R., et al., *Intracellular ferritin accumulation in neural and extraneural tissue characterizes a neurodegenerative disease associated with a mutation in the ferritin light polypeptide gene.* J Neuropathol Exp Neurol, 2004. **63**(4): p. 363-80.
45. Mackenzie, I.R., et al., *Nomenclature and nosology for neuropathologic subtypes of frontotemporal lobar degeneration: an update.* Acta Neuropathol, 2010. **119**(1): p. 1-4.

46. Hou, Y., et al., *Ageing as a risk factor for neurodegenerative disease.* Nat Rev Neurol, 2019. **15**(10): p. 565-581.
47. Maynard, S., et al., *DNA Damage, DNA Repair, Aging, and Neurodegeneration.* Cold Spring Harb Perspect Med, 2015. **5**(10).
48. López-Otín, C., et al., *The hallmarks of aging.* Cell, 2013. **153**(6): p. 1194-217.
49. Babbar, M. and M.S. Sheikh, *Metabolic Stress and Disorders Related to Alterations in Mitochondrial Fission or Fusion.* Mol Cell Pharmacol, 2013. **5**(3): p. 109-133.
50. Oh, J., Y.D. Lee, and A.J. Wagers, *Stem cell aging: mechanisms, regulators and therapeutic opportunities.* Nat Med, 2014. **20**(8): p. 870-80.
51. Inoue, K., *Genetic Risk Factors for Neurodegenerative Diseases.* 2015.
52. Corder, E.H., et al., *Gene dose of apolipoprotein E type 4 allele and the risk of Alzheimer's disease in late onset families.* Science, 1993. **261**(5123): p. 921-3.
53. Farrer, L.A., et al., *Effects of age, sex, and ethnicity on the association between apolipoprotein E genotype and Alzheimer disease. A meta-analysis. APOE and Alzheimer Disease Meta Analysis Consortium.* Jama, 1997. **278**(16): p. 1349-56.
54. Simón-Sánchez, J., et al., *Genome-wide association study reveals genetic risk underlying Parkinson's disease.* Nat Genet, 2009. **41**(12): p. 1308-12.
55. Scholz, S.W., et al., *SNCA variants are associated with increased risk for multiple system atrophy.* Ann Neurol, 2009. **65**(5): p. 610-4.
56. Bras, J., et al., *Genetic analysis implicates APOE, SNCA and suggests lysosomal dysfunction in the etiology of dementia with Lewy bodies.* Hum Mol Genet, 2014. **23**(23): p. 6139-46.
57. Gan, L., et al., *Converging pathways in neurodegeneration, from genetics to mechanisms.* Nat Neurosci, 2018. **21**(10): p. 1300-1309.
58. Nicolia, V., M. Lucarelli, and A. Fuso, *Environment, epigenetics and neurodegeneration: Focus on nutrition in Alzheimer's disease.* Exp Gerontol, 2015. **68**: p. 8-12.
59. Fuso, A., *The 'golden age' of DNA methylation in neurodegenerative diseases.* Clin Chem Lab Med, 2013. **51**(3): p. 523-34.
60. Fuso, A., et al., *S-adenosylmethionine reduces the progress of the Alzheimer-like features induced by B-vitamin deficiency in mice.* Neurobiol Aging, 2012. **33**(7): p. 1482.e1-16.
61. Li, Y.Y., et al., *Lead exposure in pheochromocytoma cells induces persistent changes in amyloid precursor protein gene methylation patterns.* Environ Toxicol, 2012. **27**(8): p. 495-502.
62. Ryu, S.H., et al., *Transcriptional repression of repeat-derived transcripts correlates with histone hypoacetylation at repetitive DNA elements in aged mice brain.* Exp Gerontol, 2011. **46**(10): p. 811-8.
63. Jowaed, A., et al., *Methylation regulates alpha-synuclein expression and is decreased in Parkinson's disease patients' brains.* J Neurosci, 2010. **30**(18): p. 6355-9.
64. Doxakis, E., *Post-transcriptional regulation of alpha-synuclein expression by mir-7 and mir-153.* J Biol Chem, 2010. **285**(17): p. 12726-34.
65. Liu, B., H.M. Gao, and J.S. Hong, *Parkinson's disease and exposure to infectious agents and pesticides and the occurrence of brain injuries: role of neuroinflammation.* Environ Health Perspect, 2003. **111**(8): p. 1065-73.
66. Pang, S.Y., et al., *The interplay of aging, genetics and environmental factors in the pathogenesis of Parkinson's disease.* Transl Neurodegener, 2019. **8**: p. 23.
67. Wang, C.S., et al., *Twin pairs discordant for neuropathologically confirmed Lewy body dementia.* J Neurol Neurosurg Psychiatry, 2009. **80**(5): p. 562-5.
68. Soto, C., *Unfolding the role of protein misfolding in neurodegenerative diseases.* Nat Rev Neurosci, 2003. **4**(1): p. 49-60.

69. Bourdenx, M., et al., *Protein aggregation and neurodegeneration in prototypical neurodegenerative diseases: Examples of amyloidopathies, tauopathies and synucleinopathies.* Prog Neurobiol, 2017. **155**: p. 171-193.
70. Berg, J.M., J.L. Tymoczko, and L. Stryer, *Biochemistry*. 2002, New York; [Basingstoke]: W.H. Freeman and Co. ; [Palgrave].
71. Dyson, H.J. and P.E. Wright, *Intrinsically unstructured proteins and their functions.* Nat Rev Mol Cell Biol, 2005. **6**(3): p. 197-208.
72. Leopold, P.E., M. Montal, and J.N. Onuchic, *Protein folding funnels: a kinetic approach to the sequence-structure relationship.* Proc Natl Acad Sci U S A, 1992. **89**(18): p. 8721-5.
73. Pace, C.N., et al., *Forces contributing to the conformational stability of proteins.* Faseb j, 1996. **10**(1): p. 75-83.
74. Callaway, D.J., *Solvent-induced organization: a physical model of folding myoglobin.* Proteins, 1994. **20**(2): p. 124-38.
75. Chen, B., et al., *Cellular strategies of protein quality control.* Cold Spring Harb Perspect Biol, 2011. **3**(8): p. a004374.
76. Uversky, V.N., *Intrinsically disordered proteins and their (disordered) proteomes in neurodegenerative disorders.* Front Aging Neurosci, 2015. **7**: p. 18.
77. Uversky, V.N. and A.L. Fink, *Conformational constraints for amyloid fibrillation: the importance of being unfolded.* Biochim Biophys Acta, 2004. **1698**(2): p. 131-53.
78. Uversky, V.N., *Amyloidogenesis of natively unfolded proteins.* Curr Alzheimer Res, 2008. **5**(3): p. 260-87.
79. Herczenik, E. and M.F. Gebbink, *Molecular and cellular aspects of protein misfolding and disease.* Faseb j, 2008. **22**(7): p. 2115-33.
80. Soto, C., *Protein misfolding and disease; protein refolding and therapy.* FEBS Lett, 2001. **498**(2-3): p. 204-7.
81. Roberts, C.J., *Non-native protein aggregation kinetics.* Biotechnol Bioeng, 2007. **98**(5): p. 927-38.
82. Nelson, R., et al., *Structure of the cross-beta spine of amyloid-like fibrils.* Nature, 2005. **435**(7043): p. 773-8.
83. Glabe, C.G., *Common mechanisms of amyloid oligomer pathogenesis in degenerative disease.* Neurobiol Aging, 2006. **27**(4): p. 570-5.
84. Walsh, D.M. and D.J. Selkoe, *A beta oligomers - a decade of discovery.* J Neurochem, 2007. **101**(5): p. 1172-84.
85. Ladiwala, A.R., J.S. Dordick, and P.M. Tessier, *Aromatic small molecules remodel toxic soluble oligomers of amyloid beta through three independent pathways.* J Biol Chem, 2011. **286**(5): p. 3209-18.
86. Wu, J.W., et al., *Fibrillar oligomers nucleate the oligomerization of monomeric amyloid beta but do not seed fibril formation.* J Biol Chem, 2010. **285**(9): p. 6071-9.
87. Yu, L., et al., *Structural characterization of a soluble amyloid beta-peptide oligomer.* Biochemistry, 2009. **48**(9): p. 1870-7.
88. Kayed, R., et al., *Common structure of soluble amyloid oligomers implies common mechanism of pathogenesis.* Science, 2003. **300**(5618): p. 486-9.
89. Kayed, R., et al., *Fibril specific, conformation dependent antibodies recognize a generic epitope common to amyloid fibrils and fibrillar oligomers that is absent in prefibrillar oligomers.* Mol Neurodegener, 2007. **2**: p. 18.
90. Caughey, B. and P.T. Lansbury, *Protofibrils, pores, fibrils, and neurodegeneration: separating the responsible protein aggregates from the innocent bystanders.* Annu Rev Neurosci, 2003. **26**: p. 267-98.

91. Jarrett, J.T. and P.T. Lansbury, Jr., *Seeding "one-dimensional crystallization" of amyloid: a pathogenic mechanism in Alzheimer's disease and scrapie?* Cell, 1993. **73**(6): p. 1055-8.
92. Meisl, G., et al., *Scaling behaviour and rate-determining steps in filamentous self-assembly.* Chem Sci, 2017. **8**(10): p. 7087-7097.
93. Marrero-Winkens, C., C. Sankaran, and H.M. Schätzl, *From Seeds to Fibrils and Back: Fragmentation as an Overlooked Step in the Propagation of Prions and Prion-Like Proteins.* Biomolecules, 2020. **10**(9).
94. *<PhDthesis_MahafuzurRahman.pdf>.*
95. Saborio, G.P., B. Permanne, and C. Soto, *Sensitive detection of pathological prion protein by cyclic amplification of protein misfolding.* Nature, 2001. **411**(6839): p. 810-3.
96. Atarashi, R., et al., *Real-time quaking-induced conversion: a highly sensitive assay for prion detection.* Prion, 2011. **5**(3): p. 150-3.
97. Atarashi, R., et al., *Simplified ultrasensitive prion detection by recombinant PrP conversion with shaking.* Nat Methods, 2008. **5**(3): p. 211-2.
98. Salvadores, N., et al., *Detection of misfolded Aβ oligomers for sensitive biochemical diagnosis of Alzheimer's disease.* Cell Rep, 2014. **7**(1): p. 261-8.
99. Fairfoul, G., et al., *Alpha-synuclein RT-QuIC in the CSF of patients with alpha-synucleinopathies.* Ann Clin Transl Neurol, 2016. **3**(10): p. 812-818.
100. Meyer, V., et al., *Amplification of Tau fibrils from minute quantities of seeds.* Biochemistry, 2014. **53**(36): p. 5804-9.
101. Scialò, C., et al., *TDP-43 real-time quaking induced conversion reaction optimization and detection of seeding activity in CSF of amyotrophic lateral sclerosis and frontotemporal dementia patients.* Brain Commun, 2020. **2**(2): p. fcaa142.
102. Yan, S.D., et al., *Receptor-dependent cell stress and amyloid accumulation in systemic amyloidosis.* Nat Med, 2000. **6**(6): p. 643-51.
103. Ii, K., et al., *Immunocytochemical co-localization of the proteasome in ubiquitinated structures in neurodegenerative diseases and the elderly.* J Neuropathol Exp Neurol, 1997. **56**(2): p. 125-31.
104. Lepock, J.R., *Role of nuclear protein denaturation and aggregation in thermal radiosensitization.* Int J Hyperthermia, 2004. **20**(2): p. 115-30.
105. Tompa, P. and G.D. Rose, *The Levinthal paradox of the interactome.* Protein Sci, 2011. **20**(12): p. 2074-9.
106. Wyss-Coray, T. and L. Mucke, *Inflammation in neurodegenerative disease--a double-edged sword.* Neuron, 2002. **35**(3): p. 419-32.
107. Abramov, A.Y., et al., *Interaction of Oxidative Stress and Misfolded Proteins in the Mechanism of Neurodegeneration.* Life (Basel), 2020. **10**(7).
108. Taylor, R.C. and A. Dillin, *Aging as an event of proteostasis collapse.* Cold Spring Harb Perspect Biol, 2011. **3**(5).
109. Soto, C. and S. Pritzkow, *Protein misfolding, aggregation, and conformational strains in neurodegenerative diseases.* Nat Neurosci, 2018. **21**(10): p. 1332-1340.
110. Verma, M., A. Vats, and V. Taneja, *Toxic species in amyloid disorders: Oligomers or mature fibrils.* Ann Indian Acad Neurol, 2015. **18**(2): p. 138-45.
111. Lambert, M.P., et al., *Diffusible, nonfibrillar ligands derived from Abeta1-42 are potent central nervous system neurotoxins.* Proc Natl Acad Sci U S A, 1998. **95**(11): p. 6448-53.
112. Surmeier, D.J., J.A. Obeso, and G.M. Halliday, *Selective neuronal vulnerability in Parkinson disease.* Nat Rev Neurosci, 2017. **18**(2): p. 101-113.
113. Brichta, L. and P. Greengard, *Molecular determinants of selective dopaminergic vulnerability in Parkinson's disease: an update.* Front Neuroanat, 2014. **8**: p. 152.

114. Muratore, C.R., et al., *Cell-type Dependent Alzheimer's Disease Phenotypes: Probing the Biology of Selective Neuronal Vulnerability.* Stem Cell Reports, 2017. **9**(6): p. 1868-1884.
115. Braak, H. and K. Del Tredici, *Neuroanatomy and pathology of sporadic Parkinson's disease.* Adv Anat Embryol Cell Biol, 2009. **201**: p. 1-119.
116. Braak, H. and E. Braak, *Neuropathological stageing of Alzheimer-related changes.* Acta Neuropathol, 1991. **82**(4): p. 239-59.
117. Glass, C.K., et al., *Mechanisms underlying inflammation in neurodegeneration.* Cell, 2010. **140**(6): p. 918-34.
118. Guo, J.L. and V.M. Lee, *Cell-to-cell transmission of pathogenic proteins in neurodegenerative diseases.* Nat Med, 2014. **20**(2): p. 130-8.
119. Stopschinski, B.E. and M.I. Diamond, *The prion model for progression and diversity of neurodegenerative diseases.* Lancet Neurol, 2017. **16**(4): p. 323-332.
120. Soto, C., *Transmissible proteins: expanding the prion heresy.* Cell, 2012. **149**(5): p. 968-77.
121. Goedert, M., *NEURODEGENERATION. Alzheimer's and Parkinson's diseases: The prion concept in relation to assembled Aβ, tau, and α-synuclein.* Science, 2015. **349**(6248): p. 1255555.
122. Jucker, M. and L.C. Walker, *Self-propagation of pathogenic protein aggregates in neurodegenerative diseases.* Nature, 2013. **501**(7465): p. 45-51.
123. Edskes, H.K., et al., *Prion variants and species barriers among Saccharomyces Ure2 proteins.* Genetics, 2009. **181**(3): p. 1159-67.
124. Wickner, R.B., et al., *Prion variants, species barriers, generation and propagation.* J Biol, 2009. **8**(5): p. 47.
125. Moore, R.A., I. Vorberg, and S.A. Priola, *Species barriers in prion diseases--brief review.* Arch Virol Suppl, 2005(19): p. 187-202.
126. Bruce, M.E., et al., *Transmissions to mice indicate that 'new variant' CJD is caused by the BSE agent.* Nature, 1997. **389**(6650): p. 498-501.
127. Marsh, A.P., *Molecular mechanisms of proteinopathies across neurodegenerative disease: a review.* Neurol Res Pract, 2019. **1**: p. 35.
128. Beekes, M., et al., *Is there a risk of prion-like disease transmission by Alzheimer- or Parkinson-associated protein particles?* Acta Neuropathol, 2014. **128**(4): p. 463-76.
129. Irwin, D.J., et al., *Evaluation of potential infectivity of Alzheimer and Parkinson disease proteins in recipients of cadaver-derived human growth hormone.* JAMA Neurol, 2013. **70**(4): p. 462-8.
130. Jaunmuktane, Z., et al., *Evidence for human transmission of amyloid-β pathology and cerebral amyloid angiopathy.* Nature, 2015. **525**(7568): p. 247-50.
131. Purro, S.A., et al., *Transmission of amyloid-β protein pathology from cadaveric pituitary growth hormone.* Nature, 2018. **564**(7736): p. 415-419.
132. Kordower, J.H., et al., *Lewy body-like pathology in long-term embryonic nigral transplants in Parkinson's disease.* Nat Med, 2008. **14**(5): p. 504-6.
133. Li, J.Y., et al., *Lewy bodies in grafted neurons in subjects with Parkinson's disease suggest host-to-graft disease propagation.* Nat Med, 2008. **14**(5): p. 501-3.
134. Eisele, Y.S., et al., *Induction of cerebral beta-amyloidosis: intracerebral versus systemic Abeta inoculation.* Proc Natl Acad Sci U S A, 2009. **106**(31): p. 12926-31.
135. Desplats, P., et al., *Inclusion formation and neuronal cell death through neuron-to-neuron transmission of alpha-synuclein.* Proc Natl Acad Sci U S A, 2009. **106**(31): p. 13010-5.
136. Luk, K.C., et al., *Intracerebral inoculation of pathological α-synuclein initiates a rapidly progressive neurodegenerative α-synucleinopathy in mice.* J Exp Med, 2012. **209**(5): p. 975-86.
137. Clavaguera, F., et al., *Brain homogenates from human tauopathies induce tau inclusions in mouse brain.* Proc Natl Acad Sci U S A, 2013. **110**(23): p. 9535-40.

138. Morales, R., et al., *De novo induction of amyloid-β deposition in vivo.* Mol Psychiatry, 2012. **17**(12): p. 1347-53.
139. Luk, K.C., et al., *Pathological α-synuclein transmission initiates Parkinson-like neurodegeneration in nontransgenic mice.* Science, 2012. **338**(6109): p. 949-53.
140. Reyes, J.F., N.L. Rey, and E. Angot, *Transmission of tau pathology induced by synthetic preformed tau filaments.* J Neurosci, 2013. **33**(16): p. 6707-8.
141. Iba, M., et al., *Synthetic tau fibrils mediate transmission of neurofibrillary tangles in a transgenic mouse model of Alzheimer's-like tauopathy.* J Neurosci, 2013. **33**(3): p. 1024-37.
142. Meyer-Luehmann, M., et al., *Exogenous induction of cerebral beta-amyloidogenesis is governed by agent and host.* Science, 2006. **313**(5794): p. 1781-4.
143. Duran-Aniotz, C., et al., *Aggregate-depleted brain fails to induce Aβ deposition in a mouse model of Alzheimer's disease.* PLoS One, 2014. **9**(2): p. e89014.
144. Tran, H.T., et al., *A-synuclein immunotherapy blocks uptake and templated propagation of misfolded α-synuclein and neurodegeneration.* Cell Rep, 2014. **7**(6): p. 2054-65.
145. Morales, R., et al., *Titration of biologically active amyloid-β seeds in a transgenic mouse model of Alzheimer's disease.* Sci Rep, 2015. **5**: p. 9349.
146. Maniecka, Z. and M. Polymenidou, *From nucleation to widespread propagation: A prion-like concept for ALS.* Virus Res, 2015. **207**: p. 94-105.
147. Westergard, T., et al., *Cell-to-Cell Transmission of Dipeptide Repeat Proteins Linked to C9orf72-ALS/FTD.* Cell Rep, 2016. **17**(3): p. 645-652.
148. Babcock, D.T. and B. Ganetzky, *Transcellular spreading of huntingtin aggregates in the Drosophila brain.* Proc Natl Acad Sci U S A, 2015. **112**(39): p. E5427-33.
149. Jeon, I., et al., *Human-to-mouse prion-like propagation of mutant huntingtin protein.* Acta Neuropathol, 2016. **132**(4): p. 577-92.
150. Peelaerts, W., et al., *α-Synuclein strains cause distinct synucleinopathies after local and systemic administration.* Nature, 2015. **522**(7556): p. 340-4.
151. Clavaguera, F., et al., *Peripheral administration of tau aggregates triggers intracerebral tauopathy in transgenic mice.* Acta Neuropathol, 2014. **127**(2): p. 299-301.
152. Eisele, Y.S., et al., *Peripherally applied Abeta-containing inoculates induce cerebral beta-amyloidosis.* Science, 2010. **330**(6006): p. 980-2.
153. Eisele, Y.S., et al., *Multiple factors contribute to the peripheral induction of cerebral β-amyloidosis.* J Neurosci, 2014. **34**(31): p. 10264-73.
154. Kuan, W.L., et al., *Systemic α-synuclein injection triggers selective neuronal pathology as seen in patients with Parkinson's disease.* Mol Psychiatry, 2021. **26**(2): p. 556-567.
155. Moreno-Gonzalez, I. and C. Soto, *Misfolded protein aggregates: mechanisms, structures and potential for disease transmission.* Semin Cell Dev Biol, 2011. **22**(5): p. 482-7.
156. Menzies, F.M., K. Moreau, and D.C. Rubinsztein, *Protein misfolding disorders and macroautophagy.* Curr Opin Cell Biol, 2011. **23**(2): p. 190-7.
157. Metcalf, D.J., et al., *Autophagy and misfolded proteins in neurodegeneration.* Exp Neurol, 2012. **238**(1): p. 22-8.
158. Kovács, G.G., et al., *Subcellular localization of disease-associated prion protein in the human brain.* Am J Pathol, 2005. **166**(1): p. 287-94.
159. Rajendran, L., et al., *Alzheimer's disease beta-amyloid peptides are released in association with exosomes.* Proc Natl Acad Sci U S A, 2006. **103**(30): p. 11172-7.
160. Lee, H.J., S. Patel, and S.J. Lee, *Intravesicular localization and exocytosis of alpha-synuclein and its aggregates.* J Neurosci, 2005. **25**(25): p. 6016-24.
161. Stuendl, A., et al., *Induction of α-synuclein aggregate formation by CSF exosomes from patients with Parkinson's disease and dementia with Lewy bodies.* Brain, 2016. **139**(Pt 2): p. 481-94.

162. Aguzzi, A. and L. Rajendran, *The transcellular spread of cytosolic amyloids, prions, and prionoids.* Neuron, 2009. **64**(6): p. 783-90.
163. Gousset, K., et al., *Prions hijack tunnelling nanotubes for intercellular spread.* Nat Cell Biol, 2009. **11**(3): p. 328-36.
164. Victoria, G.S. and C. Zurzolo, *The spread of prion-like proteins by lysosomes and tunneling nanotubes: Implications for neurodegenerative diseases.* J Cell Biol, 2017. **216**(9): p. 2633-2644.
165. Abounit, S., et al., *Tunneling nanotubes: A possible highway in the spreading of tau and other prion-like proteins in neurodegenerative diseases.* Prion, 2016. **10**(5): p. 344-351.
166. Burdick, D., et al., *Preferential adsorption, internalization and resistance to degradation of the major isoform of the Alzheimer's amyloid peptide, A beta 1-42, in differentiated PC12 cells.* Brain Res, 1997. **746**(1-2): p. 275-84.
167. Nagele, R.G., et al., *Intracellular accumulation of beta-amyloid(1-42) in neurons is facilitated by the alpha 7 nicotinic acetylcholine receptor in Alzheimer's disease.* Neuroscience, 2002. **110**(2): p. 199-211.
168. Sung, J.Y., et al., *Induction of neuronal cell death by Rab5A-dependent endocytosis of alpha-synuclein.* J Biol Chem, 2001. **276**(29): p. 27441-8.
169. Frost, B., R.L. Jacks, and M.I. Diamond, *Propagation of tau misfolding from the outside to the inside of a cell.* J Biol Chem, 2009. **284**(19): p. 12845-52.
170. Flavin, W.P., et al., *Endocytic vesicle rupture is a conserved mechanism of cellular invasion by amyloid proteins.* Acta Neuropathol, 2017. **134**(4): p. 629-653.
171. Calafate, S., et al., *Loss of Bin1 Promotes the Propagation of Tau Pathology.* Cell Rep, 2016. **17**(4): p. 931-940.
172. Morales, R., K.M. Green, and C. Soto, *Cross currents in protein misfolding disorders: interactions and therapy.* CNS Neurol Disord Drug Targets, 2009. **8**(5): p. 363-71.
173. Hamilton, R.L., *Lewy bodies in Alzheimer's disease: a neuropathological review of 145 cases using alpha-synuclein immunohistochemistry.* Brain Pathol, 2000. **10**(3): p. 378-84.
174. Tsuchiya, K., et al., *Coexistence of CJD and Alzheimer's disease: an autopsy case showing typical clinical features of CJD.* Neuropathology, 2004. **24**(1): p. 46-55.
175. Miyazono, M., et al., *Colocalization of prion protein and beta protein in the same amyloid plaques in patients with Gerstmann-Sträussler syndrome.* Acta Neuropathol, 1992. **83**(4): p. 333-9.
176. Clinton, L.K., et al., *Synergistic Interactions between Abeta, tau, and alpha-synuclein: acceleration of neuropathology and cognitive decline.* J Neurosci, 2010. **30**(21): p. 7281-9.
177. Astbury, W.T., S. Dickinson, and K. Bailey, *The X-ray interpretation of denaturation and the structure of the seed globulins.* Biochem J, 1935. **29**(10): p. 2351-2360.1.
178. Rudall, K.M., *The proteins of the mammalian epidermis.* Adv Protein Chem, 1952. **7**: p. 253-90.
179. Meredith, S.C., *Protein denaturation and aggregation: Cellular responses to denatured and aggregated proteins.* Ann N Y Acad Sci, 2005. **1066**: p. 181-221.
180. Jenkins, J. and R. Pickersgill, *The architecture of parallel beta-helices and related folds.* Prog Biophys Mol Biol, 2001. **77**(2): p. 111-75.
181. Chan, J.C., et al., *Parallel beta-sheets and polar zippers in amyloid fibrils formed by residues 10-39 of the yeast prion protein Ure2p.* Biochemistry, 2005. **44**(31): p. 10669-80.
182. Roher, A.E., et al., *Oligomerizaiton and fibril asssembly of the amyloid-beta protein.* Biochim Biophys Acta, 2000. **1502**(1): p. 31-43.
183. Chaney, M.O., et al., *Molecular modeling of the Abeta1-42 peptide from Alzheimer's disease.* Protein Eng, 1998. **11**(9): p. 761-7.
184. Eisenberg, D., et al., *The structural biology of protein aggregation diseases: Fundamental questions and some answers.* Acc Chem Res, 2006. **39**(9): p. 568-75.

185. Sawaya, M.R., et al., *Atomic structures of amyloid cross-beta spines reveal varied steric zippers.* Nature, 2007. **447**(7143): p. 453-7.
186. Miller, Y., B. Ma, and R. Nussinov, *Polymorphism in Alzheimer Abeta amyloid organization reflects conformational selection in a rugged energy landscape.* Chem Rev, 2010. **110**(8): p. 4820-38.
187. Aguzzi, A., M. Heikenwalder, and M. Polymenidou, *Insights into prion strains and neurotoxicity.* Nat Rev Mol Cell Biol, 2007. **8**(7): p. 552-61.
188. Morales, R., *Prion strains in mammals: Different conformations leading to disease.* PLoS Pathog, 2017. **13**(7): p. e1006323.
189. Poggiolini, I., D. Saverioni, and P. Parchi, *Prion protein misfolding, strains, and neurotoxicity: an update from studies on Mammalian prions.* Int J Cell Biol, 2013. **2013**: p. 910314.
190. Castilla, J., et al., *Cell-free propagation of prion strains.* Embo j, 2008. **27**(19): p. 2557-66.
191. Tian, Y., L. Meng, and Z. Zhang, *What is strain in neurodegenerative diseases?* Cell Mol Life Sci, 2020. **77**(4): p. 665-676.
192. Kam, T.I., et al., *Poly(ADP-ribose) drives pathologic α-synuclein neurodegeneration in Parkinson's disease.* Science, 2018. **362**(6414).
193. De Franceschi, G., et al., *Structural and morphological characterization of aggregated species of α-synuclein induced by docosahexaenoic acid.* J Biol Chem, 2011. **286**(25): p. 22262-74.
194. Miura, T., et al., *Metal binding modes of Alzheimer's amyloid beta-peptide in insoluble aggregates and soluble complexes.* Biochemistry, 2000. **39**(23): p. 7024-31.
195. Li, D. and C. Liu, *Hierarchical chemical determination of amyloid polymorphs in neurodegenerative disease.* Nat Chem Biol, 2021. **17**(3): p. 237-245.
196. Peng, C., J.Q. Trojanowski, and V.M. Lee, *Protein transmission in neurodegenerative disease.* Nat Rev Neurol, 2020. **16**(4): p. 199-212.
197. Scialò, C., et al., *Prion and Prion-Like Protein Strains: Deciphering the Molecular Basis of Heterogeneity in Neurodegeneration.* Viruses, 2019. **11**(3).
198. Collinge, J. and A.R. Clarke, *A general model of prion strains and their pathogenicity.* Science, 2007. **318**(5852): p. 930-6.
199. Petkova, A.T., et al., *Self-propagating, molecular-level polymorphism in Alzheimer's beta-amyloid fibrils.* Science, 2005. **307**(5707): p. 262-5.
200. Lu, J.X., et al., *Molecular structure of β-amyloid fibrils in Alzheimer's disease brain tissue.* Cell, 2013. **154**(6): p. 1257-68.
201. Stöhr, J., et al., *Distinct synthetic Aβ prion strains producing different amyloid deposits in bigenic mice.* Proc Natl Acad Sci U S A, 2014. **111**(28): p. 10329-34.
202. Watts, J.C., et al., *Serial propagation of distinct strains of Aβ prions from Alzheimer's disease patients.* Proc Natl Acad Sci U S A, 2014. **111**(28): p. 10323-8.
203. Arnold, S.E., et al., *Comparative survey of the topographical distribution of signature molecular lesions in major neurodegenerative diseases.* J Comp Neurol, 2013. **521**(18): p. 4339-55.
204. Williams, D.R., *Tauopathies: classification and clinical update on neurodegenerative diseases associated with microtubule-associated protein tau.* Intern Med J, 2006. **36**(10): p. 652-60.
205. Goedert, M., R. Jakes, and M.G. Spillantini, *The Synucleinopathies: Twenty Years On.* J Parkinsons Dis, 2017. **7**(s1): p. S51-s69.
206. Fitzpatrick, A.W.P., et al., *Cryo-EM structures of tau filaments from Alzheimer's disease.* Nature, 2017. **547**(7662): p. 185-190.
207. Kaufman, S.K., et al., *Tau Prion Strains Dictate Patterns of Cell Pathology, Progression Rate, and Regional Vulnerability In Vivo.* Neuron, 2016. **92**(4): p. 796-812.
208. Sanders, D.W., et al., *Distinct tau prion strains propagate in cells and mice and define different tauopathies.* Neuron, 2014. **82**(6): p. 1271-88.

209. Zhang, W., et al., *Novel tau filament fold in corticobasal degeneration.* Nature, 2020. **580**(7802): p. 283-287.
210. Falcon, B., et al., *Novel tau filament fold in chronic traumatic encephalopathy encloses hydrophobic molecules.* Nature, 2019. **568**(7752): p. 420-423.
211. Falcon, B., et al., *Structures of filaments from Pick's disease reveal a novel tau protein fold.* Nature, 2018. **561**(7721): p. 137-140.
212. Arakhamia, T., et al., *Posttranslational Modifications Mediate the Structural Diversity of Tauopathy Strains.* Cell, 2020. **180**(4): p. 633-644.e12.
213. Schweighauser, M., et al., *Structures of α-synuclein filaments from multiple system atrophy.* Nature, 2020. **585**(7825): p. 464-469.
214. Prusiner, S.B., et al., *Evidence for α-synuclein prions causing multiple system atrophy in humans with parkinsonism.* Proc Natl Acad Sci U S A, 2015. **112**(38): p. E5308-17.
215. Woerman, A.L., et al., *Propagation of prions causing synucleinopathies in cultured cells.* Proc Natl Acad Sci U S A, 2015. **112**(35): p. E4949-58.
216. Brettschneider, J., et al., *Converging Patterns of α-Synuclein Pathology in Multiple System Atrophy.* J Neuropathol Exp Neurol, 2018. **77**(11): p. 1005-1016.
217. Peng, C., et al., *Cellular milieu imparts distinct pathological α-synuclein strains in α-synucleinopathies.* Nature, 2018. **557**(7706): p. 558-563.
218. Bousset, L., et al., *Structural and functional characterization of two alpha-synuclein strains.* Nat Commun, 2013. **4**: p. 2575.
219. Furukawa, Y., et al., *Mutation-dependent polymorphism of Cu,Zn-superoxide dismutase aggregates in the familial form of amyotrophic lateral sclerosis.* J Biol Chem, 2010. **285**(29): p. 22221-31.
220. Nekooki-Machida, Y., et al., *Distinct conformations of in vitro and in vivo amyloids of huntingtin-exon1 show different cytotoxicity.* Proc Natl Acad Sci U S A, 2009. **106**(24): p. 9679-84.
221. Lee, A. and R.M. Gilbert, *Epidemiology of Parkinson Disease.* Neurol Clin, 2016. **34**(4): p. 955-965.
222. de Lau, L.M. and M.M. Breteler, *Epidemiology of Parkinson's disease.* Lancet Neurol, 2006. **5**(6): p. 525-35.
223. Dorsey, E.R., et al., *Projected number of people with Parkinson disease in the most populous nations, 2005 through 2030.* Neurology, 2007. **68**(5): p. 384-6.
224. Schulte, C. and T. Gasser, *Genetic basis of Parkinson's disease: inheritance, penetrance, and expression.* Appl Clin Genet, 2011. **4**: p. 67-80.
225. Langston, J.W. and P.A. Ballard, Jr., *Parkinson's disease in a chemist working with 1-methyl-4-phenyl-1,2,5,6-tetrahydropyridine.* N Engl J Med, 1983. **309**(5): p. 310.
226. Olanow, C.W. and W.G. Tatton, *Etiology and pathogenesis of Parkinson's disease.* Annu Rev Neurosci, 1999. **22**: p. 123-44.
227. Jankovic, J., *Parkinson's disease: clinical features and diagnosis.* J Neurol Neurosurg Psychiatry, 2008. **79**(4): p. 368-76.
228. Fereshtehnejad, S.M., et al., *Heterogeneous Determinants of Quality of Life in Different Phenotypes of Parkinson's Disease.* PLoS One, 2015. **10**(9): p. e0137081.
229. Kalia, L.V. and A.E. Lang, *Parkinson's disease.* Lancet, 2015. **386**(9996): p. 896-912.
230. Rajput, A.H., et al., *Course in Parkinson disease subtypes: A 39-year clinicopathologic study.* Neurology, 2009. **73**(3): p. 206-12.
231. Rodrigues, T.M., A. Castro Caldas, and J.J. Ferreira, *Pharmacological interventions for daytime sleepiness and sleep disorders in Parkinson's disease: Systematic review and meta-analysis.* Parkinsonism Relat Disord, 2016. **27**: p. 25-34.

232. Jellinger, K.A., *Neuropathobiology of non-motor symptoms in Parkinson disease.* J Neural Transm (Vienna), 2015. **122**(10): p. 1429-40.
233. Espay, A.J., P.A. LeWitt, and H. Kaufmann, *Norepinephrine deficiency in Parkinson's disease: the case for noradrenergic enhancement.* Mov Disord, 2014. **29**(14): p. 1710-9.
234. Marras, C. and K.R. Chaudhuri, *Nonmotor features of Parkinson's disease subtypes.* Mov Disord, 2016. **31**(8): p. 1095-102.
235. Giguère, N., S. Burke Nanni, and L.E. Trudeau, *On Cell Loss and Selective Vulnerability of Neuronal Populations in Parkinson's Disease.* Front Neurol, 2018. **9**: p. 455.
236. Kalia, L.V., J.M. Brotchie, and S.H. Fox, *Novel nondopaminergic targets for motor features of Parkinson's disease: review of recent trials.* Mov Disord, 2013. **28**(2): p. 131-44.
237. Chaudhuri, K.R., D.G. Healy, and A.H. Schapira, *Non-motor symptoms of Parkinson's disease: diagnosis and management.* Lancet Neurol, 2006. **5**(3): p. 235-45.
238. McCann, H., et al., *α-Synucleinopathy phenotypes.* Parkinsonism Relat Disord, 2014. **20 Suppl 1**: p. S62-7.
239. Halliday, G.M. and H. McCann, *The progression of pathology in Parkinson's disease.* Ann N Y Acad Sci, 2010. **1184**: p. 188-95.
240. Spillantini, M.G., et al., *alpha-Synuclein in filamentous inclusions of Lewy bodies from Parkinson's disease and dementia with lewy bodies.* Proc Natl Acad Sci U S A, 1998. **95**(11): p. 6469-73.
241. Kouli, A., K.M. Torsney, and W.L. Kuan, *Parkinson's Disease: Etiology, Neuropathology, and Pathogenesis*, in *Parkinson's Disease: Pathogenesis and Clinical Aspects*, T.B. Stoker and J.C. Greenland, Editors. 2018, Codon PublicationsCopyright: The Authors.: Brisbane (AU).
242. Xia, Q., et al., *Proteomic identification of novel proteins associated with Lewy bodies.* Front Biosci, 2008. **13**: p. 3850-6.
243. Hawkes, C.H., K. Del Tredici, and H. Braak, *Parkinson's disease: a dual-hit hypothesis.* Neuropathol Appl Neurobiol, 2007. **33**(6): p. 599-614.
244. Mayo, M.C. and Y. Bordelon, *Dementia with Lewy bodies.* Semin Neurol, 2014. **34**(2): p. 182-8.
245. Hogan, D.B., et al., *The Prevalence and Incidence of Dementia with Lewy Bodies: a Systematic Review.* Can J Neurol Sci, 2016. **43 Suppl 1**: p. S83-95.
246. Ransmayr, G., *Dementia with Lewy bodies: prevalence, clinical spectrum and natural history.* J Neural Transm Suppl, 2000(60): p. 303-14.
247. Weil, R.S., et al., *Current concepts and controversies in the pathogenesis of Parkinson's disease dementia and Dementia with Lewy Bodies.* F1000Res, 2017. **6**: p. 1604.
248. Moskvina, V., et al., *Analysis of genome-wide association studies of Alzheimer disease and of Parkinson disease to determine if these 2 diseases share a common genetic risk.* JAMA Neurol, 2013. **70**(10): p. 1268-76.
249. Galasko, D., *Lewy Body Disorders.* Neurol Clin, 2017. **35**(2): p. 325-338.
250. Burn, D.J., et al., *Motor subtype and cognitive decline in Parkinson's disease, Parkinson's disease with dementia, and dementia with Lewy bodies.* J Neurol Neurosurg Psychiatry, 2006. **77**(5): p. 585-9.
251. McKeith, I.G., et al., *Diagnosis and management of dementia with Lewy bodies: Fourth consensus report of the DLB Consortium.* Neurology, 2017. **89**(1): p. 88-100.
252. Harding, A.J. and G.M. Halliday, *Cortical Lewy body pathology in the diagnosis of dementia.* Acta Neuropathol, 2001. **102**(4): p. 355-63.
253. Piggott, M.A., et al., *Striatal dopaminergic markers in dementia with Lewy bodies, Alzheimer's and Parkinson's diseases: rostrocaudal distribution.* Brain, 1999. **122 (Pt 8)**: p. 1449-68.
254. Halliday, G.M., et al., *Neuropathology underlying clinical variability in patients with synucleinopathies.* Acta Neuropathol, 2011. **122**(2): p. 187-204.

255. Ballard, C., et al., *Differences in neuropathologic characteristics across the Lewy body dementia spectrum.* Neurology, 2006. **67**(11): p. 1931-4.
256. Lopez, O.L., et al., *Research evaluation and prospective diagnosis of dementia with Lewy bodies.* Arch Neurol, 2002. **59**(1): p. 43-6.
257. Wenning, G.K., et al., *The natural history of multiple system atrophy: a prospective European cohort study.* Lancet Neurol, 2013. **12**(3): p. 264-74.
258. Schrag, A., Y. Ben-Shlomo, and N.P. Quinn, *Prevalence of progressive supranuclear palsy and multiple system atrophy: a cross-sectional study.* Lancet, 1999. **354**(9192): p. 1771-5.
259. Sailer, A., et al., *A genome-wide association study in multiple system atrophy.* Neurology, 2016. **87**(15): p. 1591-1598.
260. Gilman, S., et al., *Second consensus statement on the diagnosis of multiple system atrophy.* Neurology, 2008. **71**(9): p. 670-6.
261. Fanciulli, A. and G.K. Wenning, *Multiple-system atrophy.* N Engl J Med, 2015. **372**(14): p. 1375-6.
262. Geser, F., et al., *Progression of multiple system atrophy (MSA): a prospective natural history study by the European MSA Study Group (EMSA SG).* Mov Disord, 2006. **21**(2): p. 179-86.
263. Ozawa, T., et al., *The spectrum of pathological involvement of the striatonigral and olivopontocerebellar systems in multiple system atrophy: clinicopathological correlations.* Brain, 2004. **127**(Pt 12): p. 2657-71.
264. Köllensperger, M., et al., *Red flags for multiple system atrophy.* Mov Disord, 2008. **23**(8): p. 1093-9.
265. Wenning, G.K., et al., *Multiple system atrophy.* Lancet Neurol, 2004. **3**(2): p. 93-103.
266. Yuan, J. and Y. Zhao, *Evolutionary aspects of the synuclein super-family and sub-families based on large-scale phylogenetic and group-discrimination analysis.* Biochem Biophys Res Commun, 2013. **441**(2): p. 308-17.
267. Janeczek, P. and J.M. Lewohl, *The role of α-synuclein in the pathophysiology of alcoholism.* Neurochem Int, 2013. **63**(3): p. 154-62.
268. Uéda, K., et al., *Molecular cloning of cDNA encoding an unrecognized component of amyloid in Alzheimer disease.* Proc Natl Acad Sci U S A, 1993. **90**(23): p. 11282-6.
269. George, J.M., *The synucleins.* Genome Biol, 2002. **3**(1): p. Reviews3002.
270. Giasson, B.I., et al., *A hydrophobic stretch of 12 amino acid residues in the middle of alpha-synuclein is essential for filament assembly.* J Biol Chem, 2001. **276**(4): p. 2380-6.
271. Miake, H., et al., *Biochemical characterization of the core structure of alpha-synuclein filaments.* J Biol Chem, 2002. **277**(21): p. 19213-9.
272. Kim, T.D., S.R. Paik, and C.H. Yang, *Structural and functional implications of C-terminal regions of alpha-synuclein.* Biochemistry, 2002. **41**(46): p. 13782-90.
273. Deleersnijder, A., et al., *The remarkable conformational plasticity of alpha-synuclein: blessing or curse?* Trends Mol Med, 2013. **19**(6): p. 368-77.
274. Fujiwara, H., et al., *alpha-Synuclein is phosphorylated in synucleinopathy lesions.* Nat Cell Biol, 2002. **4**(2): p. 160-4.
275. Gallegos, S., et al., *Features of alpha-synuclein that could explain the progression and irreversibility of Parkinson's disease.* Front Neurosci, 2015. **9**: p. 59.
276. Fauvet, B., et al., *α-Synuclein in central nervous system and from erythrocytes, mammalian cells, and Escherichia coli exists predominantly as disordered monomer.* J Biol Chem, 2012. **287**(19): p. 15345-64.
277. Binolfi, A., F.X. Theillet, and P. Selenko, *Bacterial in-cell NMR of human α-synuclein: a disordered monomer by nature?* Biochem Soc Trans, 2012. **40**(5): p. 950-4.
278. Bartels, T., J.G. Choi, and D.J. Selkoe, *α-Synuclein occurs physiologically as a helically folded tetramer that resists aggregation.* Nature, 2011. **477**(7362): p. 107-10.

279. Ulmer, T.S., et al., *Structure and dynamics of micelle-bound human alpha-synuclein.* J Biol Chem, 2005. **280**(10): p. 9595-603.
280. Plotegher, N., et al., *Biophysical groundwork as a hinge to unravel the biology of α-synuclein aggregation and toxicity.* Q Rev Biophys, 2014. **47**(1): p. 1-48.
281. Wang, W., et al., *A soluble α-synuclein construct forms a dynamic tetramer.* Proc Natl Acad Sci U S A, 2011. **108**(43): p. 17797-802.
282. Lashuel, H.A., et al., *The many faces of α-synuclein: from structure and toxicity to therapeutic target.* Nat Rev Neurosci, 2013. **14**(1): p. 38-48.
283. Maroteaux, L., J.T. Campanelli, and R.H. Scheller, *Synuclein: a neuron-specific protein localized to the nucleus and presynaptic nerve terminal.* J Neurosci, 1988. **8**(8): p. 2804-15.
284. Del Tredici, K. and H. Braak, *Review: Sporadic Parkinson's disease: development and distribution of α-synuclein pathology.* Neuropathol Appl Neurobiol, 2016. **42**(1): p. 33-50.
285. Iwai, A., et al., *The precursor protein of non-A beta component of Alzheimer's disease amyloid is a presynaptic protein of the central nervous system.* Neuron, 1995. **14**(2): p. 467-75.
286. Bernal-Conde, L.D., et al., *Alpha-Synuclein Physiology and Pathology: A Perspective on Cellular Structures and Organelles.* Front Neurosci, 2019. **13**: p. 1399.
287. Goers, J., et al., *Nuclear localization of alpha-synuclein and its interaction with histones.* Biochemistry, 2003. **42**(28): p. 8465-71.
288. Kontopoulos, E., J.D. Parvin, and M.B. Feany, *Alpha-synuclein acts in the nucleus to inhibit histone acetylation and promote neurotoxicity.* Hum Mol Genet, 2006. **15**(20): p. 3012-23.
289. Pinho, R., et al., *Nuclear localization and phosphorylation modulate pathological effects of alpha-synuclein.* Hum Mol Genet, 2019. **28**(1): p. 31-50.
290. Schaser, A.J., et al., *Alpha-synuclein is a DNA binding protein that modulates DNA repair with implications for Lewy body disorders.* Sci Rep, 2019. **9**(1): p. 10919.
291. Colla, E., et al., *Accumulation of toxic α-synuclein oligomer within endoplasmic reticulum occurs in α-synucleinopathy in vivo.* J Neurosci, 2012. **32**(10): p. 3301-5.
292. Grassi, D., et al., *Identification of a highly neurotoxic α-synuclein species inducing mitochondrial damage and mitophagy in Parkinson's disease.* Proc Natl Acad Sci U S A, 2018. **115**(11): p. E2634-e2643.
293. Lee, H.J., et al., *Clearance of alpha-synuclein oligomeric intermediates via the lysosomal degradation pathway.* J Neurosci, 2004. **24**(8): p. 1888-96.
294. Withers, G.S., et al., *Delayed localization of synelfin (synuclein, NACP) to presynaptic terminals in cultured rat hippocampal neurons.* Brain Res Dev Brain Res, 1997. **99**(1): p. 87-94.
295. Abeliovich, A., et al., *Mice lacking alpha-synuclein display functional deficits in the nigrostriatal dopamine system.* Neuron, 2000. **25**(1): p. 239-52.
296. Davidson, W.S., et al., *Stabilization of alpha-synuclein secondary structure upon binding to synthetic membranes.* J Biol Chem, 1998. **273**(16): p. 9443-9.
297. Varkey, J., et al., *Membrane curvature induction and tubulation are common features of synucleins and apolipoproteins.* J Biol Chem, 2010. **285**(42): p. 32486-93.
298. Chandra, S., et al., *Alpha-synuclein cooperates with CSPalpha in preventing neurodegeneration.* Cell, 2005. **123**(3): p. 383-96.
299. Burré, J., et al., *Alpha-synuclein promotes SNARE-complex assembly in vivo and in vitro.* Science, 2010. **329**(5999): p. 1663-7.
300. Perlmutter, J.D., A.R. Braun, and J.N. Sachs, *Curvature dynamics of alpha-synuclein familial Parkinson disease mutants: molecular simulations of the micelle- and bilayer-bound forms.* J Biol Chem, 2009. **284**(11): p. 7177-89.
301. Souza, J.M., et al., *Chaperone-like activity of synucleins.* FEBS Lett, 2000. **474**(1): p. 116-9.

302. Ostrerova, N., et al., *alpha-Synuclein shares physical and functional homology with 14-3-3 proteins.* J Neurosci, 1999. **19**(14): p. 5782-91.
303. Perez, R.G., et al., *A role for alpha-synuclein in the regulation of dopamine biosynthesis.* J Neurosci, 2002. **22**(8): p. 3090-9.
304. Peng, X., et al., *Alpha-synuclein activation of protein phosphatase 2A reduces tyrosine hydroxylase phosphorylation in dopaminergic cells.* J Cell Sci, 2005. **118**(Pt 15): p. 3523-30.
305. Lee, F.J., et al., *Direct binding and functional coupling of alpha-synuclein to the dopamine transporters accelerate dopamine-induced apoptosis.* Faseb j, 2001. **15**(6): p. 916-26.
306. Wersinger, C. and A. Sidhu, *Attenuation of dopamine transporter activity by alpha-synuclein.* Neurosci Lett, 2003. **340**(3): p. 189-92.
307. Lee, M., et al., *Effect of the overexpression of wild-type or mutant alpha-synuclein on cell susceptibility to insult.* J Neurochem, 2001. **76**(4): p. 998-1009.
308. Hashimoto, M., et al., *alpha-Synuclein protects against oxidative stress via inactivation of the c-Jun N-terminal kinase stress-signaling pathway in neuronal cells.* J Biol Chem, 2002. **277**(13): p. 11465-72.
309. Seo, J.H., et al., *Alpha-synuclein regulates neuronal survival via Bcl-2 family expression and PI3/Akt kinase pathway.* Faseb j, 2002. **16**(13): p. 1826-8.
310. Emamzadeh, F.N., *Alpha-synuclein structure, functions, and interactions.* J Res Med Sci, 2016. **21**: p. 29.
311. Der-Sarkissian, A., et al., *Structural organization of alpha-synuclein fibrils studied by site-directed spin labeling.* J Biol Chem, 2003. **278**(39): p. 37530-5.
312. Tuttle, M.D., et al., *Solid-state NMR structure of a pathogenic fibril of full-length human α-synuclein.* Nat Struct Mol Biol, 2016. **23**(5): p. 409-15.
313. Greenbaum, E.A., et al., *The E46K mutation in alpha-synuclein increases amyloid fibril formation.* J Biol Chem, 2005. **280**(9): p. 7800-7.
314. Li, J., V.N. Uversky, and A.L. Fink, *Effect of familial Parkinson's disease point mutations A30P and A53T on the structural properties, aggregation, and fibrillation of human alpha-synuclein.* Biochemistry, 2001. **40**(38): p. 11604-13.
315. Bertoncini, C.W., et al., *Release of long-range tertiary interactions potentiates aggregation of natively unstructured alpha-synuclein.* Proc Natl Acad Sci U S A, 2005. **102**(5): p. 1430-5.
316. Bussell, R., Jr. and D. Eliezer, *Residual structure and dynamics in Parkinson's disease-associated mutants of alpha-synuclein.* J Biol Chem, 2001. **276**(49): p. 45996-6003.
317. Rospigliosi, C.C., et al., *E46K Parkinson's-linked mutation enhances C-terminal-to-N-terminal contacts in alpha-synuclein.* J Mol Biol, 2009. **388**(5): p. 1022-32.
318. McClendon, S., C.C. Rospigliosi, and D. Eliezer, *Charge neutralization and collapse of the C-terminal tail of alpha-synuclein at low pH.* Protein Sci, 2009. **18**(7): p. 1531-40.
319. Okochi, M., et al., *Constitutive phosphorylation of the Parkinson's disease associated alpha-synuclein.* J Biol Chem, 2000. **275**(1): p. 390-7.
320. Chen, L. and M.B. Feany, *Alpha-synuclein phosphorylation controls neurotoxicity and inclusion formation in a Drosophila model of Parkinson disease.* Nat Neurosci, 2005. **8**(5): p. 657-63.
321. Fujiwara, H., et al., *α-Synuclein is phosphorylated in synucleinopathy lesions.* Nature Cell Biology, 2002. **4**(2): p. 160-164.
322. Karampetsou, M., et al., *Phosphorylated exogenous alpha-synuclein fibrils exacerbate pathology and induce neuronal dysfunction in mice.* Scientific Reports, 2017. **7**(1).
323. Smith, W.W., et al., *α-Synuclein Phosphorylation Enhances Eosinophilic Cytoplasmic Inclusion Formation in SH-SY5Y Cells.* Journal of Neuroscience, 2005. **25**(23): p. 5544-5552.
324. Chen, L., et al., *Tyrosine and serine phosphorylation of alpha-synuclein have opposing effects on neurotoxicity and soluble oligomer formation.* J Clin Invest, 2009. **119**(11): p. 3257-65.

325. Rott, R., et al., *Monoubiquitylation of alpha-synuclein by seven in absentia homolog (SIAH) promotes its aggregation in dopaminergic cells.* J Biol Chem, 2008. **283**(6): p. 3316-3328.
326. Hejjaoui, M., et al., *Towards elucidation of the role of ubiquitination in the pathogenesis of Parkinson's disease with semisynthetic ubiquitinated α-synuclein.* Angew Chem Int Ed Engl, 2011. **50**(2): p. 405-9.
327. Oh, Y., et al., *Human Polycomb protein 2 promotes α-synuclein aggregate formation through covalent SUMOylation.* Brain Res, 2011. **1381**: p. 78-89.
328. Souza, J.M., et al., *Dityrosine cross-linking promotes formation of stable alpha -synuclein polymers. Implication of nitrative and oxidative stress in the pathogenesis of neurodegenerative synucleinopathies.* J Biol Chem, 2000. **275**(24): p. 18344-9.
329. Uversky, V.N., et al., *Methionine oxidation inhibits fibrillation of human alpha-synuclein in vitro.* FEBS Lett, 2002. **517**(1-3): p. 239-44.
330. Giasson, B.I., et al., *Oxidative damage linked to neurodegeneration by selective alpha-synuclein nitration in synucleinopathy lesions.* Science, 2000. **290**(5493): p. 985-9.
331. Hodara, R., et al., *Functional consequences of alpha-synuclein tyrosine nitration: diminished binding to lipid vesicles and increased fibril formation.* J Biol Chem, 2004. **279**(46): p. 47746-53.
332. Uversky, V.N., et al., *Synergistic effects of pesticides and metals on the fibrillation of alpha-synuclein: implications for Parkinson's disease.* Neurotoxicology, 2002. **23**(4-5): p. 527-36.
333. Choi, B.K., et al., *Large α-synuclein oligomers inhibit neuronal SNARE-mediated vesicle docking.* Proc Natl Acad Sci U S A, 2013. **110**(10): p. 4087-92.
334. Wang, L., et al., *α-synuclein multimers cluster synaptic vesicles and attenuate recycling.* Curr Biol, 2014. **24**(19): p. 2319-26.
335. Danzer, K.M., et al., *Different species of alpha-synuclein oligomers induce calcium influx and seeding.* J Neurosci, 2007. **27**(34): p. 9220-32.
336. Lashuel, H.A., et al., *Alpha-synuclein, especially the Parkinson's disease-associated mutants, forms pore-like annular and tubular protofibrils.* J Mol Biol, 2002. **322**(5): p. 1089-102.
337. Lundblad, M., et al., *Impaired neurotransmission caused by overexpression of α-synuclein in nigral dopamine neurons.* Proc Natl Acad Sci U S A, 2012. **109**(9): p. 3213-9.
338. Smith, W.W., et al., *Endoplasmic reticulum stress and mitochondrial cell death pathways mediate A53T mutant alpha-synuclein-induced toxicity.* Hum Mol Genet, 2005. **14**(24): p. 3801-11.
339. Parihar, M.S., et al., *Mitochondrial association of alpha-synuclein causes oxidative stress.* Cell Mol Life Sci, 2008. **65**(7-8): p. 1272-84.
340. Luth, E.S., et al., *Soluble, prefibrillar α-synuclein oligomers promote complex I-dependent, Ca2+-induced mitochondrial dysfunction.* J Biol Chem, 2014. **289**(31): p. 21490-507.
341. Di Maio, R., et al., *α-Synuclein binds to TOM20 and inhibits mitochondrial protein import in Parkinson's disease.* Sci Transl Med, 2016. **8**(342): p. 342ra78.
342. Parihar, M.S., et al., *Alpha-synuclein overexpression and aggregation exacerbates impairment of mitochondrial functions by augmenting oxidative stress in human neuroblastoma cells.* Int J Biochem Cell Biol, 2009. **41**(10): p. 2015-24.
343. Betarbet, R., et al., *Intersecting pathways to neurodegeneration in Parkinson's disease: effects of the pesticide rotenone on DJ-1, alpha-synuclein, and the ubiquitin-proteasome system.* Neurobiol Dis, 2006. **22**(2): p. 404-20.
344. Davis, G.C., et al., *Chronic Parkinsonism secondary to intravenous injection of meperidine analogues.* Psychiatry Res, 1979. **1**(3): p. 249-54.
345. Richter, C., J.W. Park, and B.N. Ames, *Normal oxidative damage to mitochondrial and nuclear DNA is extensive.* Proc Natl Acad Sci U S A, 1988. **85**(17): p. 6465-7.

346. Martin, L.J., et al., *Parkinson's disease alpha-synuclein transgenic mice develop neuronal mitochondrial degeneration and cell death.* J Neurosci, 2006. **26**(1): p. 41-50.
347. Chen, L., et al., *A53T human α-synuclein overexpression in transgenic mice induces pervasive mitochondria macroautophagy defects preceding dopamine neuron degeneration.* J Neurosci, 2015. **35**(3): p. 890-905.
348. Eschbach, J., et al., *Mutual exacerbation of peroxisome proliferator-activated receptor γ coactivator 1α deregulation and α-synuclein oligomerization.* Ann Neurol, 2015. **77**(1): p. 15-32.
349. Zheng, B., et al., *PGC-1α, a potential therapeutic target for early intervention in Parkinson's disease.* Sci Transl Med, 2010. **2**(52): p. 52ra73.
350. Nath, S., et al., *Raised calcium promotes α-synuclein aggregate formation.* Mol Cell Neurosci, 2011. **46**(2): p. 516-26.
351. Sokolov, Y., et al., *Soluble amyloid oligomers increase bilayer conductance by altering dielectric structure.* J Gen Physiol, 2006. **128**(6): p. 637-47.
352. Bence, N.F., R.M. Sampat, and R.R. Kopito, *Impairment of the ubiquitin-proteasome system by protein aggregation.* Science, 2001. **292**(5521): p. 1552-5.
353. Xu, C., B. Bailly-Maitre, and J.C. Reed, *Endoplasmic reticulum stress: cell life and death decisions.* J Clin Invest, 2005. **115**(10): p. 2656-64.
354. Cooper, A.A., et al., *Alpha-synuclein blocks ER-Golgi traffic and Rab1 rescues neuron loss in Parkinson's models.* Science, 2006. **313**(5785): p. 324-8.
355. Paiva, I., et al., *Alpha-synuclein deregulates the expression of COL4A2 and impairs ER-Golgi function.* Neurobiol Dis, 2018. **119**: p. 121-135.
356. Wong, Y.C. and E.L. Holzbaur, *Autophagosome dynamics in neurodegeneration at a glance.* J Cell Sci, 2015. **128**(7): p. 1259-67.
357. Winslow, A.R., et al., *α-Synuclein impairs macroautophagy: implications for Parkinson's disease.* J Cell Biol, 2010. **190**(6): p. 1023-37.
358. Cuervo, A.M., et al., *Impaired degradation of mutant alpha-synuclein by chaperone-mediated autophagy.* Science, 2004. **305**(5688): p. 1292-5.
359. Martinez-Vicente, M., et al., *Dopamine-modified alpha-synuclein blocks chaperone-mediated autophagy.* J Clin Invest, 2008. **118**(2): p. 777-88.
360. Tanik, S.A., et al., *Lewy body-like α-synuclein aggregates resist degradation and impair macroautophagy.* J Biol Chem, 2013. **288**(21): p. 15194-210.
361. Volpicelli-Daley, L.A., et al., *Formation of α-synuclein Lewy neurite-like aggregates in axons impedes the transport of distinct endosomes.* Mol Biol Cell, 2014. **25**(25): p. 4010-23.
362. Giasson, B.I., et al., *Initiation and synergistic fibrillization of tau and alpha-synuclein.* Science, 2003. **300**(5619): p. 636-40.
363. Tilve, S., F. Difato, and E. Chieregatti, *Cofilin 1 activation prevents the defects in axon elongation and guidance induced by extracellular alpha-synuclein.* Sci Rep, 2015. **5**: p. 16524.
364. Mazzulli, J.R., et al., *Gaucher disease glucocerebrosidase and α-synuclein form a bidirectional pathogenic loop in synucleinopathies.* Cell, 2011. **146**(1): p. 37-52.
365. Mazzulli, J.R., et al., *α-Synuclein-induced lysosomal dysfunction occurs through disruptions in protein trafficking in human midbrain synucleinopathy models.* Proc Natl Acad Sci U S A, 2016. **113**(7): p. 1931-6.
366. Gómez-Suaga, P., et al., *ER-mitochondria signaling in Parkinson's disease.* Cell Death Dis, 2018. **9**(3): p. 337.
367. Antony, P.M.A., N.J. Diederich, and R. Balling, *Parkinson's disease mouse models in translational research.* Mammalian Genome, 2011. **22**(7-8): p. 401-419.
368. Polymeropoulos, M.H., *Mutation in the -Synuclein Gene Identified in Families with Parkinson's Disease.* Science, 1997. **276**(5321): p. 2045-2047.

369. Visanji, N.P., et al., *α-Synuclein-Based Animal Models of Parkinson's Disease: Challenges and Opportunities in a New Era.* Trends in Neurosciences, 2016. **39**(11): p. 750-762.
370. Singleton, A.B., et al., *α-Synuclein Locus Triplication Causes Parkinson's Disease.* Science, 2003. **302**(5646): p. 841-841.
371. Jackson-Lewis, V., J. Blesa, and S. Przedborski, *Animal models of Parkinson's disease.* Parkinsonism & Related Disorders, 2012. **18 Suppl 1**: p. S183-185.
372. Gonera, E.G., et al., *Symptoms and duration of the prodromal phase in parkinson's disease.* Movement Disorders, 1997. **12**(6): p. 871-876.
373. Lee, S.-J., et al., *Pathological Propagation through Cell-to-Cell Transmission of Non-Prion Protein Aggregates in Neurodegenerative Disorders.* Nature reviews. Neurology, 2010. **6**(12): p. 702-706.
374. Blesa, J. and S. Przedborski, *Parkinson's disease: animal models and dopaminergic cell vulnerability.* Frontiers in Neuroanatomy, 2014. **8**.
375. Breese, G.R. and T.D. Traylor, *Depletion of brain noradrenaline and dopamine by 6-hydroxydopamine.* Br J Pharmacol, 1971. **42**(1): p. 88-99.
376. Langston, J.W., E.B. Langston, and I. Irwin, *MPTP-induced parkinsonism in human and non-human primates--clinical and experimental aspects.* Acta Neurologica Scandinavica. Supplementum, 1984. **100**: p. 49-54.
377. Meredith, G.E., P.K. Sonsalla, and M.F. Chesselet, *Animal models of Parkinson's disease progression.* Acta Neuropathol, 2008. **115**(4): p. 385-98.
378. Schober, A., *Classic toxin-induced animal models of Parkinson's disease: 6-OHDA and MPTP.* Cell and Tissue Research, 2004. **318**(1): p. 215-224.
379. Kirik, D., et al., *Parkinson-like neurodegeneration induced by targeted overexpression of alpha-synuclein in the nigrostriatal system.* J Neurosci, 2002. **22**(7): p. 2780-91.
380. Gorbatyuk, O.S., et al., *The phosphorylation state of Ser-129 in human alpha-synuclein determines neurodegeneration in a rat model of Parkinson disease.* Proc Natl Acad Sci U S A, 2008. **105**(2): p. 763-8.
381. Ulusoy, A., et al., *Dysregulated dopamine storage increases the vulnerability to alpha-synuclein in nigral neurons.* Neurobiol Dis, 2012. **47**(3): p. 367-77.
382. Oliveras-Salva, M., et al., *rAAV2/7 vector-mediated overexpression of alpha-synuclein in mouse substantia nigra induces protein aggregation and progressive dose-dependent neurodegeneration.* Mol Neurodegener, 2013. **8**: p. 44.
383. Spillantini, M.G., et al., *Alpha-synuclein in Lewy bodies.* Nature, 1997. **388**(6645): p. 839-40.
384. Lennox, G., et al., *Diffuse Lewy body disease: correlative neuropathology using anti-ubiquitin immunocytochemistry.* J Neurol Neurosurg Psychiatry, 1989. **52**(11): p. 1236-47.
385. Recasens, A. and B. Dehay, *Alpha-synuclein spreading in Parkinson's disease.* Front Neuroanat, 2014. **8**: p. 159.
386. Serpell, L.C., et al., *Fiber diffraction of synthetic alpha-synuclein filaments shows amyloid-like cross-beta conformation.* Proc Natl Acad Sci U S A, 2000. **97**(9): p. 4897-902.
387. Crowther, R.A., S.E. Daniel, and M. Goedert, *Characterisation of isolated alpha-synuclein filaments from substantia nigra of Parkinson's disease brain.* Neurosci Lett, 2000. **292**(2): p. 128-30.
388. Luk, K.C., et al., *Pathological α-Synuclein Transmission Initiates Parkinson-like Neurodegeneration in Non-transgenic Mice.* Science (New York, N.Y.), 2012. **338**(6109): p. 949-953.
389. Luk, K.C., et al., *Intracerebral inoculation of pathological α-synuclein initiates a rapidly progressive neurodegenerative α-synucleinopathy in mice.* The Journal of Experimental Medicine, 2012. **209**(5): p. 975-986.

390. Volpicelli-Daley, L.A., K.C. Luk, and V.M.Y. Lee, *Addition of exogenous α-Synuclein Pre-formed fibrils to Primary Neuronal Cultures to seed recruitment of endogenous α-Synuclein to Lewy body and Lewy Neurite-like aggregates.* Nature protocols, 2014. **9**(9): p. 2135-2146.
391. Aulić, S., et al., *Defined α-synuclein prion-like molecular assemblies spreading in cell culture.* BMC Neuroscience, 2014. **15**(1): p. 69.
392. Luk, K.C., et al., *Exogenous α-synuclein fibrils seed the formation of Lewy body-like intracellular inclusions in cultured cells.* Proceedings of the National Academy of Sciences of the United States of America, 2009. **106**(47): p. 20051-20056.
393. Volpicelli-Daley, L.A., et al., *Exogenous α-Synuclein Fibrils Induce Lewy Body Pathology Leading to Synaptic Dysfunction and Neuron Death.* Neuron, 2011. **72**(1): p. 57-71.
394. Sacino, A.N., et al., *Conformational templating of α-synuclein aggregates in neuronal-glial cultures.* Mol Neurodegener, 2013. **8**: p. 17.
395. Kim, C., et al., *Exposure to bacterial endotoxin generates a distinct strain of α-synuclein fibril.* Scientific Reports, 2016. **6**(1).
396. Lindström, V., et al., *Extensive uptake of α-synuclein oligomers in astrocytes results in sustained intracellular deposits and mitochondrial damage.* Mol Cell Neurosci, 2017. **82**: p. 143-156.
397. Reyes, J.F., et al., *Alpha-synuclein transfers from neurons to oligodendrocytes.* Glia, 2014. **62**(3): p. 387-98.
398. Lee, J.G., et al., *Unconventional secretion of misfolded proteins promotes adaptation to proteasome dysfunction in mammalian cells.* Nat Cell Biol, 2016. **18**(7): p. 765-76.
399. Mao, X., et al., *Pathological α-synuclein transmission initiated by binding lymphocyte-activation gene 3.* Science, 2016. **353**(6307).
400. Holmes, B.B., et al., *Heparan sulfate proteoglycans mediate internalization and propagation of specific proteopathic seeds.* Proc Natl Acad Sci U S A, 2013. **110**(33): p. E3138-47.
401. Choi, Y.R., et al., *Prion-like Propagation of α-Synuclein Is Regulated by the FcγRIIB-SHP-1/2 Signaling Pathway in Neurons.* Cell Rep, 2018. **22**(1): p. 136-148.
402. Shrivastava, A.N., et al., *α-synuclein assemblies sequester neuronal α3-Na+/K+-ATPase and impair Na+ gradient.* Embo j, 2015. **34**(19): p. 2408-23.
403. Aulić, S., et al., *α-Synuclein Amyloids Hijack Prion Protein to Gain Cell Entry, Facilitate Cell-to-Cell Spreading and Block Prion Replication.* Scientific Reports, 2017. **7**(1).
404. Ferreira, D.G., et al., *α-synuclein interacts with PrPCto induce cognitive impairment through mGluR5 and NMDAR2B.* Nature Neuroscience, 2017. **20**(11): p. 1569-1579.
405. Paumier, K.L., et al., *Intrastriatal injection of pre-formed mouse α-synuclein fibrils into rats triggers α-synuclein pathology and bilateral nigrostriatal degeneration.* Neurobiology of disease, 2015. **82**: p. 185-199.
406. Sacino, A.N., et al., *Intramuscular injection of α-synuclein induces CNS α-synuclein pathology and a rapid-onset motor phenotype in transgenic mice.* Proc Natl Acad Sci U S A, 2014. **111**(29): p. 10732-7.
407. Ayers, J.I., et al., *Localized Induction of Wild-Type and Mutant Alpha-Synuclein Aggregation Reveals Propagation along Neuroanatomical Tracts.* J Virol, 2018. **92**(18).
408. Kim, S., et al., *Transneuronal Propagation of Pathologic α-Synuclein from the Gut to the Brain Models Parkinson's Disease.* Neuron, 2019. **103**(4): p. 627-641.e7.
409. Abdelmotilib, H., et al., *α-Synuclein Fibril-induced Inclusion Spread in Rats and Mice Correlates with Dopaminergic Neurodegeneration.* Neurobiology of disease, 2017. **105**: p. 84-98.
410. Ayers, J.I., et al., *Robust Central Nervous System Pathology in Transgenic Mice following Peripheral Injection of α-Synuclein Fibrils.* Journal of Virology, 2017. **91**(2).
411. Masuda-Suzukake, M., et al., *Pathological alpha-synuclein propagates through neural networks.* Acta Neuropathologica Communications, 2014. **2**.

412. Masuda-Suzukake, M., et al., *Prion-like spreading of pathological α-synuclein in brain.* Brain, 2013. **136**(4): p. 1128-1138.
413. Rey, N.L., et al., *Widespread transneuronal propagation of α-synucleinopathy triggered in olfactory bulb mimics prodromal Parkinson's disease.* The Journal of Experimental Medicine, 2016. **213**(9): p. 1759-1778.
414. Chung, H.K., et al., *Modeling α-Synuclein Propagation with Preformed Fibril Injections.* J Mov Disord, 2020. **13**(1): p. 77-79.
415. Bosboom, J.L.W., D. Stoffers, and E.C. Wolters, *Cognitive dysfunction and dementia in Parkinson?s disease.* Journal of Neural Transmission, 2004. **111**(10-11): p. 1303-1315.
416. Aarsland, D. and M.W. Kurz, *The epidemiology of dementia associated with Parkinson disease.* Journal of the Neurological Sciences, 2010. **289**(1-2): p. 18-22.
417. Ballard, C., et al., *Cognitive decline in patients with Alzheimer's disease, vascular dementia and senile dementia of Lewy body type.* Age and Ageing, 1996. **25**(3): p. 209-213.
418. Calderon, J., et al., *Perception, attention, and working memory are disproportionately impaired in dementia with Lewy bodies compared with Alzheimer's disease.* Journal of Neurology, Neurosurgery, and Psychiatry, 2001. **70**(2): p. 157-164.
419. Connor, D.J., et al., *Cognitive Profiles of Autopsy-Confirmed Lewy Body Variant vs Pure Alzheimer Disease.* Archives of Neurology, 1998. **55**(7): p. 994-1000.
420. Cykowski, M.D., et al., *Expanding the spectrum of neuronal pathology in multiple system atrophy.* Brain, 2015. **138**(Pt 8): p. 2293-309.
421. Koga, S., et al., *Profile of cognitive impairment and underlying pathology in multiple system atrophy.* Mov Disord, 2017. **32**(3): p. 405-413.
422. Aarsland, D., et al., *Neuropathology of dementia in Parkinson's disease: A prospective, community-based study.* Annals of Neurology, 2005. **58**(5): p. 773-776.
423. Apaydin, H., et al., *Parkinson Disease Neuropathology: Later-Developing Dementia and Loss of the Levodopa Response.* Archives of Neurology, 2002. **59**(1): p. 102-112.
424. Harding, A.J. and G.M. Halliday, *Cortical Lewy body pathology in the diagnosis of dementia.* Acta Neuropathologica, 2001. **102**(4): p. 355-363.
425. Hurtig, H.I., et al., *Alpha-synuclein cortical Lewy bodies correlate with dementia in Parkinson's disease.* Neurology, 2000. **54**(10): p. 1916-1921.
426. Irwin, D.J., et al., *Neuropathologic substrates of Parkinson's disease dementia.* Annals of neurology, 2012. **72**(4): p. 587-598.
427. Colosimo, C., et al., *Lewy body cortical involvement may not always predict dementia in Parkinson's disease.* Journal of Neurology, Neurosurgery, and Psychiatry, 2003. **74**(7): p. 852-856.
428. Parkkinen, L., et al., *α-Synuclein pathology does not predict extrapyramidal symptoms or dementia.* Annals of Neurology, 2005. **57**(1): p. 82-91.
429. Xuereb, J.H., et al., *Cortical and subcortical pathology in Parkinson's disease: relationship to parkinsonian dementia.* Advances in Neurology, 1990. **53**: p. 35-40.
430. Wisman, L.A.B., et al., *Functional Convergence of Dopaminergic and Cholinergic Input Is Critical for Hippocampus-Dependent Working Memory.* Journal of Neuroscience, 2008. **28**(31): p. 7797-7807.
431. Hall, H., et al., *Characterization of Cognitive Deficits in Rats Overexpressing Human Alpha-Synuclein in the Ventral Tegmental Area and Medial Septum Using Recombinant Adeno-Associated Viral Vectors.* PLOS ONE, 2013. **8**(5): p. e64844.
432. Freichel, C., et al., *Age-dependent cognitive decline and amygdala pathology in α-synuclein transgenic mice.* Neurobiology of Aging, 2007. **28**(9): p. 1421-1435.

433. Lim, Y., et al., *α-syn Suppression Reverses Synaptic and Memory Defects in a Mouse Model of Dementia with Lewy Bodies.* The Journal of neuroscience : the official journal of the Society for Neuroscience, 2011. **31**(27): p. 10076-10087.
434. Nuber, S., et al., *Neurodegeneration and Motor Dysfunction in a Conditional Model of Parkinson's Disease.* Journal of Neuroscience, 2008. **28**(10): p. 2471-2484.
435. Adamowicz, D.H., et al., *Hippocampal α-Synuclein in Dementia with Lewy Bodies Contributes to Memory Impairment and Is Consistent with Spread of Pathology.* The Journal of Neuroscience, 2017. **37**(7): p. 1675-1684.
436. Miki, Y., et al., *Hippocampal α-synuclein pathology correlates with memory impairment in multiple system atrophy.* Brain, 2020. **143**(6): p. 1798-1810.
437. Huang, C., et al., *A new method for purification of recombinant human alpha-synuclein in Escherichia coli.* Protein Expression and Purification, 2005. **42**(1): p. 173-177.
438. Paxinos, G. and C. Watson, *The rat brain in stereotaxic coordinates: hard cover edition*. 2006: Elsevier.
439. Morris, R., *Developments of a water-maze procedure for studying spatial learning in the rat.* Journal of Neuroscience Methods, 1984. **11**(1): p. 47-60.
440. Coradazzi, M., et al., *Selective noradrenaline depletion impairs working memory and hippocampal neurogenesis.* Neurobiol Aging, 2016. **48**: p. 93-102.
441. Pintus, R., et al., *Essential role of hippocampal noradrenaline in the regulation of spatial working memory and TDP-43 tissue pathology.* J Comp Neurol, 2018. **526**(7): p. 1131-1147.
442. Sasaki, A., et al., *Sensitive western blotting for detection of endogenous Ser129-phosphorylated α-synuclein in intracellular and extracellular spaces.* Scientific Reports, 2015. **5**(1).
443. West, M.J., L. Slomianka, and H.J.G. Gundersen, *Unbiased stereological estimation of the total number of neurons in the subdivisions of the rat hippocampus using the optical fractionator.* The Anatomical Record, 1991. **231**(4): p. 482-497.
444. Gundersen, H.J.G. and E.B. Jensen, *The efficiency of systematic sampling in stereology and its prediction*.* Journal of Microscopy, 1987. **147**(3): p. 229-263.
445. Vanni, S., et al., *Differential Diagnosis of Vertigo in the Emergency Department: A Prospective Validation Study of the STANDING Algorithm.* Frontiers in Neurology, 2017. **8**.
446. Livak, K.J. and T.D. Schmittgen, *Analysis of Relative Gene Expression Data Using Real-Time Quantitative PCR and the 2−ΔΔCT Method.* Methods, 2001. **25**(4): p. 402-408.
447. Bradley, V.A., J.L. Welch, and D.J. Dick, *Visuospatial working memory in Parkinson's disease.* Journal of Neurology, Neurosurgery, and Psychiatry, 1989. **52**(11): p. 1228-1235.
448. Boassa, D., et al., *Mapping the subcellular distribution of α-synuclein in neurons using genetically encoded probes for correlated light and electron microscopy: implications for Parkinson's disease pathogenesis.* J Neurosci, 2013. **33**(6): p. 2605-15.
449. Halliday, G., et al., *The progression of pathology in longitudinally followed patients with Parkinson's disease.* Acta Neuropathologica, 2008. **115**(4): p. 409-415.
450. Kim, W.S., K. Kågedal, and G.M. Halliday, *Alpha-synuclein biology in Lewy body diseases.* Alzheimer's Research & Therapy, 2014. **6**(5-8).
451. Froula, J.M., et al., *α-Synuclein fibril-induced paradoxical structural and functional defects in hippocampal neurons.* Acta Neuropathologica Communications, 2018. **6**.
452. Wu, Q., et al., *alpha-Synuclein (alphaSyn) Preformed Fibrils Induce Endogenous alphaSyn Aggregation, Compromise Synaptic Activity and Enhance Synapse Loss in Cultured Excitatory Hippocampal Neurons.* J Neurosci, 2019. **39**(26): p. 5080-5094.
453. Overk, C.R., et al., *Differential calcium alterations in animal models of neurodegenerative disease: Reversal by FK506.* Neuroscience, 2015. **310**: p. 549-60.

454. Masliah, E., et al., *Passive Immunization Reduces Behavioral and Neuropathological Deficits in an Alpha-Synuclein Transgenic Model of Lewy Body Disease.* PLoS ONE, 2011. **6**(4).
455. Larsen, K.E., et al., *α-Synuclein Overexpression in PC12 and Chromaffin Cells Impairs Catecholamine Release by Interfering with a Late Step in Exocytosis.* Journal of Neuroscience, 2006. **26**(46): p. 11915-11922.
456. Nemani, V.M., et al., *Increased Expression of Alpha-Synuclein Reduces Neurotransmitter Release by Inhibiting Synaptic Vesicle Reclustering After Endocytosis.* Neuron, 2010. **65**(1): p. 66-79.
457. Kramer, M.L. and W.J. Schulz-Schaeffer, *Presynaptic α-Synuclein Aggregates, Not Lewy Bodies, Cause Neurodegeneration in Dementia with Lewy Bodies.* Journal of Neuroscience, 2007. **27**(6): p. 1405-1410.
458. Blumenstock, S., et al., *Seeding and transgenic overexpression of alpha-synuclein triggers dendritic spine pathology in the neocortex.* EMBO Molecular Medicine, 2017. **9**(5): p. 716-731.
459. Mahmmoud, R.R., et al., *Spatial and Working Memory Is Linked to Spine Density and Mushroom Spines.* PLoS One, 2015. **10**(10): p. e0139739.
460. Anderson, J.P., et al., *Phosphorylation of Ser-129 Is the Dominant Pathological Modification of α-Synuclein in Familial and Sporadic Lewy Body Disease.* Journal of Biological Chemistry, 2006. **281**(40): p. 29739-29752.
461. Paleologou, K.E., et al., *Phosphorylation at Ser-129 but Not the Phosphomimics S129E/D Inhibits the Fibrillation of α-Synuclein.* The Journal of Biological Chemistry, 2008. **283**(24): p. 16895-16905.
462. Fiske, M., et al., *Contribution of Alanine-76 and Serine Phosphorylation in α-Synuclein Membrane Association and Aggregation in Yeasts.* Parkinson's Disease, 2011.
463. Harms, A.S., et al., *α-Synuclein fibrils recruit peripheral immune cells in the rat brain prior to neurodegeneration.* Acta Neuropathol Commun, 2017. **5**(1): p. 85.
464. Duffy, M.F., et al., *Lewy body-like alpha-synuclein inclusions trigger reactive microgliosis prior to nigral degeneration.* J Neuroinflammation, 2018. **15**(1): p. 129.
465. Olanow, C.W., et al., *Temporal evolution of microglia and α-synuclein accumulation following foetal grafting in Parkinson's disease.* Brain, 2019. **142**(6): p. 1690-1700.
466. Thakur, P., et al., *Modeling Parkinson's disease pathology by combination of fibril seeds and α-synuclein overexpression in the rat brain.* Proc Natl Acad Sci U S A, 2017. **114**(39): p. E8284-e8293.